2-25-2019 6:45 PM

Analysis and Control of Aluminum Concentration in Groundwater: Mathematical Modelling and Laboratory Study

Daria Popugaeva, *The University of Western Ontario*

Supervisor: Ray, Ajay K., *The University of Western Ontario*
Co-Supervisor: Kreyman, Konstantin, *The University of Western Ontario*
A thesis submitted in partial fulfillment of the requirements for the Doctor of Philosophy degree in Chemical and Biochemical Engineering

Abstract

The remediation of metal-contaminated natural water bodies is prioritized due to metals toxicity, non-biodegradable properties, and accumulative behaviours leading to the increased incidence of adverse health effects. Current investigation is driven by the existing problem of elevated aluminum concentrations in the groundwater of Khibiny alkaline massif (Kola Peninsula). The prohibitive aluminum level exceeding the accepted standard of 0.20 mg L^{-1} is described as a serious health concern when the groundwater used for the local water supply. The results of comprehensive field data analysis based on chemometric methods applied to the available monitoring data including 12 groundwater quality parameters are reported as well as the outcomes of laboratory study on aluminum adsorption from aqueous solutions. Computed correlation coefficients matrix revealed a statistically significant level of associations between aluminum concentrations and pH values, concentrations of SO_4^{2-}, NO_3^-, Cl^-. Mathematical models developed by using univariate and multivariate regression methods explained up to 54% of aluminum concentration temporal variability linked to pH, Cl^-, NO_3^- and up to 67.5% of the original dataset total variance. The outcomes of hierarchical cluster analysis suggested data subdivision into three clusters where Al and pH formed a separate cluster. The frequency bands describing dominant variability features of groundwater quality parameters were identified by spectral analysis based on fast Fourier transform algorithm and corresponded approximately to 5–7, 13–17, and 20–34 month periods. Calculated CCME water quality index scores identified a groundwater quality gradual deterioration from fair to marginal category during the monitoring period 1999–2012. Laboratory study of aluminum removal on adsorbents from aqueous solutions considering water-specific natural conditions showed the maximum aluminum uptake of 1.69 mg g^{-1} by montmorillonite K10 within 120 min at pH 4.0 while TiO_2 and vermiculite concrete-supported ferric oxyhydroxide adsorbent were most effective at pH 9.0 obtaining maximum adsorption capacities of 6.85 mg g^{-1} and 6.75 mg g^{-1} in 30 min and 240 min, respectively. It was shown that when these two adsorbents worked jointly the capacity reached 8.28 mg g^{-1} within 60 min at pH 9.0. The changes of each component mass allow controlling contact time to provide required aluminum removal efficiency. No apparent significant effect on aluminum removal by adsorbents tested in the presence of SO_4^{2-}, NO_3^-,

Cl^- was observed at pH 9.0. The current study identifies a possible approach and the reliable foundation of water treatment technology solving the problem of elevated aluminum concentrations in the household water of Khibiny alkaline massif area as well as other locations where the solution of this problem can improve living conditions or industrial technologies.

Keywords

Aluminum, Groundwater, Chemometric Methods, Univariate and Multivariate Regression Analysis, Fast Fourier Transform, Adsorption, Titanium Dioxide, Vermiculite, Montmorillonite, Silica Gel, Inorganic Ions, Remediation

Co-Authorship Statement

This PhD thesis includes the material that is published, "under review", prepared or in a preparation for the submission to the peer-reviewed journals as listed below.

Chapter 3: Study of Aluminum in Groundwater using Chemometric Methods

Daria Popugaeva, Konstantin Kreyman, Ajay K. Ray (2018). Study of aluminium in groundwater using chemometric methods. Published in *Environmental Technology* https://doi.org/10.1080/09593330.2018.1544667

The data analysis and writing of the manuscript were completed by Daria Popugaeva under the supervision of Dr. Konstantin Kreyman and Dr. Ajay K. Ray. The written manuscript was reviewed and revised by Dr. Konstantin Kreyman and Dr. Ajay K. Ray.

Chapter 4: Assessment of Khibiny Alkaline Massif Groundwater Quality using Statistical Methods and Water Quality Index

Daria Popugaeva, Konstantin Kreyman, Ajay K. Ray. Under peer review at *The Canadian Journal of Chemical Engineering*

The data analysis and drafting the manuscript was conducted by Daria Popugaeva under the supervision of Dr. Konstantin Kreyman and Dr. Ajay K. Ray. The feedback on written manuscript was received from the co-authors.

Chapter 5: Removal of Aluminum from Aqueous Solution by Adsorption on Montmorillonite K10, TiO_2, and SiO_2: Kinetics, Isotherms, and Effect of Ions

Daria Popugaeva, Kyriakos Manoli, Ajay K. Ray, Konstantin Kreyman. In preparation for the submission

The experimental plan, data analysis, and drafting the manuscript were completed by Daria Popugaeva under the guidance of Dr. Kyriakos Manoli, Dr. Ajay K. Ray, and Dr. Konstantin Kreyman. The written manuscript was reviewed and revised by Dr. Kyriakos Manoli, Dr. Ajay K. Ray, and Dr. Konstantin Kreyman.

Chapter 6: Removal of Aluminum from Alkaline Aqueous Solution by Adsorption on TiO_2 and Vermiculite Concrete-Supported Ferric Oxyhydroxide Adsorbent

Daria Popugaeva, Ajay K. Ray, Konstantin Kreyman. Prepared for the submission to *The Canadian Journal of Chemical Engineering*

The experimental work, data analysis, and drafting the manuscript were done by Daria Popugaeva under the guidance of Dr. Ajay K. Ray and Dr. Konstantin Kreyman. The feedback on the written manuscript was received from Dr. Ajay K. Ray and Dr. Konstantin Kreyman.

Acknowledgments

I would like to express my boundless gratitude to my supervisors, Dr. Konstantin Kreyman and Dr. Ajay K. Ray for their support, guidance, and encouragements through all stages of my graduate studies. I feel very fortunate to have had the opportunity to learn from you and to explore the intricate and amazing details of research. The knowledge and experience I have gained are invaluable.

I like to gratefully thank Apatityvodokanal company (Apatity, Russia) whose constant interest, support, and discussions facilitated this research. I thank Dr. Mikhail Khaskelberg and Dr. Dmitry Martemianov (Tomsk Polytechnic University, Tomsk, Russia) for useful discussions and providing us with the samples of vermiculite concrete-supported ferric oxyhydroxide adsorbent – one of the adsorbents that was used in this study and the supportive information.

I acknowledge the Clean Technologies for Water Refining and Nutrients and Energy Recovery (TWNER) - Natural Science and Engineering Research Council (NSERC) - Collaborative Research and Training Experience (CREATE) Training Program, Canada, for the financial support.

I would like to thank Dr. Dimitre Karamanev and Dr. Shahzad Barghi for their suggestions and discussions on my research work. I acknowledge Caitlin Corcoran, Pastor Solano-Flores, and especially Fate Hashemi for their constant support and technical assistance with my work at the laboratories.

I like to acknowledge my internship advisors Dr. Ferdinando Crapulli and Dr. Domenico Santoro (Trojan Technologies, London ON, Canada). The opportunity to work at Trojan Technologies provided me with the valuable experience for my professional future.

I thank all my colleagues and lab mates that I had a pleasure to work with or alongside at Western University, especially Malini Ghosh, Mrinmoyee Mondal, Tianfang Tian, Tiziana Venditto, Leila Azimian. Thanks to Dr. Kyriakos Manoli for sharing his knowledge and collaborating on Chapter 5. I thank the graduate coordinators, Ashley Jokhu and Cole Handsaeme for their assistance.

My appreciation is extended to my two-year in a row ES 1050 fellow TA, Dr. Fabricio Guayaquil-Sosa. It was a nice time to be involved in the design course assisting first-year engineering students together. A special thanks to Dr. Medhavi Gupta for being such a good friend.

I would like to express my very great appreciation to Lidia Kreyman for her care and encouragements.

I thank my dear family and friends from Saint Petersburg, especially my grandmother Iraida who was persistently trying to understand my research work and motivating me to move forward. Kristina, Natalia, Anna, Victoria our strong friendship over countless years is an admirable gift and support.

Finally, I am grateful to my parents, Elena and Aleksandr for their guidance and patience. Your endless support was and is a very important condition of my personal growth.

"It ain't the roads we take; it's what's inside of us that makes us turn out the way we do."

—O. Henry (William Sydney Porter), *The Roads We Take*

Table of Contents

List of Tables

List of Figures

List of Appendices

List of Abbreviations and Symbols

ANOVA	Analysis of variance
ARE	Average relative error
CA	Cluster analysis
CCME WQI	Canadian Council of Ministries of the Environment Water Quality Index
CSP	Cumulative spectral power
DFT	Discrete Fourier transform
EDX	Energy dispersive X-ray spectroscopy
EU	European Union
FA	Factor analysis
FFT	Fast Fourier transform
HCA	Hierarchical cluster analysis
HCl	Hydrochloric acid
ICP-OES	Inductively coupled plasma – optical emission spectrometry
KMO test	Kaiser-Meyer-Olkin test
MA	Multicomponent adsorbent
NaOH	Sodium hydroxide
PCA	Principal component analysis
PSD	Power spectral density
SEM	Scanning electron microscopy

SiO_2	Silica
TDS	Total dissolved solids
TiO_2	Titanium dioxide
USEPA	United States Environmental Protection Agency
VC	Vermiculite concrete-supported ferric oxyhydroxide adsorbent
VIF	Variance inflation factor
WHO	World Health Organization
ZnO	Zinc oxide
Δt	Equally spaced time interval
a_S	Sips isotherm model constant (L mg^{-1})
b	Langmuir isotherm constant (L mg^{-1})
C_0	Initial concentration of adsorbate (mg L^{-1})
C_e	Equilibrium concentration of adsorbate (mg L^{-1})
C_j	Fourier coefficient
$d(t_n)$	Value of variable d at time t_n
E^0	Redox potential (V)
E^2	Sum of squared errors
F_1	CCME WQI scope
F_2	CCME WQI frequency
F_3	CCME WQI amplitude

f	Frequency (cycle day $^{-1}$)
f_c	Nyquist critical frequency
K_F	Freundlich isotherm constant (mg g^{-1})/(mg L^{-1})^n
K_S	Sips isotherm model constant (L g^{-1})
k_1	Pseudo-first order rate constant (min^{-1})
k_2	Pseudo-second order rate constant (g (mg min) $^{-1}$)
m	Mass of the adsorbent (g)
Max	Maximum value
Min	Minimum value
N	Total number of observations
n	Discrete time observation (Chapter 3)
n	Freundlich intensity parameter (Chapters 5–6)
p	−log
$P(f)$	PSD estimate at frequency f
p-value	Probability value
Q_0	Maximum monolayer coverage capacity (mg g^{-1})
Q1	First quartile value
Q3	Third quartile value
q_e	Amount of adsorbate in the adsorbent at equilibrium (mg g^{-1})
q_t	Amount of adsorbate in the adsorbent (mg g^{-1}) at any time t

R^2	Coefficient of determination
r	Pearson correlation coefficient
r_s	Spearman correlation coefficient
S	Standard error of regression
$StDev$	Standard deviation value
T	Temperature (°C)
t	Time (min)
t-test	t-confidence interval procedure
V	Volume of solution (L)
X_{ij}	jth observation of the ith variable X
x_m	Mean value
α-$level$	Significance level
β	Cumulative equilibrium-formation constant
β_S	Sips isotherm model exponent
π	3.14
ω_j	Angular frequency

Chapter 1

1 Introduction

1.1 Rationale

Earth is known as the “blue planet” because a significant part of its surface is covered by water with just a small portion taken by fresh water resources [1]. The access to safe and easily available resources of fresh water is a fundamental aspect of sustainable development [2]. It is estimated that more than a half of a total world’s population will be living in areas experiencing high levels of water stress by 2025 and it is projected to rise [3]. Nowadays nearly 845 million people lack a rudimentary dirking water service, including millions relying on surface water [4]. The reliance on groundwater sources for household needs is becoming more and more common [5]. This happens due to several reasons. First, world’s population is increasing, and a rapid industrial development is taking place [3,6,7]. Second, the surface water sources are limited and, in many cases, is considered as unsafe due to the presence of a wide range of pollutants including toxic metals and emerging organic contaminants [7–10]. The growth of importance keeping fresh water resources harmless and readily available is essential for environmental sustainability to meet the current demands without jeopardizing future generations needs [2].

The metals are identified as one of the major pollution sources of the aqueous environments as they are toxic, non-biodegradable, and have accumulative behaviours leading to the increased incidence of negative health effects [11,12]. Among the metals, aluminum because of its neurotoxic properties is prominent making contamination of water resources with this metal the ongoing problem [13–15]. It is enough to point out that clay consists of aluminum to understand aluminum’s wide occurrence in the Earth’s crust and consequently in natural water bodies [16]. Aluminum exposure to human by means of drinking water or food can potentially cause neurotoxicity increasing the risk of neurological disorders [13,17].

Among many other locations where high aluminum concentration presented in natural water sources, the prohibitive aluminum level in the groundwater of Khibiny alkaline massif (Kola Peninsula) is considered as a serious health concern limiting the water use for the household consumption [14]. Over the past three decades, the groundwater deposit located in the southern part of the Khibiny alkaline massif became one of the vital sources of Kirovsk and Apatity water supply (Figure 1.1). The water is characterized by strong alkaline conditions and elevated aluminum concentrations that exceed the drinking water guideline of 0.20 mg L^{-1} [18] up to nine times according to the available groundwater monitoring data. To date, there is no a reliable solution solving the problem of elevated aluminum concentrations in the alkaline groundwater that is feasible to be implemented in the Khibiny area and can facilitate the household water supply management to satisfy health regulations.

A quantitative analysis of water quality data is an essential and necessary step to get an insight into such aspects of the problem as associations among investigated parameters, possible pollution sources, and overall water quality. The approach provides the reliable way to choose applicable methods and techniques revealing the key associations between the parameters under consideration. Chemometric methods of field data analysis along with various water treatments of contaminated water provide a solid foundation to investigate and solve the problem of elevated metal concentrations in aqueous environments [19–22].

Figure 1.1: Study area: Khibiny alkaline massif, Kola Peninsula.

1.2 Thesis Objectives

The need for the PhD originates from the industrial attempts to improve the groundwater quality of household water supply in Khibiny alkaline massif (Kola Peninsula) area. The approach proposed by current PhD research work to address the need combines a comprehensive field data analysis of the available groundwater quality monitoring data (1999–2012) and laboratory study on aluminum adsorption from aqueous solutions on various adsorbents. The following thesis objectives were made.

i. to quantitatively access and analyze the results of long-term field data monitoring program of Khibiny alkaline massif (Kola Peninsula) groundwater by using chemometric methods,
ii. to reveal the degree of association between the groundwater quality parameters with aluminum concentrations variability in the water intake under investigation,
iii. to study reliable adsorbents removing aluminum effectively under the water-specific natural conditions,
iv. to investigate and quantitively describe adsorption process of aluminum removal by the selected adsorbents,
v. to explore the effect of pH and ions presence on the adsorption of aluminum from aqueous solutions.

1.3 Thesis Structure

This PhD thesis is prepared in the article-integrated format in accordance with the guidelines provided by the School of Graduate and Postdoctoral Studies of the University of Western Ontario. The contents of seven chapters included in the thesis are as follows.

Chapter 1 introduces and specifies the need for this study and defines the problem of elevated aluminum concentrations in the groundwater of Khibiny alkaline massif (Kola Peninsula). The thesis specific objectives are presented.

Chapter 2 provides a literature review on the major problem-related aspects including aluminum environmental chemistry, the presence of prohibitive aluminum concentrations

in natural water bodies, the primary water treatment methods for aluminum removal from aqueous solutions, and the review and comparison of the results of studies on aluminum removal by various adsorbents.

Chapter 3 is a research article entitled *"Study of Aluminium in Groundwater using Chemometric Methods"*. The study presents the initial results of field data analysis at both time and frequency domains by using chemometric methods including Pearson correlation, multiple regression analysis and spectral analysis based on fast Fourier transform algorithm to assess and interpret the outcomes of thirteen-year field data monitoring of Khibiny alkaline massif (Kola Peninsula) groundwater. The main objective of this study was to identify the parameters associated with aluminum concentrations variability in the groundwater under consideration.

Chapter 4 is a research article entitled *"Assessment of Khibiny Alkaline Massif Groundwater Quality using Statistical Methods and Water Quality Index"*. This study extends the outcomes of univariate data analysis investigating the Khibiny alkaline massif groundwater quality by using multivariate statistical methods including factor analysis/principal component analysis and hierarchical cluster analysis, and the calculation of water quality index. The results represent the quantitative data assessment and describe influencing aluminum variability factors prior the development of plan of laboratory tests to keep aluminum concentrations in water considering water-specific natural conditions under the limits of accepted standards.

Chapter 5 is a research article entitled *"Removal of Aluminum from Aqueous Solution by Adsorption on Montmorillonite K10, TiO_2, and SiO_2: Kinetics, Isotherms, and Effect of Ions"*. The investigation of adsorption capacities of montmorillonite K10, TiO_2, and SiO_2 for the removal of aluminum from acidic aqueous solution is presented and discussed. The effects of pH, initial aluminum concentration, adsorbent amount, contact time, and the ions – Ca^{2+}, Mg^{2+}, SO_4^{2-}, HCO_3^-, Na^+, and Cl^- that usually present in natural water bodies were investigated.

Chapter 6 is a research article entitled *"Removal of Aluminum from Alkaline Aqueous Solution by Adsorption on TiO_2 and Vermiculite Concrete-Supported Ferric*

Oxyhydroxide Adsorbent". Considering the results discussed in Chapters 3–5, this study is aimed at the investigation of aluminum adsorption from aqueous solution reflecting the main features of physico-chemical composition of Khibiny alkaline massif groundwater (Kola Peninsula) on TiO_2, vermiculite concrete-supported ferric oxyhydroxide adsorbent, and a multicomponent adsorbent – the vermiculite-based adsorbent enriched with TiO_2. The results obtained evidence in favour of that the application of this adsorbent can be an effective way to decrease and control aluminum concentrations below the drinking water guideline at the local Khibiny water treatment facility and at the other locations where high aluminum concentration in the alkaline aqueous solutions limits the water use for the household needs.

Chapter 7 includes the discussion on PhD thesis major findings followed by scientific contribution of the study, study limitations, and future work recommendations.

1.4 References

[1] R.B. Singh, D. Kumar, Water Scarcity, in: S. Eslamian (Ed.), Handb. Eng. Hydrol. Environ. Hydrol. Water Manag., CRC Press, Boca Raton, 2014: pp. 519–544.

[2] United Nations, Sustainable Development Goals Report 2018, New York, 2018.

[3] N.W. Arnell, Climate change and global water resources, Glob. Environ. Chang. 9 (1999) S31–S49.

[4] World Health Organization (WHO) and the United Nations Children's Fund (UNICEF), Progress on Drinking Water, Sanitation and Hygiene: 2017 update and SDG baselines, Geneva, 2017.

[5] World Health Organization (WHO), Protecting Groundwater for Health, IWA Publishing, London, 2006.

[6] I. Ali, New generation adsorbents for water treatment, Chem. Rev. 112 (2012) 5073–5091. doi:10.1021/cr300133d.

[7] L.I. Ezemonye, P.O. Adebayo, A.A. Enuneku, I. Tongo, E. Ogbomida, Potential health risk consequences of heavy metal concentrations in surface water, shrimp (Macrobrachium macrobrachion) and fish (Brycinus longipinnis) from Benin River, Nigeria, Toxicol. Reports. 6 (2019) 1–9. doi:10.1016/j.toxrep.2018.11.010.

[8] Q. Gao, K.M. Blum, P. Gago-Ferrero, K. Wiberg, L. Ahrens, P.L. Andersson, Impact of on-site wastewater infiltration systems on organic contaminants in groundwater and recipient waters, Sci. Total Environ. 651 (2019) 1670–1679. doi:10.1016/j.scitotenv.2018.10.016.

[9] A.L. Paschoalini, L.A. Savassi, F.P. Arantes, E. Rizzo, N. Bazzoli, Heavy metals accumulation and endocrine disruption in Prochilodus argenteus from a polluted neotropical river, Ecotoxicol. Environ. Saf. 169 (2019) 539–550. doi:10.1016/j.ecoenv.2018.11.047.

[10] C. Becouze-Lareure, A. Dembélé, M. Coquery, C. Cren-Olivé, J.L. Bertrand-Krajewski, Assessment of 34 dissolved and particulate organic and metallic micropollutants discharged at the outlet of two contrasted urban catchments, Sci. Total Environ. 651 (2019) 1810–1818. doi:10.1016/j.scitotenv.2018.10.042.

[11] L. de Pablo, M.L. Chávez, M. Abatal, Adsorption of heavy metals in acid to alkaline environments by montmorillonite and Ca-montmorillonite, Chem. Eng. J. 171 (2011) 1276–1286. doi:10.1016/j.cej.2011.05.055.

[12] S.H. Peng, R. Wang, L.Z. Yang, L. He, X. He, X. Liu, Biosorption of copper, zinc, cadmium and chromium ions from aqueous solution by natural foxtail millet shell, Ecotoxicol. Environ. Saf. 165 (2018) 61–69. doi:10.1016/j.ecoenv.2018.08.084.

[13] T.P. Flaten, Aluminium as a risk factor in Alzheimer's disease, with emphasis on drinking water, Brain Res. Bull. 55 (2001) 187–196.

[14] D. Popugaeva, K. Kreyman, A.K. Ray, Study of aluminium in groundwater using chemometric methods, Environ. Technol. (2018). doi:10.1080/09593330.2018.1544667.

[15] M. Frankowski, A. Zioła-Frankowska, I. Kurzyca, K. Novotný, T. Vaculovič, V. Kanický, M. Siepak, J. Siepak, Determination of aluminium in groundwater samples by GF-AAS, ICP-AES, ICP-MS and modelling of inorganic aluminium complexes, Environ. Monit. Assess. 182 (2011) 71–84. doi:10.1007/s10661-010-1859-8.

[16] C.T. Driscoll, W.D. Schecher, The chemistry of aluminum in the environment, Environ. Geochem. Health. 12 (1990) 28–49. doi:10.1007/BF01734046.

[17] Z. Wang, X. Wei, J. Yang, J. Suo, J. Chen, X. Liu, X. Zhao, Chronic exposure to aluminum and risk of Alzheimer's disease: a meta-analysis, Neurosci. Lett. 610 (2016) 200–206. doi:10.1016/j.neulet.2015.11.014.

[18] U.S. Environmental Protection Agency (USEPA), 2018 Edition of the Drinking Water Standards and Health Advisories Tables, Washington, DC, 2018.

[19] M.A. Hashim, S. Mukhopadhyay, J.N. Sahu, B. Sengupta, Remediation technologies for heavy metal contaminated groundwater, J. Environ. Manage. 92 (2011) 2355–2388. doi:10.1016/j.jenvman.2011.06.009.

[20] K. Nosrati, M. Van Den Eeckhaut, Assessment of groundwater quality using multivariate statistical techniques in Hashtgerd Plain, Iran, (2012) 331–344. doi:10.1007/s12665-011-1092-y.

[21] J. Wang, Statistical study on distribution of multiple dissolved elements and a water quality assessment around a simulated stackable fly ash, Ecotoxicol. Environ. Saf. 159 (2018) 46–55. doi:10.1016/j.ecoenv.2018.04.057.

[22] S. Chowdhury, M.A.J. Mazumder, O. Al-attas, T. Husain, Heavy metals in drinking water: Occurrences, implications, and future needs in developing countries, Sci. Total Environ. 569–570 (2016) 476–488. doi:10.1016/j.scitotenv.2016.06.166.

Chapter 2

2 Literature Review

2.1 Introduction

Aluminum (Al) is widely distributed in the environment comprising about 8% of the Earth's outer crust. Al containing agents have been used in many applications including food, drinking water, and medicine [1,2]. Al compounds are currently extensively used in the industrial sector as well as in pharmaceutical sector comprising cosmetics, food additives, and household products. Aluminum-based salts such as aluminum chloride and aluminum sulphate are one of the most commonly used coagulating agents in the water treatment industry. The application of aluminum-based agents in various modern engineering technologies more often leads to the by-products generation including increased Al level in water [3].

Al is known as a powerful neurotoxicant [4,5]. Several studies have implicated that Al accumulation in human body can cause neurotoxicity leading to the increased risk of neurological disorders such as Alzheimer's disease [5–7]. The recommended upper boundary limit of Al concentration in drinking water is 0.05–0.20 mg L^{-1} [8]. In a number of cases, the elevated concentrations of Al that have been found in both acidic and alkaline surface and ground waters are recognized as a serious concern in many countries in the worldwide [9–11].

A number of methods have been proposed for Al removal from aqueous solutions including ion exchange, adsorption, membrane filtration, and electrodialysis [12,13]. Among available water treatment technologies adsorption is considered as a suitable method for metal removal from aqueous solutions having advantages such as the availability of the wide range of adsorbents, low-cost, ease of operation, and efficiency [14]. Various sorbents substantially organic such as activated carbon and its modified forms, (bio)polymers, char, marble wastes, natural zeolite were tested for the Al removal from aqueous solutions [12,15–18].

2.2 Al Occurrence in the Environment

The chemistry, bioavailability, and toxicity of Al in the aquatic environment are complex and affected by various water quality characteristics [19,20]. Al is released by both anthropogenic and natural sources and is present in all types of natural water bodies [9,21]. The major features of the biogeochemical cycle of aluminum include leaching of aluminum from geochemical formations and soil particulates to aqueous environments, adsorption onto soil or sediment particulates, and wet and dry deposition from the air to land and surface water [21]. The inorganic monomeric Al – aqua aluminum (Al^{3+}) or its complexes by dissolved constituents such as OH^{-}, F^{-}, PO_4^{-}, and SO_4^{2-} are prevalent in the natural water bodies [22]. According to the World Health Organization dissolved Al concentration in natural water sources varies dramatically from 0.001 to 90.0 mg L^{-1} depending on various physico-chemical and mineralogical factors [23]. Acid rain in recent years has transformed the insoluble aluminum-containing minerals into a more soluble form causing an accumulation of Al in food through drinking water sources [2]. The diversity of aluminum-based minerals found in nature are wide. The Al leaching from soil and bedrock into the aqueous solutions are widely occurring [21]. For example, in Sweden, Norway, and USA (Adirondacks), during the springtime a big amount of Al goes out from soil creating a glistening, silvery coat on the surface of lakes and ponds [24]. The elevated concentrations of Al in industrial waters can appear due to a side effect of applying Al-based coagulants in treatment processes resulting in a significant increase of Al concentration in the treated water [3].

2.3 Al Water Chemistry

The behaviour of aluminum in the aqueous environment depends upon its coordination chemistry and the characteristics of the local environment, especially pH [21]. Within the aqueous phase, Al may be associated with a variety of inorganic and organic complexes [22]. Investigation of Al speciation in aqueous solutions is important due to several reasons. Firstly, the toxicity of Al depends primarily on its chemical forms. Secondly, some monomeric inorganic complexes may interfere with analytical techniques to

determine Al concentration. Thirdly, the hydrolysis products of Al are believed to be important in mineral phase formation and transportation, in the mobility of Al in soils and aquatic systems, and in the toxicity of Al to plants and aquatic organisms [20,25].

The chemistry of Al in aqueous solution can be characterized by following properties [22,25–27]:

- it has a strong tendency to hydrolyze in the solution,
- its formation is strongly pH dependent,
- its hydroxide forms are amphoteric,
- its toxicity determines by the chemical form,
- it forms stable soluble complexes with other substances present in the water.

Total Al in water can be divided into three main fractions [13,22]:

- monomeric aluminum organic complexes,
- monomeric inorganic aluminum,
- colloidal, polymeric, and organic complexes.

Monomeric organic aluminum complexes are the ones associated with dissolved organic carbon. Monomeric inorganic aluminum includes aqua aluminum (Al^{3+}) and its hydroxide, fluoride, and sulphate complexes. Polymeric organic complexes form when the number of Al ions in the complexes increases. The fraction of interest of most investigators is monomeric inorganic Al complexes [22,26]. These complexes of Al are dominant forms of the metal present in water bodies and the primary form (> 80%) of it is Al^{3+} [13,20]. Al^{3+} is a small (ionic radius 0.51 Å), highly positive trivalent ion surrounded by six water molecules in an octahedral configuration. The chemical formula can be represented as $Al(H_2O)_6^{3+}$ [22]. Because of the high positive charge of Al^{3+} these water molecules form a tightly bound primary hydration shell giving a rise to the several

hydrolytic species, which are formed in accordance with the equilibrium constants [22]. This process is known as a hydrolysis and the resulting hydrolytic Al species are called hydrolysis products. At any pH above 3.5–4.0 various combinations of Al with hydroxide ions occur [26].

2.3.1 Al Hydrolysis in Aqueous Solution

The hydrolysis of Al ion is the progressive loss of hydration shell protons to water molecules in the surrounding bulk solution to maintain dissociation equilibrium. Aluminum hydrolysis reactions formed in accordance with the Al hydrolysis constants data pβ at constant temperature (25 °C) and zero ion strength are presented as follows [22]:

the first hydrolysis reaction,

$$Al(H_2O)_6^{3+} + H_2O = Al(H_2O)_5OH^{2+} + H_3O^+ \qquad \text{p}\beta = 5.5 \qquad (2.1)$$

the reaction can be abbreviated to the more common expression,

$$Al^{3+} + H_2O = Al(OH)^{2+} + H^+ \qquad \text{p}\beta = 5.5 \qquad (2.2)$$

second hydrolysis reaction,

$$Al^{3+} + 2H_2O = Al(OH)_2^+ + 2H^+ \qquad \text{p}\beta = 10.5 \qquad (2.3)$$

third hydrolysis reaction,

$$Al^{3+} + 3H_2O = Al(OH)_3^0 + 3H^+ \qquad \text{p}\beta = 17.3 \qquad (2.4)$$

fourth hydrolysis reaction,

$$Al^{3+} + 4H_2O = Al(OH)_4^- + 4H^+ \qquad \text{p}\beta = 23.5 \qquad (2.5)$$

2.3.2 pH Dependence

Al is most soluble in strongly acidic environments such as volcanic areas and in strongly alkaline environments including alkaline lakes or groundwater. Amorphous aluminum hydroxide $Al(OH)_3^0$ is amphoteric [27]. It dissolves in acidic solutions as a cationic mono- or dihydroxo complex or in the alkaline solution having excess of hydroxo-ions as aluminate anion. Positively charged soluble Al^{3+}, $Al(OH)^{2+}$, and $Al(OH)_2^+$ are most abundant below pH 5.0. At pH below 3.0, Al^{3+} is the dominant species in the solution. Insoluble aluminum hydroxide $Al(OH)_3^0$ is the predominant form in the pH range 5.2–8.0 (T = 25 °C). In the alkaline conditions pH above 8.0, soluble aluminate anion $Al(OH)_4^-$ is a dominating species and it is the only species present above pH 10.0 (T = 25 °C) [19–21,27].

Dissolution of aluminum hydroxide under different pH values are presented as follows:

$$Al(OH)_3^0 \leftrightarrow Al^{3+} + 3OH^- \quad (2.6)$$

$$Al(OH)_3^0 \leftrightarrow Al(OH)^{2+} + 2OH^- \quad (2.7)$$

$$Al(OH)_3^0 \leftrightarrow Al(OH)_2^+ + OH^- \quad (2.8)$$

$$Al(OH)_3^0 + OH^- \leftrightarrow Al(OH)_4^- \quad (2.9)$$

$Al(OH)_3^0$ is mainly insoluble in the pH range of 6.5 to 7.5 depending on the temperature of the system. The solubility is enhanced under acidic conditions and alkaline conditions pH < 6.0 and pH > 8.0, respectively [13,27]. The most toxic forms of Al are soluble Al^{3+} and hydrated monomers $Al(OH)^{2+}$ and $Al(OH)_2^+$ which occur in acidic water conditions [20,22]. These forms represent a greater danger to living organisms rather than organic complexes of Al. Conditions for Al adsorption from aqueous solution are best at pH around 4.0 where the most toxic aluminum species Al^{3+}, $Al(OH)^{2+}$, and $Al(OH)_2^+$ are presented [27].

2.4 Accepted Guidelines for Al Concentration in Water

According to the World Health Organization (WHO) and the council of the European Union (EU) the recommended value for Al in water of 0.20 mg L^{-1} was established in 1984 and 1998, respectively [28,29]. The U.S. Environmental Protection Agency (USEPA) announced the drinking water contaminant candidate list in 1998 where Al was included due to the recognition of a potential link between Al and adverse neurological effects [30]. The recommended secondary drinking water standard of Al concentration is 0.05–0.20 mg L^{-1} in accordance with USEPA [8]. There is no health-based guideline provided for Al by Health Canada. However, it is recommended that the water treatment plants using Al-based coagulants optimize their operational conditions to decrease residual Al concentration in the treated water to the lowest extent possible according to the Guidelines for Canadian Drinking Water Quality. The operational guidance value of < 0.10 mg L^{-1} is established for conventional treatment plants using Al-based coagulants, for other types of treatment systems using such coagulants, the operational guidance value is < 0.20 mg L^{-1} [31].

According to a recent WHO global overview of national regulations and standards for drinking-water quality, out of 97 countries and territories specifying a value for Al, 84 of them set a value of 0.20 mg L^{-1} [32].

2.5 Negative Health Effect

Food and drinking water are among the main sources of Al exposure to human [1]. Al interferes with numerous essential metals and metalloids in the human organism by altering their bioavailability [27]. Adverse effects of Al are currently known to be far more chronic than acute [33]. Aluminum accumulation can cause neurotoxicity leading to the increased risk of neurological disorders such as dementia [5]. In 1973, after the first report of elevated concentration of Al in the brains of patients with Alzheimer's disease was published, an increased number of epidemiological studies on Al in drinking water and Alzheimer's disease has been observed [5,34]. Alzheimer's disease accounts for

more than 60% of dementia cases and is the fourth cause of mortality in the elderly [4]. Epidemiological studies performed in several countries have reported the presence of an association between Al in drinking water and Alzheimer's disease [4,35,36]. The recent research showed the elevated Al concentrations in drinking water correlate with the increased incidence of neurological disorders [6,7,37]. Moreover, low Al levels can lead to behavioural and morphological changes associated with Alzheimer's disease and age-related neurodegeneration as the recent research indicated [38].

2.6 High Al Level in Water Bodies Worldwide

The problem of high Al concentrations presented in natural water sources and wastewater has a worldwide scale and in most cases is recognized as a serious health concern. Table 2.1 specifies just several locations where prohibitive Al concentrations exceeding the drinking water guidelines of 0.20 mg L^{-1} (sometimes up to more than 30–78 times) were observed in raw and/or treated water sources. The natural processes such as Al leaching from minerals, the application of aluminum-containing coagulants like aluminum sulphate (alum), and anthropogenic influence are within the main reasons responsible for elevated Al concentrations in the water bodies. The high Al level in the freshwater resources has been recognized as a serious health issue in several countries (Table 2.1). The data from Table 2.1 show that in most cases, the prohibitive concentrations of Al have been observed in both acidic and alkaline surface and ground waters. For example, a study on the water quality assessment conducted in Iquitos, Peru showed that the groundwater having dissolved Al concentrations of up to 3.33 mg L^{-1} is acidic [39]. The outcomes of water quality assessment led in China defined Al as one of the dominant contaminants in the analyzed groundwater where Al concentrations were almost up to 25 times higher than the local drinking water guidelines [40]. Al concentrations in the surface water of Sehwan Sharif, Pakistan significantly exceeds the drinking water guidelines reaching up to 4.27 mg L^{-1} with a mean value of 2.1 mg L^{-1} under alkaline conditions [41]. Studies on the assessment of groundwater recourses conducted in Cacheu and Oio regions, Guinea Bissau revealed that maximum Al concentrations exceeding the guidelines up to 22 times were observed at pH values of 5.8–6.2 [42].

Table 2.1: Elevated Al concentration in water bodies worldwide.

Location	Water type	Al, mg L^{-1}	pH	Water treatment method	Residual Al, mg L^{-1}	Reference
Turkey *) *Biga Peninsula*	Spring water	13.17–15.70	< 4.0	N/D	N/D	[10]
Peru *) *Iquitos*	Groundwater	0.001–3.33	4.2–5.5	N/D	N/D	[39]
Guinea Bissau *Cacheu, Oio*	Groundwater	0.13–4.48	5.0–7.3	N/D	N/D	[42]
India *) *Ghaziabad*	Groundwater	1.33–6.30	6.1–7.7	N/D	N/D	[43]
Poland *) *Poznan*	Groundwater	0.001–0.75	6.2–8.1	N/D	N/D	[11]
Russia *) *Kola Peninsula*	Groundwater	0.19–1.81	8.7–9.6	UV disinfection	0.19–1.81	[44]
China	Groundwater	0.001–4.92	N/D	N/D	N/D	[40]
Canada *Sudbury*	Surface water	0.15–1.15	4.3–7.0	Liming	N/D	[45]
Spain *Galicia*	Surface water	N/D	5.3–7.4	Coagulation: Alum	0.008–0.65	[46]
Pakistan *) *Sehwan Sharif*	Surface water	0.91–4.27	7.4–8.9	N/D	N/D	[41]
Canada *Toronto*	Surface water	0.001–0.12	N/D	Coagulation: Alum	0.05–0.29	[3]
Canada *Windsor*	Surface water	0.03–2.50	N/D	Coagulation: Alum	0.001–5.10	[3]
United States *California, Nevada*	Surface water	N/D	N/D	Coagulation: Alum	0.001–1.12	[47]
United Kingdom *Nottinghamshire*	Wastewater	0.05–0.18	7.3	Coagulation: Alum	0.001–1.00	[48]
Russia *Angarsk*	Wastewater	N/D	N/D	N/D	(5.0÷15.0) $\times 10^3$	[49]

*) Water is used for the drinking and household water supply.

It is not seldom when high exceeding guidelines Al concentrations are found in the wastewater effluents. The potential source of wastewater contamination with Al is the industrial application of aluminum chloride as a catalyst for ethylbenzene production [50]. The drastically elevated concentrations of Al (5.0÷15.0) × 10^3 mg L^{-1} due to the use of aluminum chloride as a catalyst in the alkylation technology were reported in the wastewater effluent of polymer plant, Angarsk, Russia [49].

According to the Table 2.1 the water treatment using alum as a coagulant can lead to the increased residual Al concentrations in the treated water. Studies led in the United Kingdom revealed Al concentration in wastewater effluent treated by alum as high as 1.0 mg L^{-1} [48]. The Al concentration in the treated water of Lake Ontario (Toronto, Canada) and Detroit River (Windsor, Canada) increased more than twice compared to the Al concentration observed in raw water. Al concentrations in these surface water sources changed from 0.12 to 0.29 mg L^{-1} and from 2.50 to 5.10 mg L^{-1}, respectively [3].

Elevated Al concentration in the groundwater of Miocene (Poznan, Poland) and Khibiny alkaline massif (Kola Peninsula, Russia) aquifers are the examples of serious health concerns when the groundwater is used for the local household water supply [11,44]. For example, the groundwater deposit located in the southern part of the Khibiny alkaline massif which belongs to the Baltic hydrogeological massif (Kola Peninsula) over the past three decades became one of the essential sources of household water supply in the area. The groundwater of this deposit has strong alkaline conditions (pH mean value 9.56) and elevated Al concentrations that are 4–9 higher than the acceptable drinking water guideline.

2.7 Methods Removing Heavy Metals and Aluminum from Water

Studies on metal removal from water are mainly focused on heavy metals including Cd, Cr, Cu, Fe, Hg, Ni, Pb, and Zn. Numerous chemical and physico-chemical methods were

proposed for metal removal from aqueous solutions including but not limited to chemical precipitation, ion exchange, adsorption, membrane processes, electrochemical methods [51,52]. Among the most widely used water treatment methods, coagulation/precipitation, lime softening, ion exchange (cation resin), electrodialysis, reverse osmosis, and adsorption are within the most suitable for the removal of Al from aqueous solution [12,13,53,54]. Some of these methods such as ion exchange and reverse osmosis are expensive and likely to be impractical for the industrial application in low-income countries with high demand for safe household water [51].

2.7.1 Chemical Precipitation

Chemical precipitation is an effective and one of the most widely used process in water and wastewater treatment industries having advantages such as low-cost and ease of operation. The process can be combined with other water treatment methods including ion exchange, coagulation, filtration. In precipitation processes, chemicals react with metals ions forming insoluble precipitates which further separated from water by sedimentation or filtration. The conventional chemical precipitation processes include hydroxide and sulphate precipitations [55]. The application of chemical precipitation for the removal of metal cations such as Zn^{2+}, Cu^{2+}, Pb^{2+} showed a removal efficiency reaching up to more than 95% [56]. Although widely used, the application of chemical precipitation has some weaknesses including the generation of large amount of precipitated waste and extra operational cost for its disposal and possible formation of colloidal precipitates that can cause some separation problems in either settling or filtration processes. In addition, the process is not suitable for the removal of low metal ion concentrations and amphoteric metals hydroxides such for example as $Al(OH)_3$ [55,57].

2.7.2 Ion Exchange

Ion exchange processes for metals removal from water are beneficial due to high removal efficiency and fast kinetics. The main advantages of ion exchange over chemical precipitation are selectivity and low waste generation [55]. In the ion exchange process, ions accumulated on the surface of ion exchange resin are exchanged for the metal ions having similar charge. Among materials used in ion exchange processes, synthetic resins are commonly preferred as they are effective to remove metal ions from aqueous solution [58]. For example, a complete removal of Co^{2+}, Ni^{2+}, and Cr^{3+} was obtained using cation-exchange resin [59]. The application of cation-exchange resin for the Al removal reached the efficiency of more than 90% [13]. Periodic acid treatment is necessary to exchange accumulated Al off the resin due to high resin affinity for Al making self-regenerating cation-exchange systems impractical for the residential use [13]. Despite the effectiveness of ion exchange application, the treatment of large amount of water having low metal concentration can be expensive, moreover the regeneration of exhausted ion exchange resins by chemical reagents can cause serious secondary pollution [55].

2.7.3 Coagulation and Flocculation

Coagulation and flocculation in a conjunction with sedimentation and filtration is a commonly used water treatment approach for the metal removal. Coagulation involves the addition of coagulants to the aqueous solution to destabilize colloids by neutralizing the forces that keep them apart, flocculation forms the agglomerates (flocs) of destabilized particles that can further be removed or separated by filtration [55]. Various coagulants including ferric chloride, ferrous sulphate, aluminum sulphate (alum) are widely used showing a high efficiency toward metal removal. For example, tungsten removal reached up to 99% using ferric chloride as a coagulant in the treatment process [60]. The application of Al-containing coagulants may either increase or decrease Al concentration in the treated water depending on its speciation in the source water and water treatment conditions [3,13]. In most cases, the application of alum leads to a rise of Al concentrations in the treated water [46,48]. Additionally, it is difficult to control the

coagulant species formed when Al-based salts are used. Generally, the application of coagulation and flocculation is not sufficient for metals removal and must be combined with other treatment techniques such as precipitation, filtration [55].

2.7.4 Membrane Filtration

The membrane processes including reverse osmosis, nanofiltration, electrodialysis, and ultrafiltration are promising toward metal removal from water and wastewater. Membrane processes rely on a membrane defined as a phase that acts as a barrier between other phases to remove contaminants from water [61]. The application of these processes is advantageous as it is easy to operate, they are space-saver, and high metal removal efficiency can be archived [55]. Both electrodialysis and reverse osmosis showed an excellent Al removal reaching more than 90% [13]. A study on the application of nanofiltration for Al removal from coagulant effluent water obtained nearly 100% removal [53]. The application of reverse osmosis successfully removed other metals such as Ca^{2+} and Ni^{2+} ions where 99.5% removal was achieved [62]. It has been reported that the semi-permeable membrane used in reverse osmosis for removing metal ions lowers the pH of water making it acidic [63]. The high cost, process complexity, and membrane fouling limited the application of membrane processes for the metal removal from aqueous solution [55].

2.7.5 Adsorption

Among available water treatment technologies adsorption is considered as a suitable method for the removal of various toxic pollutants including heavy metals and organic chemicals from aqueous solutions [64]. The adsorption process offers numerous advantages including cost-effectiveness, flexibility in design and operation, wide variety of adsorbents available, effective removal of metal ions even in low concentrations. A recent review on the adsorption of heavy metals by clay minerals showed that these minerals have an excellent feasibility in removing different toxic aquatic metal pollutants

[14]. The use of metal oxides which have a favourable sorption to metals in terms of high capacity and selectivity has also been widely investigated [65].

The adsorption process is described as a mass transfer process by which a substance is transferred from the liquid phase to the surface of a solid (adsorbent) and becomes bound by physical and/or chemical interactions [57]. Depending on the value of the adsorption enthalpy, adsorption can be characterized as chemical adsorption (chemisorption) or physical adsorption (physisorption) (Figure 2.1a,b). Chemisorption is carried out by the chemical interaction of molecules of the adsorbent and adsorbate, whereas physisorption is driven by the van der Waals forces (dipole-dipole interactions, dispersion forces, induction forces). The accumulation of adsorbate on the surface of adsorbent can form a monolayer or multilayer coverage (Figure 2.1c,d).

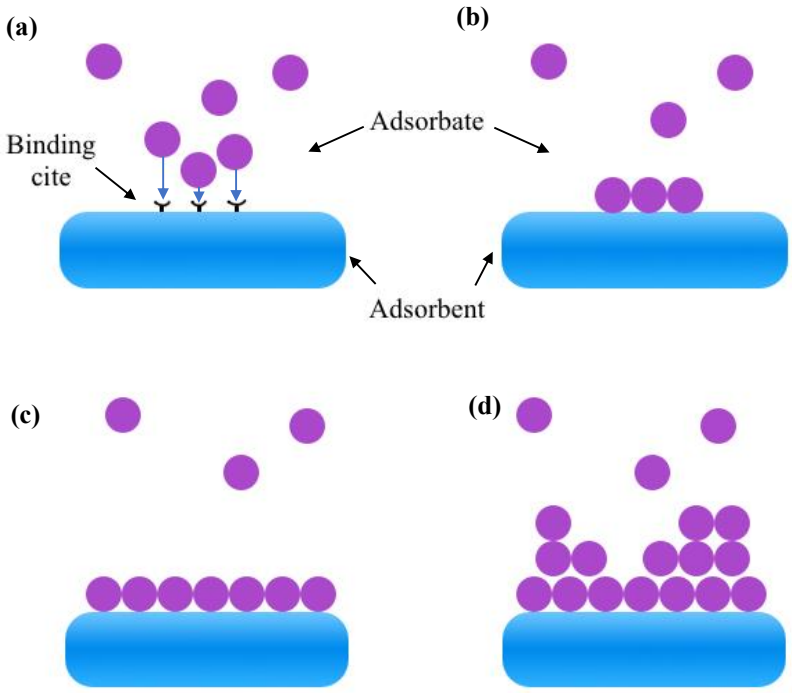

Figure 2.1: Adsorption in aqueous solution: chemisorption (a), physisorption (b), monolayer coverage (c), multilayer coverage (d).

Mathematically adsorption process can be described by using kinetic and isotherm models [66]. The physico-chemical parameters of kinetic and isotherm models along with the underlying thermodynamic assumptions provide an insight into the adsorption mechanism, surface properties, and the degree of affinity of the adsorbents [67]. Among various isotherm models describing adsorption process in aqueous phase such as Sips model [68], Toth model, the Brunauer-Emmett-Teller (BET) model, the Dubinin-Radushkevich model [67] – Freundlich [69] and Langmuir [70] are the most commonly used isotherm models.

Langmuir isotherm refers to the homogeneous adsorption assuming a monolayer adsorbent surface coverage. Freundlich isotherm widely applied in heterogeneous systems describes a multilayer adsorption process [67]. The choice of experimental variables to obtain laboratory equilibrium adsorption data narrows generally down to the following two: adsorbate concentration and adsorbent dose where either one or both can be varied [71]. In the study of adsorption kinetics, two kinetic reaction models – the pseudo-first order and pseudo-second order adsorption kinetic models, the Elovich or Roginsky-Zeldovich models, and the intraparticle diffusion model are commonly used to describe the intrinsic kinetic adsorption constant mathematically [66,72]. The application of nonlinear optimization techniques such as nonlinear regression instead of the linear methods are recommended for an accurate estimation of the adsorption kinetic and isotherm models parameters [66].

2.8 The Application of Adsorption for Al Removal

According to the literature survey metals removal by means of adsorption was found to be the method of choice [51,73]. The general tendency is to find cost-effective adsorbents which remove metals from aqueous solutions effectively. The data from Table 2.2 show that mainly organic or having organic components sorbents are capable for Al removal from water most of which were previously investigated. Various materials including activated carbon and its modified forms [12,15,33,74,75], (bio)polymers (poly(γ-glutamic acid), ionic imprinted polymer IIP-PEI/SiO_2, polyacrylonitrile (PAN) beads) [2,54,76],

alizarin yellow-attached magnetic poly(2-hydroxyethyl methacrylate) (mPHEMA) beads [77], silica gel grafted with polymer containing a functional monomer for metal chelating [78], char [18,75], marble wastes [17], natural zeolite [16], marine alga (*Cystoseira Baccata, Sargassurn fluitans*) [79,80], powder and ash of leaves (*Achiranthus Aspera*) [81], fluted pumpkin (*Telfairia Occidentalis*) waste biomass [82], aluminosilicate clay minerals (montmorillonite, kaolinite, vermiculite) [83], clay and starch [84] showed their effectiveness toward Al removal from aqueous solution (Table 2.2). The outcomes of literature sources on Al adsorption can be briefly summarized as follows:

- adsorption can be an effective method, various materials are capable to remove up to 95–98% of Al concentration from water,
- the efficiency of Al adsorption in most cases is strongly pH dependent and the sorbent choice is based on the treated water characteristics,
- at the optimal solution pH the adsorption equilibrium is reached within 0.5–360 min and in most cases 60 min or less depending on the initial Al concentration and sorbent dose is sufficient to reach the equilibrium,
- the variation in the results of Al removal can be attributed to the different nature of each sorbent,
- a very limited number of investigations on the process of Al adsorption from strong alkaline solutions ($pH \geq 8.0$) has been studied,
- the limited number of studies investigating the effect of ions usually present in natural water bodies on the removal of Al by adsorption has been carried out.

Table 2.2: Comparison of sorption performance of various materials under optimal experimental conditions for Al removal from aqueous solutions.

	Sorbent	pH	Temperature, °C	Sorbent dose, g L^{-1}	Initial Al concentration, mg L^{-1}	Equilibrium/contact time, min	Al removal, %	Effect of ions study	References
1.	Date-pit activated carbon	4.0	22	2.0	5.0	1440 **)	52 *)	–	[33]
					50.0	1440 **)	18 *)		
2.	BDH activated carbon	4.0	22	2.0	5.0	1440 **)	53 *)	–	[33]
					50.0	1440 **)	18 *)		
3.	Activated carbon	4.0	N/D	20.0	3.0	5	95 *)	–	[74]
4.	Beach cast seaweed	4.0	23	2.5	10.0	30 **)	80	–	[79]
					100.0	30 **)	80		
5.	Biopolymer	4.0	37	0.6	10.0	1 **)	81	+	[2]
					50.0	1 **)	96		
6.	Marine algae	4.0	N/D	1.0	N/D	600	80	–	[80]
7.	Aluminosilicate clay minerals	4.0	25	N/D	N/D	0.5	N/D	–	[83]
8.	Rice husk char	4.2	30	2.0	3.0	120	98	–	[75]
9.	Magnetic activated carbon/tungsten nanocomposite	5.0	24	0.3	10.0	45	90	+	[12]
10.	Fluted pumpkin waste	5.0	24	5.0	10	120	95 *)	–	[82]
11.	Surface imprinted polymer	5.0	25	2.0	N/D	30	N/D	–	[76]

Table 2.2. ***Continuation.***

12. mPHEMA beads	5.0	25	2.0	100.0	60	98	+	[77]
13. PAN-based adsorbent	5.6	20	N/D	1.0	1440	>99	–	[54]
14. Silica gel grafted with polymer	6.0	20	1.0	0.5	80	92	+	[78]
15. Powder of leaves	6.0	N/D	2.5	50.0	60	>99	+	[81]
16. Ash of leaves	6.0	N/D	2.0	50.0	30	>99	+	[81]
17. Natural zeolite	6.0	30	2.0	1.6	60	66	–	[16]
				40.0		85		
18. Clay	6.5	30	0.25	100.0	90	90	–	[84]
19. Starch	6.5	30	0.25	100.0	90	90	–	[84]
20. Powdered marble wastes	7.0	25	0.1	1.0, 3.0	5	>99	+	[17]
				4.0, 8.0	25	>99		
21. Refuse derived char	8.0	23	2.0	100.0	120	93	–	[18]
22. Granular activated carbon with $FeCl_3$	8.0	20	5.0	2.15	360	83 *)	–	[15]
				10.3	360	92 *)		

*) Al removal % calculated using the data reported in journal articles.

**) Contact time.

N/D: not detected.

Presence (+) or absence (−) of the ions tests results.

pH scale: acidic, neutral, alkaline solution.

The data of Table 2.2 show that a limited number of inorganic adsorbents applied to Al removal from aqueous solution was previously studied and most of investigations was performed in the acidic pH range. The recent study on the adsorption of metal cations Cd^{2+}, Cu^{2+}, and Pb^{2+} from water onto vermiculite concrete and aerated autoclaved light concrete (aerocrete) modified with iron oxyhydroxide showed an effective metal removal [85]. The cost of vermiculite concrete and aerocrete vary within US $6–11 per $tonne^{-1}$ making it economically feasible [85]. In recent years, the number of application of titanium dioxide (TiO_2) as an adsorbent which is relatively cheap, non-toxic, insoluble in water, and stable under operational conditions increases. It has been studied for the removal of toxic aquatic metal pollutants from aqueous solutions and showed a good adsorption performance [86,87]. Among other oxides, silica (SiO_2) has also received a considerable attention, because of the large surface area and the ability to effectively adsorb metal ions from aqueous solutions [88].

The investigation of low-cost and reliable inorganic adsorbents for Al removal from aqueous solution needs further insights. The application of this group of adsorbents can be suitable for the removal of Al from natural water bodies with a potential to increase removal efficiency and reduce the contact time to reach equilibrium, to use low adsorbent doses allowing to decrease Al concentration below the guidelines, and to study the Al adsorption in both acidic and alkaline water solutions.

2.9 References

[1] D. Krewski, R.A. Yokel, E. Nieboer, D. Borchelt, J. Cohen, J. Harry, S. Kacew, J. Lindsay, A.M. Mahfouz, V. Rondeau, Human health risk assessment for aluminium, aluminium oxide, and aluminium hydroxide, J. Toxicol. Environ. Heal. Part B. 10:S1 (2007) 1–269. doi:10.1080/10937400701597766.

[2] Y.C. Rajan, B.S. Inbaraj, B.H. Chen, In vitro adsorption of aluminum by an Edible Biopolymer Poly(γ-glutamic acid), J. Agric. Food Chem. 62 (2014) 4803–4811. doi:10.1021/jf5011484.

[3] P.F. Henshaw, J.K. Bewtra, N. Biswas, Occurrence of aluminum, lead, and trihalomethanes in drinking water from the Great Lakes, J. Great Lakes Res. 19 (1993) 521–532. doi:10.1016/S0380-1330(93)71238-1.

[4] E. Gauthier, I. Fortier, F. Courchesne, P. Pepin, J. Mortimer, D. Gauvreau, Aluminum forms in drinking water and risk of Alzheimer's disease, Environ. Res. 84 (2000) 234–246. doi:10.1006/enrs.2000.4101.

[5] T.P. Flaten, Aluminium as a risk factor in Alzheimer's disease, with emphasis on drinking water, Brain Res. Bull. 55 (2001) 187–196.

[6] Z. Wang, X. Wei, J. Yang, J. Suo, J. Chen, X. Liu, X. Zhao, Chronic exposure to aluminum and risk of Alzheimer's disease: a meta-analysis, Neurosci. Lett. 610 (2016) 200–206. doi:10.1016/j.neulet.2015.11.014.

[7] J. Nie, Neurotoxicity of Aluminum, in: Q. Niu (Ed.), Adv. Exp. Med. Biol., Springer, Singapore, 2018: pp. 99–111. doi:10.1007/978-981-13-1370-7_6.

[8] U.S. Environmental Protection Agency (USEPA), 2018 Edition of the Drinking Water Standards and Health Advisories Tables, Washington, DC, 2018. https://www.epa.gov/sites/production/files/2018-03/documents/dwtable2018.pdf.

[9] C.T. Driscoll, W.D. Schecher, The chemistry of aluminum in the environment, Environ. Geochem. Health. 12 (1990) 28–49. doi:10.1007/BF01734046.

[10] C. Bakar, H.I.Ö. Karaman, A. Baba, F. Şengünalp, Effect of high aluminum concentration in water resources on human health, case study: Biga Peninsula, northwest part of Turkey, Arch. Environ. Contam. Toxicol. 58 (2010) 935–944. doi:10.1007/s00244-009-9435-3.

[11] M. Frankowski, A. Zioła-Frankowska, I. Kurzyca, K. Novotný, T. Vaculovič, V. Kanický, M. Siepak, J. Siepak, Determination of aluminium in groundwater samples by GF-AAS, ICP-AES, ICP-MS and modelling of inorganic aluminium complexes, Environ. Monit. Assess. 182 (2011) 71–84. doi:10.1007/s10661-010-1859-8.

[12] A. Saleh, M. Tuzen, A. Sarı, Magnetic activated carbon loaded with tungsten oxide nanoparticles for aluminum removal from waters, J. Environ. Chem. Eng. 5 (2017) 2853–2860. doi:10.1016/j.jece.2017.05.038.

[13] P.T. Srinivasan, T. Viraraghavan, K.S. Subramanian, Aluminium in drinking water: an overview, Water SA. 25 (1999) 47–55.

[14] M.K. Uddin, A review on the adsorption of heavy metals by clay minerals, with special focus on the past decade, Chem. Eng. J. 308 (2017) 438–462. doi:10.1016/j.cej.2016.09.029.

[15] M. Mahdavi, A. Ebrahimi, A.H. Mahvi, A. Fatehizadeh, F. Karakani, H. Azarpira, Experimental data for aluminum removal from aqueous solution by raw and iron-modified granular activated carbon, Data Br. 17 (2018) 731–738. doi:10.1016/j.dib.2018.01.063.

[16] A.M. Abdullah, Aluminum pollution removal from water using a natural zeolite, J. Pollut. Eff. Control. 2 (2014) 1–4. doi:10.4172/2375-4397.1000120.

[17] S.E. Ghazy, S.E. Samra, A.M. Mahdy, S.M. El-Morsey, Kinetic investigation of the removal of aluminum from water samples by adsorption onto powdered marble wastes, Sep. Sci. Technol. 40 (2005) 1797–1815. doi:10.1081/SS-200064573.

[18] C. Nobre, M. Gonçalves, D. Resende, C. Vilarinho, B. Mendes, Removal of Chromium and Aluminum from Aqueous Solutions Using Refuse Derived Char, in: L. Camarinha-Matos, A.J. Falcão, N. Vafaei, S. Najdi (Eds.), Technol. Innov. Cyber-Physical Syst., Springer International Publishing, Costa de Caparica, 2016: pp. 515–522. doi:DOI: 10.1007/978-3-319-31165-4_48.

[19] R.W. Gensemer, R.C. Playle, The bioavailability and toxicity of aluminum in aquatic environments, Crit. Rev. Environ. Sci. Technol. 29 (1999) 315–450. doi:10.1080/10643389991259245.

[20] A.S. Cardwell, W.J. Adams, R.W. Gensemer, E. Nordheim, R.C. Santore, A.C. Ryan, W.A. Stubblefield, Chronic toxicity of aluminum, at a pH of 6, to freshwater

organisms: empirical data for the development of international regulatory standards/criteria, Environ. Toxicol. Chem. 37 (2018) 36–48. doi:10.1002/etc.3901.

[21] Agency for Toxic Substances and Disease Registry (ATSDR), Toxicological Profile for Aluminum, Atlanta, GA, 2008.

[22] G. Sposito, The Environmental Chemistry of Aluminum, 2nd edition, Lewis Publishers, Boca Raton, FL, 1996.

[23] World Health Organization (WHO), Aluminium in Drinking-water, Geneva, 2010. https://www.who.int/water_sanitation_health/water-quality/guidelines/chemicals/aluminium.pdf.

[24] T. Pawlick, A killing rain. The global threat of acid precipitation, Sierra Club Books, San Francisco, CA, 1984.

[25] J. Ščančar, R. Milačič, Aluminium speciation in environmental samples: a review, Anal. Bioanal. Chem. 386 (2006) 999–1012. doi:10.1007/s00216-006-0422-5.

[26] J.D. Hem, C.E. Roberson, Form and Stability of Aluminum Hydroxide Complexes in Dilute Solution, United States goverment printing office, Washington, 1967.

[27] J. Namiésnik, A. Rabajczyk, The speciation of aluminum in environmental samples, Crit. Rev. Anal. Chem. 40 (2010) 68–88. doi:10.1080/10408340903153234.

[28] World Health Organization (WHO), Guidelines for Drinking-water Quality, Geneva, 1984. http://www.who.int/water_sanitation_health/publications/gdwq1-vol1/en/.

[29] The Council of the European Union, Council Directive 98/83/EC of 3 November 1998 on the Quality of Water Intended for Human Consumption, 1998. https://eur-lex.europa.eu/legal-content/EN/TXT/PDF/?uri=CELEX:31998L0083&from=EN.

[30] U.S. Environmental Protection Agency (USEPA), Announcment of the Drinking Water Contaminant Candidate List, Washington, 1998.

[31] Federal-Provincial-Territorial Committee on Drinking Water, Guidelines for Canadian Drinking Water Quality, Ottawa, 2017. http://publications.gc.ca/collections/collection_2017/sc-hc/H129-24-2017-eng.pdf.

[32] World Health Organization (WHO), A global overview of national regulations and standards for drinking-water quality, Switzerland, 2018. http://apps.who.int/iris/bitstream/handle/10665/272345/9789241513760-eng.pdf.

[33] S.A. Al-Muhtaseb, M.H. El-Naas, S. Abdallah, Removal of aluminum from aqueous solutions by adsorption on date-pit and BDH activated carbons, J. Hazard. Mater. 158 (2008) 300–307. doi:10.1016/j.jhazmat.2008.01.080.

[34] D.R. Crapper, S.S. Krishnan, A.J. Dalton, Brain aluminum distribution in Alzheimer's disease and experimental neurofibrillary degeneration, Science. 180 (1973) 511–513.

[35] V. Rondeau, D. Commenges, H. Jacqmin-Gadda, J.F. Dartigues, Relation between aluminum concentrations in drinking water and Alzheimer's disease: an 8-year follow-up study, Am. J. Epidemiol. 152 (2000) 59–66. doi:10.1093/aje/152.1.59.

[36] C.N. Martyn, C. Osmond, J.A. Edwardson, D.J. Barker, E.C. Harris, R.F. Lacey, Geographical relation between Alzheimer's disease and aluminum in drinking water, Lancet. 1 (1989) 59–62.

[37] L. Xu, W. Zhang, X. Liu, C. Zhang, P. Wang, X. Zhao, Circulatory levels of toxic metals (aluminum, cadmium, mercury, lead) in patients with Alzheimer's disease: a quantitative meta-analysis and systematic review, J. Alzheimer's Dis. 62 (2018) 361–372.

[38] S.C. Bondy, Low levels of aluminum can lead to behavioral and morphological changes associated with Alzheimer's disease and age-related neurodegeneration, Neurotoxicology. 52 (2016) 222–229. doi:10.1016/j.neuro.2015.12.002.

[39] C.M.C. de Meyer, J.M. Rodríguez, E.A. Carpio, P.A. García, C. Stengel, M. Berg, Arsenic, manganese and aluminum contamination in groundwater resources of Western Amazonia (Peru), Sci. Total Environ. 607–608 (2017) 1437–1450. doi:10.1016/j.scitotenv.2017.07.059.

[40] J. Wang, Statistical study on distribution of multiple dissolved elements and a water quality assessment around a simulated stackable fly ash, Ecotoxicol. Environ. Saf. 159 (2018) 46–55. doi:10.1016/j.ecoenv.2018.04.057.

[41] T.G. Kazi, M.B. Arain, M.K. Jamali, N. Jalbani, H.I. Afridi, R.A. Sarfraz, J.A. Baig, A.Q. Shah, Assessment of water quality of polluted lake using multivariate statistical techniques: a case study, Ecotoxicol. Environ. Saf. 72 (2009) 301–309. doi:10.1016/j.ecoenv.2008.02.024.

[42] M. Ferrante, S.S. Signorelli, L.S. Ferlito, A. Grasso, A. Dimartino, C. Copat, Groundwater-based water wells characterization from Guinea Bissau (Western Africa): a risk evaluation for the local population, Sci. Total Environ. 619–620 (2018) 916–926. doi:10.1016/j.scitotenv.2017.11.176.

[43] S. Kumari, A.K. Singh, A.K. Verma, N.P.S. Yaduvanshi, Assessment and spatial distribution of groundwater quality in industrial areas of Ghaziabad, India, Env. Monit Assess. 186 (2014) 501–514. doi:10.1007/s10661-013-3393-y.

[44] D. Popugaeva, K. Kreyman, A.K. Ray, Study of aluminium in groundwater using chemometric methods, Environ. Technol. (2018). doi:10.1080/09593330.2018.1544667.

[45] W.A. Scheider, B. Cave, J. Jones, Reclamation of Acidified Lakes near Sudbury Ontario by Neutralization and Fertilization, Rexdale, ON, 1975.

[46] D.A. Rubinos, M. Arias, C. Aymerich, F. Diaz-Fierros, Aluminum contents in drinking water from public water supplies of Galicia (Northwest Spain), in: Water Celt. Ctries. Quant. Qual. Clim. Var. Fourth Inter-Celtic Colloq. Hydrol. Manag. Water Resour., IAHS Press, Guimarães, 2005: pp. 113–119.

[47] G. V Alexeeff, A.M. Fan, Public Health Goal for Aluminum in Drinking Water, California Environmental Protection Agency, CA, 2001.

[48] S.D.W. Comber, M.J. Gardner, J. Churchley, Aluminium speciation: implications of wastewater effluent dosing on river water quality, Chem. Speciat. Bioavailab. 17 (2005) 117–128. doi:10.3184/095422905782774874.

[49] E.S. Khlebnikova, Intensification of the process obtaining ethylbenzene in a reactor unit with a preliminary mixing of reagents, Tomsk Polytechnic University, 2018.

[50] I.O. Dolganova, N.S. Belinskaya, E.N. Ivashkina, V.V. Martemyanova, E.V. Tkachev, Improving the efficiency of technology producing ethylbenzene by using mathematical modeling, Fundam. Res. 8 (2013) 595–600. http://www.fundamental-research.ru/ru/article/view?id=31964.

[51] S. Chowdhury, M.A.J. Mazumder, O. Al-attas, T. Husain, Heavy metals in drinking water: occurrences, implications, and future needs in developing countries, Sci. Total Environ. 569–570 (2016) 476–488. doi:10.1016/j.scitotenv.2016.06.166.

[52] L. Lin, X. Xu, C. Papelis, T.Y. Cath, P. Xu, Sorption of metals and metalloids from reverse osmosis concentrate on drinking water treatment solids, Sep. Purif. Technol. 134 (2014) 37–45. doi:10.1016/j.seppur.2014.07.008.

[53] W. Wang, H. Yang, H. Zhao, Z. Jiang, Transfer and transport of aluminum in filtration unit, J. Environ. Sci. 19 (2007) 897–901. doi:https://doi.org/10.1016/S1001-0742(07)60149-1.

[54] Z. Aly, A. Graulet, N. Scales, T. Hanley, Removal of aluminium from aqueous solutions using PAN-based adsorbents: characterisation, kinetics, equilibrium and thermodynamic studies, Environ. Sci. Pollut. Res. 21 (2014) 3972–3986. doi:10.1007/s11356-013-2305-6.

[55] F. Fu, Q. Wang, Removal of heavy metal ions from wastewaters: a review, J.

Environ. Manage. 92 (2011) 407–418. doi:10.1016/j.jenvman.2010.11.011.

[56] M.T. Alvarez, C. Crespo, B. Mattiasson, Precipitation of Zn(II), Cu(II) and Pb(II) at bench-scale using biogenic hydrogen sulfide from the utilization of volatile fatty acids, Chemosphere. 66 (2007) 1677–1683. doi:10.1016/j.chemosphere.2006.07.065.

[57] M.A. Barakat, New trends in removing heavy metals from industrial wastewater, Arab. J. Chem. 4 (2011) 361–377. doi:10.1016/j.arabjc.2010.07.019.

[58] B. Alyüz, S. Veli, Kinetics and equilibrium studies for the removal of nickel and zinc from aqueous solutions by ion exchange resins, J. Hazard. Mater. 167 (2009) 482–488. doi:10.1016/j.jhazmat.2009.01.006.

[59] S. Kang, J. Lee, S. Moon, K. Kim, Competitive adsorption characteristics of Co2+, Ni2+, and Cr3+ by IRN-77 cation exchange resin in synthesized wastewater, Chemosphere. 56 (2004) 141–147. doi:10.1016/j.chemosphere.2004.02.004.

[60] M. Plattes, A. Bertrand, B. Schmitt, J. Sinner, F. Verstraeten, J. Welfring, Removal of tungsten oxyanions from industrial wastewater by precipitation, coagulation and flocculation processes, J. Hazard. Mater. 148 (2007) 613–615. doi:10.1016/j.jhazmat.2007.03.016.

[61] B. Halling-Sorensen, S.E. Jorgensen, The removal of nitrogen compounds from wastewater, in: Stud. Environ. Sci., Elsevier, New York, 1993: pp. 337–353. doi:https://doi.org/10.1016/S0166-1116(08)70532-6.

[62] M. Mohsen-Nia, P. Montazeri, H. Modarress, Removal of Cu2+ and Ni2+ from wastewater with a chelating agent and reverse osmosis processes, Desalination. 217 (2007) 276–281. doi:10.1016/j.desal.2006.01.043.

[63] M. Bhatia, R. Satish Babu, S.H. Sonawane, P.R. Gorate, A. Girdhar, E.R. Reddy, M. Pola, Application of nanoadsorbents for removal of lead from water, Int. J. Environ. Sci. Technol. 14 (2017) 1135–1154. doi:10.1007/s13762-016-1198-6.

[64] Y. Zhang, C. Zhu, F. Liu, Y. Yuan, H. Wu, A. Li, Effects of ionic strength on removal of toxic pollutants from aqueous media with multifarious adsorbents: a review, Sci. Total Environ. 646 (2019) 265–279. doi:10.1016/j.scitotenv.2018.07.279.

[65] M. Hua, S. Zhang, B. Pan, W. Zhang, L. Lv, Q. Zhang, Heavy metal removal from water/wastewater by nanosized metal oxides: a review, J. Hazard. Mater. 211–212 (2012) 317–331. doi:10.1016/j.jhazmat.2011.10.016.

[66] H.N. Tran, S.-J. You, A. Hosseini-Bandegharaei, H.-P. Chao, Mistakes and inconsistencies regarding adsorption of contaminants from aqueous solutions: a critical review, Water Res. 120 (2017) 88–116. doi:10.1016/j.watres.2017.04.014.

[67] K.Y. Foo, B.H. Hameed, Insights into the modeling of adsorption isotherm systems, Chem. Eng. J. 156 (2010) 2–10. doi:10.1016/j.cej.2009.09.013.

[68] R. Sips, On the structure of a catalyst surface, J. Chem. Phys. 16 (1948) 490–495. doi:10.1063/1.1746922.

[69] H.M.F. Freundlich, Over the adsorption in solution, J. Phys. Chem. 57 (1906) 385–471.

[70] I. Langmuir, The constitution and fundamental properties of solids and liquids. Part I. Solids, J. Am. Chem. Soc. 38 (1916) 2221–2295. doi:10.1021/ja02268a002.

[71] B. Volesky, Biosorption and me, Water Res. 41 (2007) 4017–4029. doi:10.1016/j.watres.2007.05.062.

[72] X. Xie, R. Deng, Y. Pang, Y. Bai, W. Zheng, Y. Zhou, Adsorption of copper(II) by sulfur microparticles, Chem. Eng. J. 314 (2017) 434–442. doi:10.1016/j.cej.2016.11.163.

[73] H.Z. Fu, M.H. Wang, Y.S. Ho, Mapping of drinking water research: a bibliometric analysis of research output during 1992-2011, Sci. Total Environ. 443 (2013) 757–765. doi:10.1016/j.scitotenv.2012.11.061.

[74] P.G. Pour, M.A.L.I. Takassi, T. Hamoule, Removal of aluminum from water and industrial waste water, Orient. J. Chem. 30 (2014) 1365–1369. doi:http://dx.doi.org/10.13005/ojc/300356.

[75] T.S. Singh, B. Parikh, K. Pant, Investigation on the sorption of aluminium in drinking water by low-cost adsorbents, Water SA. 32 (2006) 49–54. doi:http://dx.doi.org/10.4314/wsa.v32i1.5239.

[76] F. An, B. Gao, X. Huang, Y. Zhang, Y. Li, Y. Xu, Z. Zhang, J. Gao, Z. Chen, Selectively removal of Al(III) from Pr(III) and Nd(III) rare earth solution using surface imprinted polymer, React. Funct. Polym. J. 73 (2013) 60–65. doi:10.1016/j.reactfunctpolym.2012.08.022.

[77] A. Denizli, R. Say, E. Piskin, Removal of aluminium by Alizarin Yellow-attached magnetic poly (2-hydroxyethyl methacrylate) beads, React. Funct. Polym. 55 (2003) 99–107.

[78] E. Moniri, H.A. Panahi, Y.G. Mohammadi, H. Gaforian, Removal of aluminum(III) from environmental samples by siliceous support grafted with poly[1-(N,N-bis-carboxymethyl)amino-3- allylglycerol-co-dimethylacrylamide] brushes, Can. J. Chem. Eng. 92 (2014) 1414–1420. doi:10.1002/cjce.22003.

[79] P. Lodeiro, Á. Gudiña, L. Herrero, R. Herrero, M.E. Sastre de Vicente, Aluminium removal from wastewater by refused beach cast seaweed. Equilibrium and dynamic studies, J. Hazard. Mater. 178 (2010) 861–866. doi:10.1016/j.jhazmat.2010.02.017.

[80] H.S. Lee, Biosorption of Cr, Cu and Al by Sargassum biomass, Biotechnol. Bioprocess Eng. 2 (1997) 126–131. doi:https://doi.org/10.1007/BF02932340.

[81] A.A. Kumari, K. Ravindhranath, Removal of aluminium(III) from polluted waters using biosorbents derived from Achiranthus Aspera and Cassia Occidentalis, Int. J. Water Resour. Environ. Sci. 1 (2012) 8–19. doi:10.5829/idosi.ijwres.2012.1.1.1101.

[82] M.J. Horsfall, A. Spiff, Equilibrum sorption study of Al3+, Co2+ and Ag+ in aqueous solutions by fluted pumpkin (Telfairia occidentals HOOK f) waste biomass, Acta Chim. Slov. 52 (2005) 174–181. doi:10.1021/jp5050628.

[83] W.J. Walker, C.S. Cronan, H.H. Patterson, A kinetic study of aluminum adsorption by aluminosilicate clay minerals, Geochim. Cosmochim. Acta. 52 (1988) 55–62. doi:10.1016/0016-7037(88)90056-7.

[84] P.M. Choksi, V.Y. Joshi, Adsorption kinetic study for the removal of nickel(II) and aluminum(III) from an aqueous solution by natural adsorbents, Desalination. 208 (2007) 216–231. doi:10.1016/j.desal.2006.04.081.

[85] D. Martemianov, B. Xie, T. Yurmazova, M. Khaskelberg, F. Wang, C. Wei, S. Preis, Cellular concrete-supported cost-effective adsorbents for aqueous arsenic and heavy metals abatement, J. Environ. Chem. Eng. 5 (2017) 3930–3941. doi:10.1016/j.jece.2017.07.063.

[86] Y.C. Sharma, V. Srivastava, V.K. Singh, S.N. Kaul, C.H. Weng, Nano-adsorbents for the removal of metallic pollutants from water and wastewater, Environ. Technol. 30 (2009) 583–609. doi:10.1080/09593330902838080.

[87] I. Ali, New generation adsorbents for water treatment, Chem. Rev. 112 (2012) 5073–5091. doi:10.1021/cr300133d.

[88] M.E. Mahmoud, I.M.M. Kenawy, M.A.H. Hafez, R.R. Lashein, Removal, preconcentration and determination of trace heavy metal ions in water samples by AAS via chemically modified silica gel N-(1-carboxy-6-hydroxy) benzylidenepropylamine ion exchanger, Desalination. 250 (2010) 62–70. doi:10.1016/j.desal.2009.09.009.

Chapter 3

3 Study of Aluminum in Groundwater using Chemometric Methods

3.1 Introduction

It is enough to point out that Aluminum (Al) is a part of clay composition to understand its wide occurrence in the Earth crust [1,2]. The metal is present in all types of natural water sources and additionally comes to drinking and industrial waters from alum used as a coagulant in water treatment technologies [3,4]. In soil and natural waters, Al ions can form complexes with a series of organic and inorganic ligands. However, the information on speciation of dissolved Al is rather limited. Furthermore, the chemical behaviour of Al species and their ecological and health effect are even less understood [5]. The recommended upper boundary limit of Al concentration in drinking water is 0.20 mg L^{-1} in accordance with the U.S. Environmental Protection Agency [6]. The recent research showed the elevated Al concentrations in drinking water correlate with the increased incidence of neurological disorders [7].

The high Al level in the freshwater resources has been recognized as a serious problem in many countries, for example, Canada, China, Poland, India, etc. [8–12]. One of the locations where prohibitive Al concentrations in natural waters have been found is the Khibiny alkaline massif area which belongs to the Baltic hydrogeological massif (Kola Peninsula) [13,14]. The main objective of current study is revealing and analyzing the patterns of Al concentration variability in the Khibiny area and its possible associations with various groundwater quality parameters by applying chemometric methods.

Chemometric methods have several advantages including a broad range of applications, the ease of use and results interpretation. The chemometrics in environmental analysis comprises a variety of mathematical methods aiming to the identification, assessment, modelling, and prediction purposes depending on the data structures and the objective of study [15,16]. The univariate and multivariate regression methods are successfully used for the water quality assessment. The efficiency of the approach has been demonstrated

by a number of recent water quality monitoring research where the application of regression methods results in a possibility of evaluation spatial and temporal variations in drinking water quality and identification of pollution sources [17–19].

The spectral analysis based on fast Fourier transform (FFT) algorithm as a part of chemometric methods is extensively used in various fields of engineering and science to analyze laboratory and field data. Its application to environmental data allows researchers solving a number of tasks related to water quality as well as biological and climatological problems [20–23]. Fourier transform decomposes a periodic time series into a linear superposition of sinusoids of different frequencies [22]. The main advantage of this approach lies in its capability to explain the patterns of dynamics and strength of variations of various components under consideration.

The data of groundwater quality monitoring were analyzed by applying chemometric methods including Pearson correlation, multiple linear regression, and spectral analysis based on FFT algorithm. This combination of methods and proposed analysis framework not only allows for identifying the degree of association between Al concentrations and other physico-chemical parameters of groundwater but also revealing the frequency bands describing the strength of variations of various groundwater quality parameters (Appendix A).

3.2 Study Area and Materials

3.2.1 Location and Environmental Conditions

The area of interest – the Khibiny alkaline massif located between two lakes Imandra and Umbozero at the central part of Kola Peninsula. The Khibiny alkaline massif area occupies 1327 km^2 and has a ring structure. More than 90% of massif area is taken by nepheline syenite, where about 21% of its chemical composition is Al_2O_3 [14,24]. The massif is a place of the large-scale industrial production of apatite. The mining industry defines the social and economic region development. The influence of mining industry is considered as a threat to ecosystem’s sustainably in the region. It has changed the natural

landscape, increased the level of air pollution and dramatically lowered the quality of surface waters [25]. Up to 9.0×10^6 m^3 of industrial wastewater enter the natural water bodies without a sufficient pre-treatment annually. This resulted in a serious contamination of surface water with aluminum, strontium, iron, manganese, zinc, alkali and alkaline earth metals, which in high concentrations have a negative effect on aquatic organisms and humans [26]. Several natural water bodies such as lake Imandra, Belaya and Zhemchuzhnaya rivers are considered as contaminated making the groundwater resources an alternative option for water supply of the area [25].

A deposit of groundwater has been discovered in the southern part of the Khibiny alkaline massif and used as a local freshwater source for more than 40 years. Over the past 25–30 years groundwater became the main source of household water supply in the area. A current water treatment method – UV disinfection does not allow decreasing Al concentration to keep it below the guidelines [13]. Under these circumstances, the analysis of available field dataset as well as the development of effective water treatment method are becoming predominant tasks of local water supply.

3.2.2 Field Dataset

There are two groundwater intakes – “Central” and “Bolotny” that supply with water the city of Kirovsk with a population of approximately 27,000. The water of “Central” water intake having prohibitive Al concentrations and pH values that are much higher than local standards is the main water supply source, while water of “Bolotny” intake is under the drinking water guidelines [13]. A systematic monitoring of household water supply source “Central” has a seasonal basis – water samples in most cases were collected four times a year in winter, spring, summer, and fall. It includes ten operating wells equipped with centrifugal submersible pumps having an average discharge of 185 m^3 $hour^{-1}$ each. The operating wells have a depths range of 72–131 m. The field dataset for each well includes 12 physico-chemical characteristics of groundwater: Al, pH, fluoride F^-, nitrate NO_3^-, chloride Cl^-, sulphate SO_4^{2-}, total dissolved solids TDS, turbidity, colour, hardness, calcium Ca^{2+}, magnesium Mg^{2+}. The observations of each variable covered the

period of 112–161 months during 1999–2012 depending on the well (Table S3.1 of Appendix B).

3.3 Methods

3.3.1 Time Domain Analysis

The initial step of analysis included the application of descriptive statistics to assess and summarize the basic properties of groundwater characteristics of each well. Prior calculating the descriptive statistics, the time series plots were examined with the application of the Grubbs' outlier test to identify and remove unusual observations – outliers [27].

The Pearson correlation and multiple linear regression analysis were applied to groundwater monitoring time series by using Minitab software to relate Al concentrations as a response variable to a set of predictor variables. The linearity and normality were the main assumptions for the regression analysis. The commonly used significance level (*α-level*) of 0.05 was a criterion for interpreting the significance of calculated statistical parameters [28]. In consideration of the established *α-level*, the guidelines for interpretation of statistically significant Pearson correlation coefficient *r* values were chosen as follows: $|r| \leq 0.3$ indicates a poor or no linear relationship, $0.3 < |r| < 0.7$ – a moderate linear relationship and $|r| \geq 0.7$ – a strong linear relationship. To improve the strength of linear correlation between Al level and other statistically significant variables the exponential, logarithmic, power, and quadratic transformations [28] were applied to the time series and after that, the correlation coefficients were recalculated.

Multiple linear regression analysis was applied to examine the association between Al and predictor variables and to develop a mathematical model describing quantitatively this association. The forward selection of variables procedure was used to test the statistical significance of groundwater quality parameters under consideration in multiple regression [28].

It is important to diagnose multicollinearity that arises when at least two highly correlated predictor variables are assessed simultaneously in a multiple regression model. The adverse impact of multicollinearity in regression analysis is very well recognized and much attention to its effect is documented in the literature [29]. In current study, multicollinearity was assessed by the value of variance inflation factor (VIF). VIFs get their name from the fact that they report how much the variance of the estimated coefficients increases is due to collinear predictor variables. Specifically, VIF reports how much of a particular regressor's variability is explained by the rest of regressors in the model due to correlation among those regressors [30].

3.3.2 Frequency Domain Analysis

The spectral analysis based on discrete Fourier transform (DFT) allowed converting time domain series (e.g. the results of groundwater monitoring) into the frequency domain. The Fourier coefficients, power spectral density (PSD) and cumulative spectral power (CSP) estimates were calculated to identify and quantify the dominant frequencies, to characterize periodicities of variations and explore the strength of variations, so-called energies, of each variable for all ten water wells. The spectral analysis was performed using MATLAB. The Fourier coefficients C_j were calculated as follows [31]:

$$C_j = \sum_{n=1}^{N} d(t_n) \cdot exp\left(-i\omega_j t_n\right) \tag{3.1}$$

where $d(t_n)$ – value of variable at time t_n, $i = \sqrt{-1}$, n – number of discrete time observations, $n = 1,...,N$, $j = 0,\ldots,N-1$, $\omega_j = 2\times\pi f_j$ – angular frequency, f_j – ordinary frequency. Based on this the one-sided PSD estimates showing the strength of variation as a function of frequency were calculated with the normalizing factor considering the Parseval's theorem [32]:

$$P\left(f_j\right) = (2 \cdot (\Delta t/N))\ |C_j|^2 \tag{3.2}$$

where $P(f_j)$ – PSD estimates at frequency f_j, Δt – an equally spaced time interval. The PSD estimates were integrated over the frequency range to obtain CSP estimates which allowed to identify the frequency range where the main energy inflow is accumulated.

The computations related to spectral analysis of dataset required pre-processing to make the time series of each separate well stationary and regularly sampled [33,34]. The application of linear detrending eliminated trends from the time series by taking a difference between consecutive observations. The missing observations in the groundwater monitoring data series were filled in with 35-day step data interpolation. When choosing the 35-day interval, the Nyquist critical frequency $f_c=(2\times\Delta t)^{-1}$ was taken into consideration to prevent the problem of aliasing [31,32].

3.4 Results and Discussion

3.4.1 Descriptive Statistics

The descriptive statistics measures (Table 3.1) allowed assessing the central tendencies and variabilities of field data characteristics. The calculations exhibited that the pH mean value is 9.56 and its variation is insignificant within 13 years according to the *StDev* value of pH time series. This concludes that there are constant alkaline conditions in the groundwater. The range of TDS concentrations falls within the maximum allowable limit of 500 mg L^{-1} [6]. The concentrations of anions are varied considerably, although at the relatively low levels. For example, the concentrations of SO_4^{2-} and Cl^- vary in the ranges 0.77–27.80 and 0.15–6.86 mg L^{-1} respectively. The Al concentration in groundwater exceeds the drinking water guideline of 0.20 mg L^{-1} up to nine times while the variation range is 0.19–1.81 mg L^{-1}. The difference between *Q3* and *Q1* indicates that the middle 50% of all observations of Al concentrations are within the range of 0.67–1.10 mg L^{-1} that in 3–5 times exceeds the acceptable level.

The results of calculations showed that most of the time the “Central” intake water does not meet established drinking water standards at least for two factors: the level of pH and concentration of Al. The mean, median and mode values for Al are almost equal that

indicates a normal distribution of Al concentrations**.** The distribution is centered at the concentration of 0.88 mg L^{-1} that significantly exceeds the guideline (Figure 3.1).

Table 3.1: Calculated descriptive statistics measures assessing the central tendencies and variabilities of field data characteristics of "Central" water intake 1999–2012.

Parameters	Units	Mean	StDev	Min	Q1	Median	Q3	Max	Mode
Al	mg L^{-1}	0.88	0.32	0.19	0.67	0.88	1.10	1.81	0.87
pH	–	9.56	0.25	8.74	9.43	9.63	9.74	9.96	9.62
F^-	mg L^{-1}	0.13	0.10	0.00	0.04	0.10	0.19	0.62	0.04
NO_3^-	mg L^{-1}	2.14	2.55	0.04	0.48	1.00	2.58	13.12	0.44
Cl^-	mg L^{-1}	1.86	0.88	0.15	1.22	1.70	2.25	6.86	1.00
SO_4^{2-}	mg L^{-1}	7.15	5.66	0.77	3.11	5.30	9.20	27.80	2.06
TDS	mg L^{-1}	55.81	21.90	25.20	40.25	48.00	62.95	126.00	38.70
Turbidity	mg L^{-1}	0.27	0.27	0.00	0.05	0.25	0.40	1.84	0.00
Colour	colour units	1.48	1.52	0.00	0.40	0.90	2.21	8.18	0.00
Hardness	mmol L^{-1}	0.03	0.05	0.00	0.00	0.02	0.03	0.51	0.00
Ca^{2+}	mmol L^{-1}	0.16	0.33	0.00	0.00	0.00	0.10	2.00	0.00
Mg^{2+}	mmol L^{-1}	0.05	0.11	0.00	0.00	0.00	0.02	0.60	0.00

StDev – standard deviation; *Min* – minimum; *Max* – maximum; *Q1*, *Q3* – first and third quartiles.

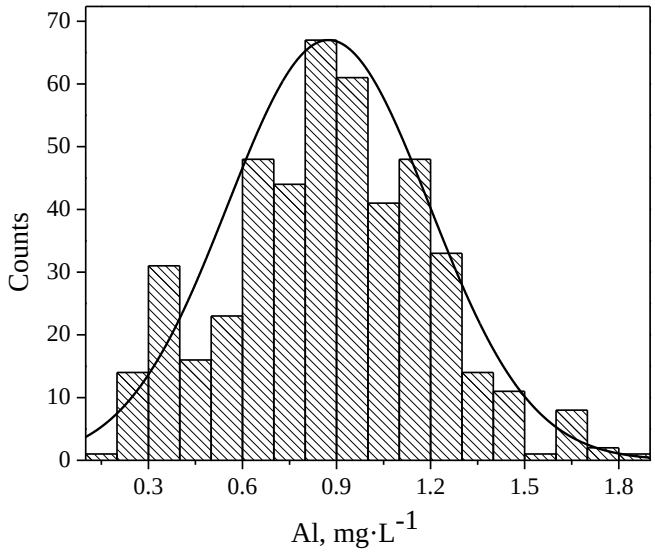

Figure 3.1: The distribution of Al concentrations in water of intake "Central", 1999–2012; solid line indicates the fitted normal distribution; counts correspond to the number of times a specific Al concentration occurs.

3.4.2 Pearson Correlation

The Pearson correlation coefficients *r* describing the association between Al concentrations and predictor variables showed a resembling strength and a tendency of variation among all wells. The correlation matrix reflecting the whole dataset (Table 3.2) contains *r* values exhibiting relationships between two variables and their corresponding probability values (*p-values*). The application of exponential transformation technique to initial data provided up to 15% improvement in correlation strength between Al concentrations and other variables. Calculated results revealed the moderate linear relationships between Al concentrations and pH values, concentrations of NO_3^-, SO_4^{2-}, Cl^-, and TDS as well as the strong and moderate linear relationships between some predictor variables (Table 3.2). The Al concentrations have a positive correlation with pH values, while its pairwise correlations with concentrations of NO_3^-, SO_4^{2-}, Cl^-, and TDS have a negative interconnection. The investigation of a possible connection between Al concentrations and physical characteristics of water intake "Central" such as well discharge and depth did not show any statistically significant correlations.

The results of computations supported the dependency between TDS and major anions as TDS is determined by the amount of dissolved substances. The calculated degree of association between Al and pH agrees with the theory describing the pH-dependency of Al and considering that the Al^{3+} ion, which is released to natural waters from Al-bearing minerals such, for example, as a nepheline syenite of Khibiny alkaline massif, is octahedrally coordinated with six water molecules and exists as $Al(H_2O)_6^{3+}$. This ion is a proton donor and moderately acidic and its hydrolysis in natural waters is thus the rule rather than the exception [5]. In accordance with a commonly used concept, there are four mononuclear species of Al: $Al(OH)^{2+}$, $Al(OH)_2^+$, $Al(OH)_3^0$, and $Al(OH)_4^-$ which formation is strongly pH dependent and deals with hydrolysis reactions [1]. In the alkaline conditions – that is one of the major features of Khibiny massif groundwater – the fourth of a set of Al hydrolysis reactions takes place:

$$Al^{3+} + 4H_2O = Al(OH)_4^- + 4H^+ \quad (3.3)$$

This reaction and the fact that a mean pH value of "Central" intake water is 9.56 evidence in favour of the hypothesis that the dominant Al specie in water is $Al(OH)_4^-$.

Table 3.2: Calculated Pearson correlation coefficient matrix of "Central" water intake field data 1999–2012.

N=464	ln Al	pH	F^-	NO_3^-	Cl^-	SO_4^{2-}	TDS	Turbidity	Colour	Hardness	Ca^{2+}
pH	**0.66** *)										
	0.00 **)										
F^-	–0.02	–0.05									
	0.94	0.28									
NO_3^-	**–0.68**	**–0.67**	–0.05								
	0.00	0.00	0.32								
Cl^-	**–0.40**	**–0.36**	–0.04	**0.40**							
	0.00	0.00	0.35	0.00							
SO_4^{2-}	**–0.59**	**–0.61**	–0.04	**0.75**	**0.43**						
	0.00	0.00	0.35	0.00	0.00						
TDS	**–0.69**	**–0.67**	–0.06	**0.86**	**0.44**	**0.78**					
	0.00	0.00	0.21	0.00	0.00	0.00					
Turbidity	0.13	–0.10	0.01	0.03	–0.08	–0.06	0.03				
	0.01	0.09	0.84	0.50	0.10	0.17	0.58				
Colour	0.02	–0.14	–0.11	0.17	0.04	0.10	0.14	**0.45**			
	0.66	0.00	0.02	0.00	0.42	0.03	0.03	0.00			
Hardness	–0.21	–0.24	–0.06	0.28	0.09	0.21	0.24	0.01	0.20		
	0.00	0.00	0.18	0.00	0.06	0.00	0.00	0.90	0.00		
Ca^{2+}	–0.03	–0.15	0.15	0.12	0.18	0.16	0.10	–0.05	0.01	0.30	
	0.56	0.00	0.00	0.00	0.00	0.00	0.03	0.30	0.78	0.00	
Mg^{2+}	–0.15	–0.06	0.07	0.21	0.00	0.12	0.19	0.06	0.16	0.30	0.10
	0.01	0.40	0.16	0.00	0.98	0.01	0.00	0.20	0.00	0.00	0.03

Cell Contents: Pearson correlation coefficient *r*
p-value (*α-level* = 0.05)

*) Bolded values indicate moderate and strong relationships.
**) *p-value* = 0.00 corresponds to the *p-value* < 0.001.
N – the total number of observations.

3.4.3 Multiple Linear Regression

Among the investigated parameters (Table 3.1), pH, NO_3^-, SO_4^{2-}, Cl^-, and TDS were

identified by Pearson correlation as statistically significant variables and were examined by the application of multiple linear regression analysis. In accordance with the results of calculation pH, NO_3^-, and Cl^- time series were used to develop a multiple regression mathematical model while SO_4^{2-} time series did not meet a minimum criterion (*p-value* ≤ 0.05) to stay in it. The TDS time series were also excluded from the further analysis based on the results of multicollinearity check (Table S3.2 of Appendix B). Calculations showed that they have the highest VIF value (close to five) explained by strong and moderate correlations between this variable and the rest of assessed predictor variables (Table 3.2).

The next step of data examination has been done with the application of analysis of variance (ANOVA) method which allows separating the contributions of various sources to the total variation of response variable in a set of experimental data [17]. The coefficient of determination R^2 giving the proportion of Al variation explained by the predictor variables is 0.54 (54%). The sequential chain of contribution to the R^2 percentage is as follows: pH > NO_3^- > Cl^-. The numerical results of ANOVA are statistically significant in accordance with their corresponding *p-values* (≤ 0.05) and a multiple regression model can be given as follows:

$$ln\,Al = -5.86 + 0.62 \times pH - 0.07 \times NO_3^- - 0.06 \times Cl^- \quad (3.4)$$

The *r* value corresponding to the model above is 0.74 that falls within a strong correlation range. The model shows a pH-dependency and quantitative impact of pH on the Al concentration variability when other predictor variables are held constant is the highest.

The calculated VIF values for pH, NO_3^-, and Cl^- time series were less than two concluding that multicollinearity is negligible when these variables are assessed simultaneously in the proposed mathematical regression model (Table S3.3 of Appendix B). Figure 3.2 shows a variability of spatially averaged within the whole "Central" water intake time series of various variables included in equation (3.4). The Al and pH time series showed a general increase with the 8.6×10^{-5} mg L^{-1} day^{-1} and 1.6×10^{-5} day^{-1} rate of change respectively while the Cl^- and NO_3^- time series exhibited a decline.

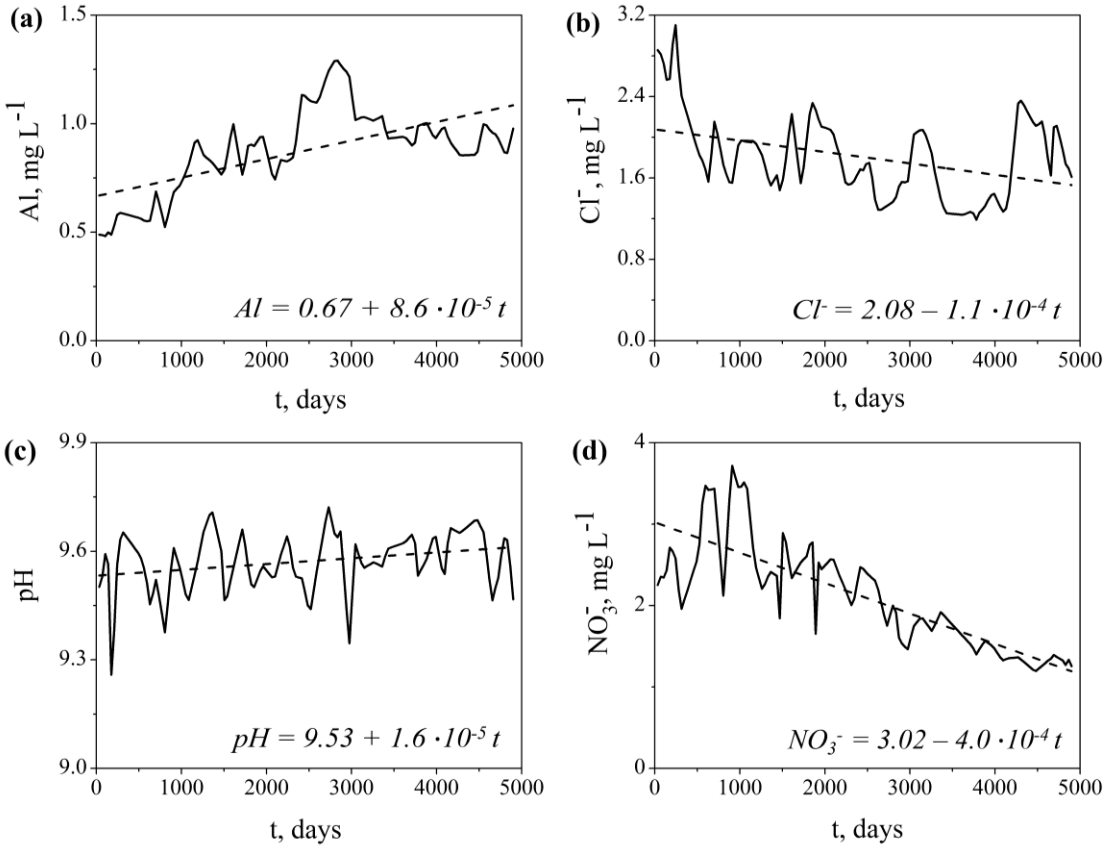

Figure 3.2: Spatially averaged within water intake "Central" Al (a), Cl^- (b), pH (c), and NO_3^- (d) time series; dashed lines denote linear fits within 13 years.

3.4.4 Spectral Analysis Based on FFT

The spectral analysis revealed that the energy spectrums of Al, pH, NO_3^-, and Cl^- have similar patterns of variability in frequency domain throughout the all ten groundwater wells of "Central" water intake. The calculations of PSD estimates allowed to identify the major frequency bands corresponding approximately to 5–7, 13–17, and 20–34 month periods. The fluctuations within these periods contribute mostly to the total temporal variability of time series under consideration. Figure 3.3 and Figure S3.1 (Appendix B) represent characteristic for the "Central" water intake examples of calculated energy spectrums of Al, pH, NO_3^-, and Cl^-. There is a good agreement between the main features of Al, pH, NO_3^-, and Cl^- energy spectrums including spikes identified by calculated PSD estimates. For example, there is a typical for all variables spike

corresponding to the period of approximately seven months although its intensity differs depending on the particular variable. The spikes within 5–7 months and 13–17 frequency bands can possibly reflect the semi-annual and annual cycles respectively. There are also appeared considerable low-frequency variations in the range of 20–34 months period in Al, NO_3^-, and Cl^- spectrums. The low-frequency variation in pH spectrum also exists but with the lower intensity compared to other variables. These long-term fluctuations can potentially describe anthropogenic influence.

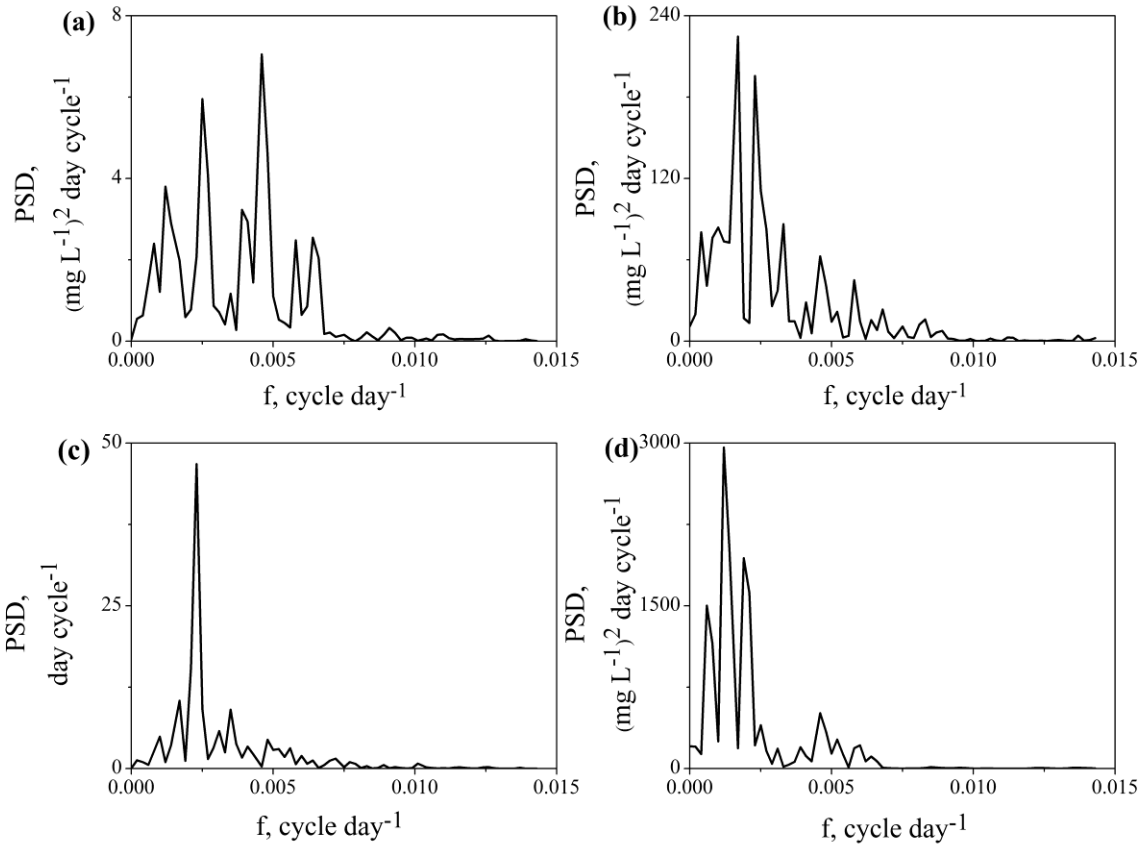

Figure 3.3: Calculated PSD of Al (a), Cl^- (b), pH (c), and NO_3^- (d) time series, well 8 of water intake "Central".

The calculated CSP estimates of all four investigated variables showed that the main energy inflows fall within a frequency range of $(1.0 \div 5.0) \times 10^{-3}$ cycle day^{-1} corresponding

to the period extend of 6.7–33.3 months (Figure 3.4a). Calculations identified the similar patterns of exponential decay of PSD values with frequency increasing. It is proportional approximately to the −4 power characterizing the falloff in the strength of variations. The decay occurs depending on the well at the frequency $(2.1 \div 5.0) \times 10^{-3}$ cycle day^{-1} (Figure 3.4b).

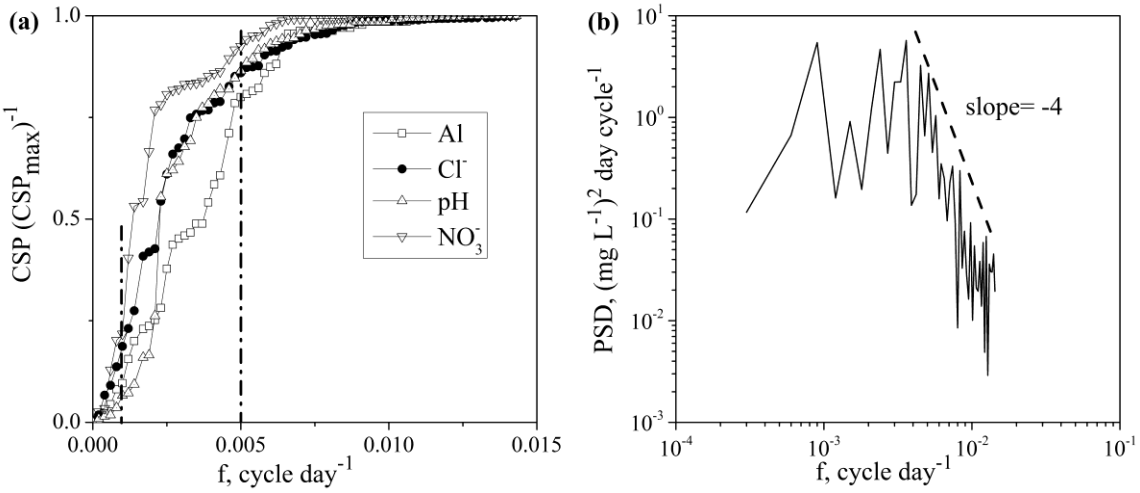

Figure 3.4: Calculated PSD and CSP estimates based on Al time series of the water intake "Central": Calculated CSP estimates of Cl^-, pH, and NO_3^-, well 8 (a); vertical dashed-dotted lines denote the frequency boundaries of main energy impact; an example of PSD changes over frequency range with the typical pattern of energy decay, well 7 (b); dashed line denotes a slope describing the falloff in the strength of variations.

The raw data of water quality monitoring have an element of irregularity in sampling periods that can obstruct the direct application of FFT algorithm. The examination using Lomb-Scargle periodogram method [35] was performed to identify the influence and applicability of data interpolation that was used in current study. The method was applied to the Al, pH, NO_3^-, and Cl^- time series with irregular sampling interval. The calculations using both Lomb-Scargle and FFT algorithms revealed the close results especially within

the range of frequencies where the main energy inflow falls (Figure 3.5). The MATLAB code used for the spectral analysis calculations is shown in Appendix C.

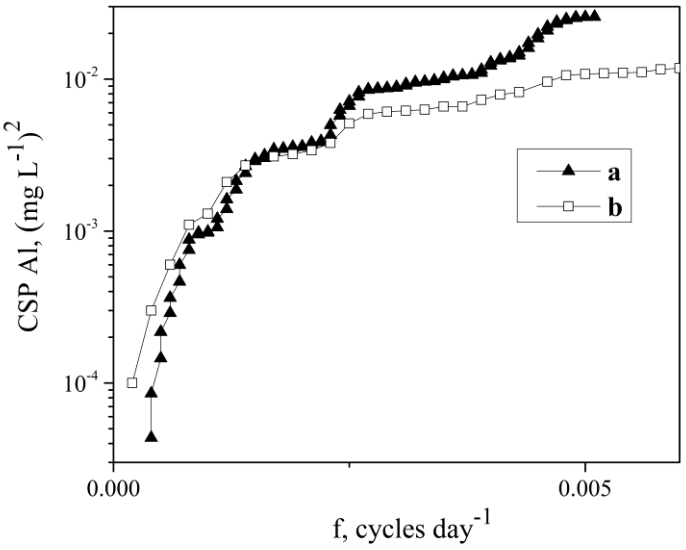

Figure 3.5: Calculated CSP estimates of Al with application of FFT algorithm (a) and Lomb-Scargle method (b); well 8 of water intake "Central".

3.5 Conclusions

The current study presents the first results of chemometric methods application to assess and interpret the outcome of long-term field data monitoring of Khibiny alkaline massif (Kola Peninsula) groundwater with the prohibitive concentrations of Al limiting the use of groundwater for the local household water supply. The results of analysis allow better understanding the major features of Al concentration variability as well as associations between Al and other groundwater quality parameters examined at both time and frequency domains. Among 11 considered physico-chemical parameters pH values, concentrations of NO_3^-, SO_4^{2-}, Cl^-, and TDS were the main statistically significant factors associated with the Al concentration variation in groundwater. It was revealed that exponential data transformation technique applied to the raw field data provided up to 15% improvement in pairwise correlation. Multiple regression model (Equation (3.4))

considering the result of multicollinearity check explained up to 54% of Al concentration variability linked to pH values, concentrations of Cl^- and NO_3^-.

Spectral analysis based on FFT algorithm applied to Al, pH, NO_3^-, and Cl^- time series identified similar variability patterns and three major frequency bands corresponding approximately to 5–7, 13–17, and 20–34 month periods. The periodicities within these frequency bands are responsible for most of the total temporal variation of variables under consideration. The main energy inflow is accumulated in the frequency range of $(1.0 \div 5.0) \times 10^{-3}$ cycle day^{-1} as calculated CSP estimates showed.

The results obtained in this study represent an initial quantitative data analysis step preceding the development of effective technology keeping Al concentrations under the guideline of accepted water quality standards. The current study of groundwater parameters dynamics did not reveal the evidence of direct anthropogenic influence on the elevated Al concentration in groundwater of "Central" water intake. It rather supports the outcomes of recent geochemical analysis according to which at the big depths of Khibiny alkaline massif there are reduction conditions promoting the Aluminum leaching [14]. On the other hand, the long-period variations (20–34 months) revealed by the spectral analysis can potentially describe anthropogenic influence. However, more data are needed to investigate this.

The incorporation of additional factors reflecting industrial activities in the area such as waste discharge and its changes into the analysis and modelling will be beneficial to further examination of Al concentration variability. Although the current investigation has been done for the particular metal and groundwater source, a similar approach can be successfully applied to any other groundwater sources and can be extended to various toxic metals.

3.6 References

[1] G. Sposito, The Environmental Chemistry of Aluminum, 2nd edition, Lewis Publishers, Boca Raton, FL, 1996.

[2] D. Mendeleev, Osnovi Himii [The Princliples of Chemistry], 7th edition, Frolova's typolitography, Saint Petersburg, 1903.

[3] C.T. Driscoll, R.D. Letterman, Chemistry and fate of Al(III) in treated drinking water, Environ. Enginering. 114 (1988) 21–37. doi:10.1061/(ASCE)0733-9372(1988)114:1(21).

[4] C. Sollars, S. Bragg, A. Simpson, R. Perry, Aluminium in European drinking water, Environ. Technol. Lett. 10 (1989) 131–150. doi:10.1080/09593338909384727.

[5] B. Stewart, Advance in Soil Science, 1st edition, Springer-Verlag, New York, 1988.

[6] U.S. Environmental Protection Agency (USEPA), 2018 Edition of the Drinking Water Standards and Health Advisories Tables, Washington, DC, 2018.

[7] Z. Wang, X. Wei, J. Yang, J. Suo, J. Chen, X. Liu, X. Zhao, Chronic exposure to aluminum and risk of Alzheimer's disease: a meta-analysis, Neurosci. Lett. 610 (2016) 200–206. doi:10.1016/j.neulet.2015.11.014.

[8] M. Frankowski, A. Zioła-Frankowska, I. Kurzyca, K. Novotný, T. Vaculovič, V. Kanický, M. Siepak, J. Siepak, Determination of aluminium in groundwater samples by GF-AAS, ICP-AES, ICP-MS and modelling of inorganic aluminium complexes, Environ. Monit. Assess. 182 (2011) 71–84. doi:10.1007/s10661-010-1859-8.

[9] W. Wang, H. Li, X. Wang, Y. Liu, Spatial variations of aluminum species in drinking water supplies in Xi'an studied applying geographic information system, J. Environ. Sci. 22 (2010) 519–525. doi:10.1016/S1001-0742(09)60136-4.

[10] W.A. Scheider, B. Cave, J. Jones, Reclamation of Acidified Lakes near Sudbury Ontario by Neutralization and Fertilization, Rexdale, ON, 1975.

[11] P.F. Henshaw, J.K. Bewtra, N. Biswas, Occurrence of aluminum, lead, and

trihalomethanes in drinking water from the Great Lakes, J. Great Lakes Res. 19 (1993) 521–532. doi:10.1016/S0380-1330(93)71238-1.

[12] S. Kumari, A.K. Singh, A.K. Verma, N.P.S. Yaduvanshi, Assessment and spatial distribution of groundwater quality in industrial areas of Ghaziabad, India, Env. Monit Assess. 186 (2014) 501–514. doi:10.1007/s10661-013-3393-y.

[13] K. Marchenko, Aluminum v podzyemnih vodah Hibinskogo gornogo massiva [Aluminum in groundwater of Khibiny alkaline massif], in: V.. Trushko, L.. Sinkov, U.. Sischuk (Eds.), Proc. Int. Forum Young Res. "Topical Issues Subsoil Usage," Saint Petersburg Mining University Press, Saint Petersburg, 2011: pp. 173–175.

[14] S.I. Mazukhina, V.A. Masloboev, K. V Chudnenko, V.A. Bychinsky, A. V Svetlov, S. V Muraviev, Monitoring and physical-chemical modeling of conditions of natural surface and underground waters forming in the Kola North, J. Environ. Sci. Heal. Part A. 47 (2012) 657–668. doi:10.1080/10934529.2012.660037.

[15] J. Einax, H. Zwanziger, S. Geiss, Chemometrics in Environmental Analysis, VCH, Weinheim, 1997.

[16] S. Mas, A. de Juan, R. Tauler, A.C. Olivieri, G.M. Escandar, Application of chemometric methods to environmental analysis of organic pollutants: a review, Talanta. 80 (2010) 1052–1067. doi:10.1016/j.talanta.2009.09.044.

[17] A. Astel, M. Biziuk, A. Przyjazny, J. Namiesnik, Chemometrics in monitoring spatial and temporal variations in drinking water quality, Water Res. 40 (2006) 1706–1716. doi:10.1016/j.watres.2006.02.018.

[18] R. Osman, N. Saim, H. Juahir, M.P. Abdullah, Chemometric application in identifying sources of organic contaminants in Langat river basin, Environ. Monit. Assess. 184 (2016) 1001–1014. doi:10.1007/s10661-011-2016-8.

[19] H. Gu, B. Chi, H. Li, J. Jiang, W. Qin, H. Wang, Assessment of groundwater quality and identification of contaminant sources of Liujiang basin in

Qinhuangdao, North China, Environ. Earth Sci. 73 (2015) 6477–6493. doi:10.1007/s12665-014-3870-9.

[20] R. Fagbenle, Fourier analysis of climatological data series in a tropical environment, Int. J. Energy Res. 19 (1995) 117–123.

[21] P.H. Whitfield, Identification and characterization of transient water quality events by Fourier analysis, Environ. Int. 21 (1995) 571–575. doi:10.1016/0160-4120(95)00059-T.

[22] J.D. Leaver, C.P. Unsworth, Fourier analysis of short-period water level variations in the Rotorua geothermal field, New Zealand, Geothermics. 36 (2007) 539–557. doi:10.1016/j.geothermics.2007.07.001.

[23] Y.B. Mel'nikova, Evaluation of parameters of a plankton community's biological rhythms under the natural environment of the Black Sea using the Fourier transform method, Luminescence. 32 (2017) 321–326. doi:10.1002/bio.3181.

[24] A.O. Kalashnikov, N.G. Konopleva, Y.A. Pakhomovsky, G.Y. Ivanyuk, Rare earth deposits of the Murmansk Region, Russia - a review, Econ. Geol. 111 (2016) 1529–1559. doi:10.2113/econgeo.111.7.1529.

[25] V. Konukhin, A. Kozyrev, A. Orlov, U. Smirnov, Isslyedovaniye podzyemnih istochnikov dlya vodosnabzhyeniya gorodov Zapolyar'ya ekologichyeski chistoy vodoy na primyerye goroda Apatiti [The research of underground sources for water supply of cities in the North (city of Apatity as an example)], Arct. Ecol. Econ. 2 (2012) 58–65.

[26] S. Sandimirov, N. Kashoolin, G. Yevdokimova, V. Koshkin, GIS-analiz tyehnogyennogo zagryaznyeniya hibinskih ryek i ozyer v ryezool'tatye dyeyatyel'nosti gornogo i obogatityel'nogo proizvodstva. [GIS-analysis of lakes and rivers contamination due to the anthropogenic influence caused by the mining industry], ArcReview. 4 (2004).

[27] F. Grubbs, Procedures for detecting outlying observations in samples,

Technometrics. 11 (1969) 1–21. doi:10.1080/00401706.1969.10490657.

[28] S. Chatterjee, A. Hadi, Regression Analysis by Example, 5th edition, Wiley, Hoboken, NJ, 2012.

[29] K.P. Vatcheva, M. Lee, J.B. McCormick, M.H. Rahbar, Multicollinearity in regression analyses conducted in epidemiologic studies, Epidemiology. 6 (2016) 227. doi:10.4172/2161-1165.1000227.

[30] T.A. Craney, J.G. Surles, Model-dependent variance inflation factor cutoff values, Qual. Eng. 14 (2002) 391–403. doi:10.1081/QEN-120001878.

[31] W. Menke, J. Menke, Environmental Data Analysis with Matlab, Elsevier, London, 2016.

[32] M. Elson, J. Bennett, Calculation of the power spectral density from surface profile data, Appl. Opt. 34 (1995) 201–208. doi:https://doi.org/10.1364/AO.34.000201.

[33] G. Jenkins, D. Watts, Spectral Analysis and its Applications, Holden-Day, San Francisco, CA, 1968.

[34] R. Warner, Spectral Analysis of Time-series Data, Guilford Press, New York, NY, 1998.

[35] N. Lomb, Least-squares frequency analysis of unequally spaced data, Astrophys. Space Sci. 39 (1975) 447–462.

Chapter 4

4 Assessment of Khibiny Alkaline Massif Groundwater Quality using Statistical Methods and Water Quality Index

4.1 Introduction

It is well-known that natural processes and anthropogenic influence can change the quality of natural water resources limiting the water use for drinking, industrial, and agricultural purposes [1]. The contamination of drinking water with metals, due to their potential acute (occurring in the short term) and/or chronic (occurring over the long term) adverse effect on human health can lead to life-threatening cancers and neurological disorders [2,3]. Negative health effects make metal pollution of natural water resources an ongoing global environmental problem nowadays.

Aluminum (Al) is widely distributed in the environment comprising about 8% of the Earth outer crust [4]. It is released by both anthropogenic and natural sources and is present in all types of natural water bodies including wastewater [4]. The prohibitive concentrations of Al in natural water sources exceeding the recommended standard of 0.20 mg L^{-1} according to the U.S. Environmental Protection Agency [5] are recognized as a serious issue in many countries in the worldwide as a growing number of epidemiological studies suggested the association between the increased incidence of neurological diseases and the elevated Al concentrations in drinking water [6].

A study on the water quality assessment conducted in China defined Al as one of the dominant contaminants in the analyzed groundwater where Al concentrations were almost up to 25 times higher than the local drinking water guidelines [7]. The surface water assessment led in Pakistan revealed that Al concentrations significantly exceeded the drinking water guidelines ranging from 1.01 to 4.27 mg L^{-1} with a mean value of 2.10 mg L^{-1} [8]. One of the locations where prohibitive Al level in groundwater is described as a serious health concern when used for the household water supply is the Khibiny

alkaline massif area which belongs to the Baltic hydrogeological massif (Kola Peninsula) [9].

The analysis of environmental monitoring data includes the application of various mathematical methods working toward achieving a quantitative description, modeling, and forecasting purposes depending on the objectives of research and data structures. The multivariate statistical methods such as cluster analysis (CA), factor analysis (FA), and principal component analysis (PCA) are powerful tools which are widely applied for the comprehensive water quality assessment [10–12]. CA is the data classification method while FA and PCA are methods used for the data reduction [13,14]. The commonly used FA type, namely exploratory FA is often applied to identify several factors and variables that belong to specific factors. PCA is one of the exploratory factor analytic procedures [14]. The water quality indices (WQI) mathematically combine the water quality parameters providing a general and readily understood description of the water source under consideration [15]. Providing interpretation and communication of environmental data, WQI can be applied to reduce the multivariate nature of water quality data [16–18]. Among various WQI the Canadian Council of Ministries of the Environment Water Quality Index (CCME WQI) is used extensively in Canada and throughout the world for reporting on the state of water quality [15].

A limited number of studies on Khibiny alkaline massif groundwater quality assessment by means of field data statistical analysis has been reported in the literature until now [9,19]. Taking this into consideration as well as a harmful influence of elevated aluminum concentration on groundwater quality, the current study has been conducted. The present paper is focused on the application of univariate and multivariate statistical methods and CCME WQI to assess and interpret the Khibiny alkaline massif groundwater quality field dataset with an emphasis on elevated Al concentrations. The main objectives are (i) quantitative description of interactions between groundwater quality parameters and (ii) evaluation of temporal variation of groundwater quality parameters. The results obtained can be used for water management and to develop and implement the treatment technology maintaining Al concentrations below the drinking water standards.

4.2 Materials and Methods

4.2.1 Environmental Conditions of Study Area and Field Dataset

The Khibiny massif has been investigated since the 19th century. Occupying the area of 1327 km^2, the Khibiny massif is located at the central part of Kola Peninsula and is considered as the world's largest alkaline complex [20]. The local climate is strongly affected by the North Atlantic Current and is classified as slightly continental with an annual temperature and precipitation of −3.7℃ and 1070 mm, respectively [21,22]. The region geology is mainly represented by Precambrian crystalline rocks related to Fennoscandian crystalline massif [22]. Khibiny area is a minor intermontane aquifer system including Quaternary and bedrock aquifers. The groundwater of these aquifers is recharged from precipitation in the catchment area of Lake Bolshoy Vudyavr [19].

Over 90% of the total area of the Khibiny massif is occupied with nepheline syenites, where almost 21% of its chemical composition is aluminum oxide [23]. The apatite reserves have driven a large-scale industrial production of apatite in Khibiny alkaline massif area. The impact of well-developed mining industry is considered as a negative factor influencing the local ecosystem's sustainably. It has contributed to the increasing level of air pollution and contamination of surrounding surface water sources [24].

Over the past three decades, the groundwater aquifer located in the southern part of the Khibiny alkaline massif became one of the essential sources of local household water supply. The water intakes "Central" and "Bolotny" are two groundwater intakes supplying the city of Kirovsk and area with water. The water of "Central" intake is the main local water supply source having restrictively high Al concentrations and high pH level, while the water quality parameters of intake "Bolotny" are within the drinking water standards [25]. The household water contamination with Al has become a serious concern in the organization and management of the local water supply. These conditions making the analysis of available field monitoring data of "Central" water intake aiming the development of an effective water treatment method becomes a predominant initial task of the water supply in the area.

The “Central” water intake includes ten operating groundwater wells. Each well is equipped with centrifugal submersible pumps providing an average discharge of 185 m^3 $hour^{-1}$. The depths of operating wells are 72–131 m with an average depth of 115.6 m. The data for each of ten operating groundwater wells of intake “Central” comprises 12 groundwater quality parameters: Al, pH, fluoride F^-, nitrate NO_3^-, chloride Cl^-, sulphate SO_4^{2-}, total dissolved solids TDS, turbidity, colour, hardness, calcium Ca^{2+}, magnesium Mg^{2+} that in most cases were collected seasonally. The total of 462 samples of each variable collected from 1999 to 2012 were analyzed by univariate and multivariate statistical methods.

4.2.2 Descriptive Statistics and Multivariate Methods

The major descriptive statistics measures (mean x_m, standard deviation *StDev*, min, max, quartiles – 25%, median, 75%) and Spearman correlation coefficient matrix were calculated to assess and summarize the basic properties of groundwater parameters of each well and to quantitively analyze the associations between Al concentration and other groundwater quality parameters. The Spearman correlation coefficient r_s is a widely used nonparametric measure assessing how well an arbitrary monotonic function can describe a relationship between two variables and is computed over the ranked data [11,26]. The application of r_s does not require to make any assumptions regarding the frequency distribution of the variables and is not as sensitive to outliers (unusual observations within the dataset) as for example Pearson correlation coefficient [27]. The guidelines for interpretation of statistically significant r_s values were chosen as follows: when the absolute value of r_s is $|r_s| \leq 0.3$, $0.3 < |r_s| < 0.7$ and $|r_s| \geq 0.7$, the two variables would be regarded having a poor or no correlation, a moderate correlation and a strong correlation, respectively. The commonly used significance level (*α-level*) of 0.05 was a criterion for interpreting the statistical significance of computed r_s values. The statistical significance was set at probability value (*p-value*) ≤ 0.05 [9,26].

The application of multivariate statistical methods to environmental monitoring datasets is beneficial when the results of basic statistics reveal statistically significant correlation

coefficients for several dataset parameters. The factor analysis (FA), principal component analysis (PCA) and cluster analysis (CA) are the most commonly used multivariate analysis methods for complex environmental datasets assessment [1,28]. Complex structures within the datasets could be extracted without losing any information by reducing them to a few dominating factors. FA/PCA is a convenient data reduction method which uses the extraction of eigenvalues and eigenvectors from the correlation matrix [28]. Each factor is extracted by means of PCA method and interpretation is based on the rotated factors and loadings (a measure of how much the variable contributes to the factor) [28]. The suitability of data to be applied to FA/PCA is assessed using Kaiser-Meyer-Olkin (KMO) and Bartlett's sphericity tests [3,29]. The KMO test is a measure of sampling adequacy indicating the proportion of variance that is common, i.e., the variance that may be caused by underlying factors [30]. A high KMO value (close to 1) generally indicates that FA/PCA may be useful. The Bartlett's sphericity test examines the hypothesis that the correlation matrix comes from a population in which the variables are independent, i.e., an identity matrix [30]. The hypothesis is rejected when the significance of Bartlett's sphericity test is < 0.05 indicating that the data are adequate for FA/PCA [3,30].

A well-recognized method for identifying groups called clusters from multivariate data objects is a cluster analysis (CA) [31]. Clustering procedures based on hierarchical, partitioning or two-step clustering methods are used to determine how clusters are to be formed [13]. Applied to environmental datasets, the hierarchical clustering methods allow combining the variables of similar observations into one group, followed by the next most similar observation into another group [28]. Having numerous advantages, the minor drawback of hierarchical clustering methods is a limited guidance to make a decision on the number of clusters. The only meaningful indicator relates to the distances at which the objects are grouped [13]. The application of hierarchical cluster analysis (HCA) using Euclidean distance as a measure of distance and Ward's method as a linkage rule produces the most distinctive clusters between the variables [28]. A dendrogram can be composed to illustrate the hierarchical arrangements of clusters produced.

The data standardization is recommended for FA/PCA and HCA to avoid misclassification due to the wide differences in data dimensionality [11,32]. One of the most commonly used data standardization technique so-called z-scale transformation for *n* variables each with *N* observations is calculated as follows:

$$Z_{ij} = (X_{ij} - x_m)/StDev \quad (4.1)$$

where Z_{ij} is a *j*th value of the standardized variable Z_i, X_{ij} is a the jth observation of the *i*th variable, $i = 1, \ldots, n$, $j = 1, \ldots, N$, x_m stands for the mean value, *StDev* is a standard deviation [32].

The FA/PCA and HCA were performed on the to z-scale transformed Khibiny alkaline massif groundwater dataset to reduce the dimensionality of the dataset variables to several factors and group them into clusters. The calculated values of factor loadings using FA/PCA were classified as strong, moderate, and weak according to the absolute loading values of > 0.75, 0.75–0.50, and 0.50–0.30, respectively [1]. The HCA results were interpreted using a dendrogram displaying the distance level at which there is a merger of objects and clusters. The distance was rescaled to a range of 0–25, i.e., the last merging step to a one-cluster solution occurs at the rescaled distance of 25 [13].

4.2.3 Water Quality Index Calculation

A water quality index (WQI) is a means by which the water quality datasets including several parameters can be summarized and expressed in a simple, concise, and consistent number representing the overall water quality. The Canadian Council of Ministries of the Environment Water Quality Index (CCME WQI) is extensively used worldwide to characterize the quality of water for several intended uses including agriculture, the protection of aquatic life and treated drinking water as well as a tool to characterize water intended as a source for drinking purposes [15,16]. CCME WQI is an objective-based index that reflects the results of comparison between measured parameters of water quality and accepted guidelines and produces a single score ranging from 0, representing

worst quality, to 100, representing best quality [15]. The CCME WQI incorporates three elements and can be calculated as follows:

$$CCMEWQI = 100 - (\sqrt{F_1^2 + F_2^2 + F_3^2}/1.732) \quad (4.2)$$

where F_1 (scope) represents the percentage of parameters that do not meet their corresponding guidelines at least once during the considered period of time, F_2 (frequency) states for the percentage of individual tests that do not meet the guidelines, F_3 (amplitude) represents the amount by which failed test values do not meet their guidelines, the divisor 1.732 normalizes the resultant values to a range between 0 and 100 [15]. Based on the calculated CCME WQI score value the water quality falls into one of the following categories: 95–100 indicates an excellent water quality, 80–94 a good water quality, 65–79 a fair water quality, 45–64 a marginal water quality, and 0–44 a poor water quality [15,16].

The multivariate data processing was performed by using SPSS 16.0 statistical software package. The CCME WQI calculator 2.0 was used to compute CCME WQI score values from groundwater quality monitoring data [15].

4.3 Results and Discussion

4.3.1 Descriptive Statistics of Groundwater Quality and Spearman Correlation

The calculated descriptive statistics measures revealed that among 12 analyzed groundwater quality variables the concentration of Al and level of pH did not satisfy with the recommended drinking water quality standards. The amount of Al in groundwater exceeded the drinking water guideline of 0.20 mg L^{-1} up to nine times where the mean value was 0.88 mg L^{-1}. Within the variation range of 0.19 to 1.81 mg L^{-1} only once during the 13-year monitoring period Al observation fell below the guideline value (Figure 4.1). The concentrations of anions Cl^-, NO_3^-, and SO_4^{2-} were varied at the relatively low levels with respect to their guidelines values. The TDS concentrations were

varied significantly below the guideline of 500 mg L^{-1} in the range of 25.20 to 126 mg L^{-1} (Figure 4.1). According to pH mean value of 9.56 and corresponding standard deviation of 0.25 the groundwater under consideration has constant alkaline conditions. The observations of some organoleptic and physical characteristics of groundwater, as well as cations Ca^{2+} and Mg^{2+}, were predominantly near not detectable level (< 0.001).

Low concentrations of major anions such as Cl^{-}, NO_3^{-}, and F^{-} in groundwater suggest that anthropogenic influence most likely do not influence its quality. The groundwater can be characterized as soft and low-mineralized according to the hardness and TDS levels, respectively.

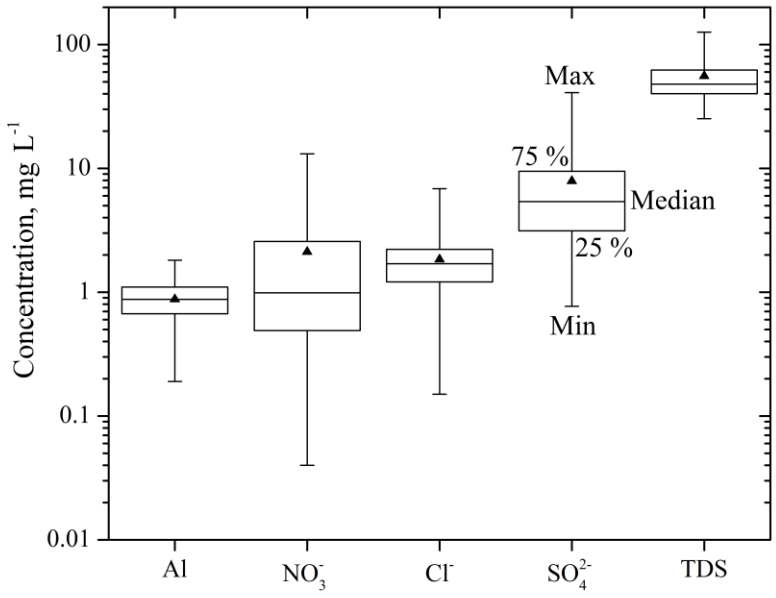

Figure 4.1: The variation of Al, major anions, and TDS concentrations in the groundwater of "Central" intake 1999–2012; quartiles 25%, 50% (median), and 75% divide the data distribution into four parts; black-coloured triangle corresponds to the mean value.

The calculated Spearman correlation coefficient matrix (Table 4.1) revealed statistically significant correlations between each pair of groundwater quality parameters with r_s values varying from |0.31| to |0.82|. Both pH and Al had statistically significant correlations with major anions NO_3^-, SO_4^{2-}, Cl^-, and TDS. Al and pH were interconnected with a moderate correlation coefficient equal to 0.50. The speciation and solubility of Al are strongly affected by pH according to the theory describing Al chemistry in the aqueous solution [4].

Table 4.1: Calculated Spearman correlation coefficient matrix of field monitoring data of "Central" water intake 1999–2012.

	Al	pH	F^-	NO_3^-	Cl^-	SO_4^{2-}	TDS	Turbidity	Colour	Hardness	Ca^{2+}	Mg^{2+}
Al	1.00											
pH	**0.50** *) 0.00 **)	1.00										
F^-	−0.07 0.06	−0.10 0.02	1.00									
NO_3^-	**−0.51** 0.00	**−0.55** 0.00	−0.13 0.00	1.00								
Cl^-	**−0.44** 0.00	**−0.37** 0.00	−0.04 0.19	**0.56** 0.00	1.00							
SO_4^{2-}	**−0.45** 0.00	**−0.42** 0.00	−0.07 0.06	**0.74** 0.00	**0.50** 0.00	1.00						
TDS	**−0.49** 0.00	**−0.47** 0.00	−0.15 0.00	**0.82** 0.00	**0.57** 0.00	**0.73** 0.00	1.00					
Turbidity	0.21 0.00	−0.05 0.14	0.10 0.01	−0.07 0.08	−0.08 0.04	−0.12 0.00	−0.04 0.22	1.00				
Colour	0.10 0.02	−0.12 0.00	−0.08 0.04	0.21 0.00	0.04 0.19	0.17 0.00	0.14 0.00	**0.49** 0.00	1.00			
Hardness	**−0.34** 0.00	−0.28 0.00	−0.04 0.21	**0.49** 0.00	**0.31** 0.00	**0.48** 0.00	**0.43** 0.00	**−0.32** 0.00	0.10 0.01	1.00		
Ca^{2+}	−0.16 0.00	−0.19 0.00	0.07 0.08	0.30 0.00	**0.33** 0.00	**0.31** 0.00	0.25 0.00	−0.25 0.00	0.05 0.17	**0.68** 0.00	1.00	
Mg^{2+}	−0.30 0.00	−0.21 0.00	−0.02 0.31	**0.34** 0.00	0.09 0.03	**0.35** 0.00	**0.35** 0.00	−0.07 0.06	0.17 0.00	**0.44** 0.00	−0.11 0.01	1.00

Cell contents: Spearman correlation coefficient
p-value (*α-level* = 0.05)

*) Bolded values: statistically significant correlation coefficients.

**) *p-value* = 0.00 corresponds to the *p-value* < 0.001.

4.3.2 Multivariate Analysis Results

The application of FA/PCA with the extraction constraint of the eigenvalue > 1 revealed four dominating influencing factors from the z-scale transformed dataset (Figure S4.1 of Appendix D). The factor contributions are presented in Table 4.2. All four factors included 12 groundwater quality parameters but the loading of a separate variable to each of the factors had a different magnitude. The analyzed data were considered adequate for the FA/PCA application as the calculated value of KMO test equal to 0.82 and the significance of Bartlett's sphericity test < 0.001 suggested.

Altogether the extracted four factors were accounted for 67.36% of the dataset total variance. The eigenvalues of these factors were 3.95, 1.55, 1.50, and 1.11, and corresponding variance loadings were 32.89%, 12.88%, 12.49%, and 9.28%, respectively. Factor 1 had values of strong positive loadings of TDS (0.90), NO_3^- (0.88), and SO_4^{2-} (0.85), as well as values of strong negative loadings of pH (−0.81) and Al (−0.77). Hardness and F^- contributed the most to the variance of Factor 2 and Factor 4, respectively. Factor 3 included colour and turbidity having strong positive loadings values of 0.87 and 0.76, respectively (Table 4.2).

According to the results of calculation, Factor 1 evidenced in favor of the weathering processes responsible for Al release to groundwater due to pH changes. This conclusion supports the results of recent geochemical research suggesting that at the big depths of Khibiny alkaline massif the reduction conditions are formed promoting the Al leaching [23]. Factor 2 and Factor 3 including hardness, colour and turbidity represented the physical and organoleptic characteristics of the groundwater explaining 25.37% of the dataset total variance.

Table 4.2: Varimax rotated matrix for "Central" water intake field data 1999–2012.

Variable	Factor 1	Factor 2	Factor 3	Factor 4
Al	**−0.77** *)	−0.06	0.17	0.01
pH	**−0.81**	−0.06	−0.14	−0.10
F^-	0.02	−0.04	0.02	**0.93**
NO_3^-	**0.88**	0.17	0.13	−0.05
Cl^-	0.59	0.03	−0.17	0.03
SO_4^{2-}	**0.85**	0.12	0.01	0.03
TDS	**0.90**	0.12	0.10	−0.06
Turbidity	−0.03	0.09	**0.87**	0.09
Colour	0.04	0.31	**0.76**	−0.15
Hardness	0.18	**0.79**	0.02	−0.12
Ca^{2+}	0.08	0.58	-0.16	0.44
Mg^{2+}	0.06	0.65	0.19	0.01
Eigenvalues	3.95	1.55	1.50	1.11
Cumulative (%)	32.89	45.77	58.26	67.53
Variance (%)	32.89	12.88	12.49	9.28

Extraction method: Principal component analysis.
Rotation method: Varimax with Kaiser normalization.
*) Bolded values: strong loadings values.

The HCA applied to group the monitored groundwater quality parameters into clusters based on the similarity revealed three clusters (Figure 4.2). The calculations showed that among analyzed parameters pH and Al — variables considerably exceeding their corresponding guideline values — were grouped into one cluster indicating a metal pollution at the strong alkaline water conditions. Cluster 1 included major anions and TDS reflecting the mineralization content of groundwater, whereas Cluster 3 represented organoleptic parameters and hardness. According to the results of HCA and Spearman correlation, the parameters included in Cluster 1 were highly associated with each other and Al concentrations whereas Cluster 3 combined the parameters that have a low level of association with Al concentrations.

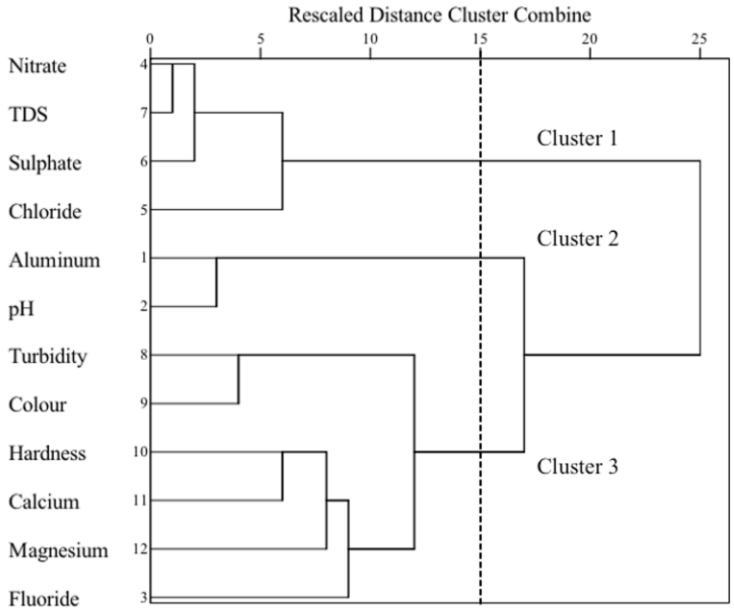

Figure 4.2: HCA dendrogram for 12 groundwater quality parameters of "Central" water intake 1999–2012; dash line represents the chosen distance defining number of clusters.

4.3.3 Groundwater Quality Assessment using CCME WQI

The observations (1999–2012) of six monitored groundwater quality parameters Al, Cl^-, pH, NO_3^-, SO_4^{2-}, TDS from ten wells and the corresponding drinking water guidelines [5] were used to calculate CCME WQI score values. The selection of groundwater quality parameters was based on the results of descriptive statistics and FA/PCA. The calculated CCME WQI score values showed that groundwater quality fell into the fair to marginal water quality category depending on the monitoring year (Figure 4.3). The score values decreased from 69.9 (fair) to 64.8 (marginal) during the monitoring period. Exceeding their acceptable drinking water guidelines, Al concentrations and pH values influenced the calculation results the most. In accordance with the results of calculations, the stable increase of Al concentrations over the years mainly caused the deterioration of groundwater quality and the decreasing WQI values.

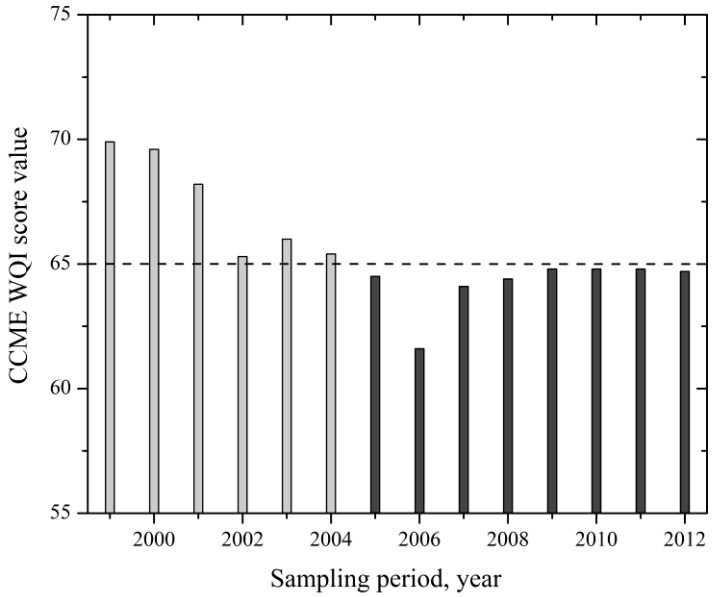

Figure 4.3: Calculated CCME WQI score values 1999–2012; dash line represents the boundary between fair (light grey – CCME WQI > 65) and marginal (dark grey – CCME WQI < 65) water quality categories.

4.4 Conclusions

The present study describes the results of multivariate analysis methods and water quality index application to the outcome of long-term field data groundwater monitoring of Khibiny alkaline massif (Kola Peninsula). The results of analysis provided the assessment and interpretation of the water quality with an emphasis on elevated aluminum concentrations and pH level narrowing the use of groundwater for the local household water supply. Among all considered physico-chemical parameters pH values, concentrations of nitrate, sulphate, and total dissolved solids were the main statistically significant variables associated with the aluminum concentration variation in the groundwater. The application of factor analysis using principal component analysis extraction method (FA/PCA) allowed the reduction of 12 groundwater quality parameters into four dominating influencing factors. These factors explained 67.53% of the original dataset total variance. The first factor including aluminum and pH, nitrate, sulphate, total

dissolved solids – parameters influencing the variation of aluminum concentrations – accounted for about 33% of the total variance.

In accordance with the results of hierarchical cluster analysis (HCA), 12 monitored groundwater quality parameters were grouped into three clusters where Cluster 1 represented major anions and total dissolved solids, Cluster 2 indicated the groundwater contaminants and Cluster 3 consisted of organoleptic parameters and hardness. The calculated Canadian Council of Ministries of the Environment Water Quality Index (CCME WQI) scores values describing the groundwater quality as fair to marginal indicated its gradual deterioration during the monitoring period 1999–2012.

The outcomes of present study using univariate and multivariate statistical methods and the calculated values of WQI are in the agreement with the results of fulfilled earlier univariate analysis of Khibiny alkaline massif groundwater quality suggesting the natural processes as the main cause of prohibitive high aluminum concentrations in the groundwater [9]. The results obtained represent the quantitative data assessment prior to the development of effective technology keeping aluminum concentrations in groundwater under the limits of accepted water quality guidelines. It is believed that the results could be useful to the local authorities in the efforts on the pollution control and water quality management.

4.5 References

[1] J. Wang, G. Liu, H. Liu, P.K.S. Lam, Multivariate statistical evaluation of dissolved trace elements and a water quality assessment in the middle reaches of Huaihe River, Anhui, China, Sci. Total Environ. 583 (2017) 421–431. doi:10.1016/j.scitotenv.2017.01.088.

[2] S.A. Al-Muhtaseb, M.H. El-Naas, S. Abdallah, Removal of aluminum from aqueous solutions by adsorption on date-pit and BDH activated carbons, J. Hazard. Mater. 158 (2008) 300–307. doi:10.1016/j.jhazmat.2008.01.080.

[3] S. Li, J. Li, Q. Zhang, Water quality assessment in the rivers along the water conveyance system of the Middle Route of the South to North Water Transfer Project (China) using multivariate statistical techniques and receptor modeling, J. Hazard. Mater. 195 (2011) 306–317. doi:10.1016/j.jhazmat.2011.08.043.

[4] C.T. Driscoll, W.D. Schecher, The chemistry of aluminum in the environment, Environ. Geochem. Health. 12 (1990) 28–49. doi:10.1007/BF01734046.

[5] U.S. Environmental Protection Agency (USEPA), 2018 Edition of the Drinking Water Standards and Health Advisories Tables, Washington, DC, 2018. https://www.epa.gov/sites/production/files/2018-03/documents/dwtable2018.pdf.

[6] Z. Wang, X. Wei, J. Yang, J. Suo, J. Chen, X. Liu, X. Zhao, Chronic exposure to aluminum and risk of Alzheimer's disease: a meta-analysis, Neurosci. Lett. 610 (2016) 200–206. doi:10.1016/j.neulet.2015.11.014.

[7] J. Wang, Statistical study on distribution of multiple dissolved elements and a water quality assessment around a simulated stackable fly ash, Ecotoxicol. Environ. Saf. 159 (2018) 46–55. doi:10.1016/j.ecoenv.2018.04.057.

[8] T.G. Kazi, M.B. Arain, M.K. Jamali, N. Jalbani, H.I. Afridi, R.A. Sarfraz, J.A. Baig, A.Q. Shah, Assessment of water quality of polluted lake using multivariate statistical techniques: a case study, Ecotoxicol. Environ. Saf. 72 (2009) 301–309. doi:10.1016/j.ecoenv.2008.02.024.

[9] D. Popugaeva, K. Kreyman, A.K. Ray, Study of aluminium in groundwater using chemometric methods, Environ. Technol. (2018). doi:10.1080/09593330.2018.1544667.

[10] V. Simeonov, J.A. Stratis, C. Samara, G. Zachariadis, D. Voutsa, A. Anthemidis, M. Sofoniou, T. Kouimtzis, Assessment of the surface water quality in Northern Greece, Water Res. 37 (2003) 4119–4124. doi:10.1016/S0043-1354(03)00398-1.

[11] K.P. Singh, A. Malik, D. Mohan, S. Sinha, Multivariate statistical techniques for the evaluation of spatial and temporal variations in water quality of Gomti River

(India)— a case study, Water Res. 38 (2004) 3980–3992. doi:10.1016/j.watres.2004.06.011.

[12] H. Wei, H. Yu, G. Zhang, H. Pan, C. Lv, F. Meng, Revealing the correlations between heavy metals and water quality, with insight into the potential factors and variations through canonical correlation analysis in an upstream tributary, Ecol. Indic. 90 (2018) 485–493. doi:10.1016/j.ecolind.2018.03.037.

[13] M. Sarstedt, E. Mooi, Cluster Analysis, in: A Concise Guid. to Mark. Res. Process. Data, Methods Using IBM SPSS Stat., Springer Berlin Heidelberg, Berlin, Heidelberg, 2014: pp. 273–324. doi:10.1007/978-3-662-56707-4.

[14] M. Sarstedt, E. Mooi, Factor Analysis, in: A Concise Guid. to Mark. Res. Process. Data, Methods Using IBM SPSS Stat., Springer Berlin Heidelberg, Berlin, Heidelberg, 2014: pp. 235–272. doi:10.1007/978-3-642-53965-7_8.

[15] Canadian Council of Ministers of the Environment, Canadian Water Quality Guidelines for the Protection of Aquatic Life CCME Water Quality Index, Winnipeg, 2017. https://www.ccme.ca/files/Resources/water/water_quality/WQI Manual EN.pdf.

[16] T. Hurley, R. Sadiq, A. Mazumder, Adaptation and evaluation of the Canadian Council of Ministers of the Environment Water Quality Index (CCME WQI) for use as an effective tool to characterize drinking source water quality, Water Res. 46 (2012) 3544–3552. doi:10.1016/j.watres.2012.03.061.

[17] Khanoranga, S. Khalid, An assessment of groundwater quality for irrigation and drinking purposes around brick kilns in three districts of Balochistan province, Pakistan , through water quality index and multivariate statistical approaches, J. Geochemical Explor. 197 (2019) 14–26. doi:10.1016/j.gexplo.2018.11.007.

[18] N. Adimalla, P. Li, S. Venkatayogi, Hydrogeochemical evaluation of groundwater quality for drinking and irrigation purposes and integrated interpretation with water quality index studies, Environ. Process. 5 (2018) 363–383.

doi:https://doi.org/10.1007/s40710-018-0297-4.

[19] A. V Gudkov, I.L. Kamensky, G.S. Melikhova, V.I. Skiba, I. V Tokarev, I.N. Tolstikhin, The tritium–helium-3 method and its application to groundwater dating by the example of the Kirovsk mine region, Murmansk oblast, Geochemistry Int. 52 (2014) 646–653. doi:10.1134/S001670291405005X.

[20] A.O. Kalashnikov, N.G. Konopleva, Y.A. Pakhomovsky, G.Y. Ivanyuk, Rare earth deposits of the Murmansk Region, Russia - a review, Econ. Geol. 111 (2016) 1529–1559. doi:10.2113/econgeo.111.7.1529.

[21] I.E. Mathisen, A. Mikheeva, O. V Tutubalina, S. Aune, A. Hofgaard, Fifty years of tree line change in the Khibiny Mountains, Russia: advantages of combined remote sensing and dendroecological approaches, Appl. Veg. Sci. 17 (2014) 6–16. doi:10.1111/avsc.12038.

[22] Y.M. Kononov, M. Friedrich, T. Boettger, Regional Summer Temperature Reconstruction in the Khibiny Low Mountains (Kola Peninsula, NW Russia) by Means of Tree-ring Width during the Last Four Centuries, Arctic, Antarct. Alp. Res. 41 (2009) 460–468. doi:10.1657/1938-4246-41.4.460.

[23] S.I. Mazukhina, V.A. Masloboev, K. V Chudnenko, V.A. Bychinsky, A. V Svetlov, S. V Muraviev, Monitoring and physical-chemical modeling of conditions of natural surface and underground waters forming in the Kola North, J. Environ. Sci. Heal. Part A. 47 (2012) 657–668. doi:10.1080/10934529.2012.660037.

[24] V. Konukhin, A. Kozyrev, A. Orlov, U. Smirnov, Isslyedovaniye podzyemnih istochnikov dlya vodosnabzhyeniya gorodov Zapolyar'ya ekologichyeski chistoy vodoy na primyerye goroda Apatiti [The research of underground sources for water supply of cities in the North (city of Apatity as an example)], Arct. Ecol. Econ. 2 (2012) 58–65.

[25] D. Popugaeva, K. Kreyman, A.K. Ray, Analysis and control of Al concentration in groundwater based on mathematical modeling and laboratory tests, in: 2018

AIChE Annu. Meet., American Institute of Chemical Engineers (AIChE), Pittsburgh, PA, (October 28–November 2, 2018).

[26] R. Bouza-Deano, M. Ternero-Rodrıguez, A.J. Fernandez-Espinosa, Trend study and assessment of surface water quality in the Ebro River (Spain), J. Hydrol. 361 (2008) 227–239. doi:10.1016/j.jhydrol.2008.07.048.

[27] J. Hauke, T. Kossowski, Comparison of values of Pearson's and Spearman's correlation coefficients, Quaest. Geogr. 30 (2011) 87–93. doi:10.2478/v10117-011-0021-1.

[28] M. Jampani, S. Huelsmann, R. Liedl, S. Sonkamble, S. Ahmed, P. Amerasinghe, Spatio-temporal distribution and chemical characterization of groundwater quality of a wastewater irrigated system: a case study, Sci. Total Environ. 636 (2018) 1089–1098. doi:10.1016/j.scitotenv.2018.04.347.

[29] J. Wang, Statistical study on distribution of multiple dissolved elements and a water quality assessment around a simulated stackable fly ash, Ecotoxicol. Environ. Saf. 159 (2018) 46–55. doi:10.1016/j.ecoenv.2018.04.057.

[30] M. Varol, Assessment of heavy metal contamination in sediments of the Tigris River (Turkey) using pollution indices and multivariate statistical techniques, J. Hazard. Mater. 195 (2011) 355–364. doi:10.1016/j.jhazmat.2011.08.051.

[31] W. Härdle, L. Simar, Cluster Analysis, in: Appl. Multivar. Stat. Anal., 2nd edition, Springer, Heidelberg, 2007: pp. 271–285. doi:10.1007/978-3-540-72244-1.

[32] C. Liu, K. Lin, Y. Kuo, Application of factor analysis in the assessment of groundwater quality in a blackfoot disease area in Taiwan, Sci. Total Environ. 313 (2003) 77–89. doi:10.1016/S0048-9697(02)00683-6.

Chapter 5

5 Removal of Aluminum from Aqueous Solution by Adsorption on Montmorillonite K10, TiO_2, and SiO_2: Kinetics, Isotherms, and Effect of Ions

5.1 Introduction

There is an increasing concern related to the contamination of drinking water sources (e.g. surface waters such as lakes and rivers, and groundwater) with metals, due to their potential acute (occurring in the short term) and/or chronic (occurring over the long term) adverse effects on the human health [1–3]. Aluminum (Al) is the most abundant metallic element in the Earth's outer crust comprising about 8% of its mass. It is released to the environment from both natural e.g. weathering of rocks and minerals as well as from anthropogenic sources [4,5]. Many natural water bodies are severely influenced by acidification as a consequence of anthropogenic impacts promoting the release of Al into the aquatic environments [6].

The negative effects of Al are currently recognized to be far more chronic than acute [7] while the toxicity of Al depends primarily on its specific forms [8]. The recent research evidenced in favour of that the increased incidence of neurological diseases correlates with the high Al concentrations in drinking water [9,10]. The U.S. Environmental Protection Agency recommended secondary drinking water standards of Al concentration as 0.05–0.20 mg L^{-1} [11]. In a number of cases, the concentrations of Al that have been found in both acidic and alkaline surface and ground waters are recognized as a serious concern in many countries worldwide [4,12]. Several studies on the assessment of groundwater quality revealed drastically elevated Al concentrations. For example, groundwater sources in two regions of Guinea Bissau and in the industrial areas of Ghaziabad, India have Al concentrations reaching up to 4.48 mg L^{-1} and 6.30 mg L^{-1}, respectively [13,14]. Most of springs used for a drinking water supply in Kirazli region, Turkey are described as acidic Al-rich waters having excessive Al concentrations ranging from 13.17 to 15.70 mg L^{-1} [15]. It is not seldom when high exceeding guidelines Al concentrations are found in the wastewater effluents. The drastically elevated

concentrations of Al (5.0÷15.0) × 10^3 mg L^{-1} due to the use of aluminum chloride as a catalyst in the alkylation technology were reported in the wastewater effluent of polymer plant, Angarsk, Russia [16]. The water treatment using alum as a coagulant can also lead to the increased residual Al concentrations in the treated water. Studies led in the United Kingdom revealed Al concentration in wastewater effluent treated by alum as high as 1.0 mg L^{-1} [17,18].

Studies on the removal of various toxic metals from natural water bodies and wastewater have been intensively reported over the past decades [19]. Numerous methods have been proposed for Al removal from aqueous solutions including cation exchange, adsorption, chemical precipitation, membrane filtration, and electrodialysis [7,20–22]. Among available water treatment technologies adsorption is considered as a reliable method for metal removal from aqueous solutions, due to the significant advantages such as low-cost, ease of operation, efficiency, and the availability of the wide range of adsorbents [19]. The current work is focused on Al adsorption from acidic aqueous solution in which Al^{3+}, $Al(OH)^{2+}$, and $Al(OH)_2^{+}$ — the most toxic aluminum species — are presented [8].

The Al removal from water by adsorption by using various organic materials such as starch, activated charcoal, wood charcoal, date-pit and commercially available BDH activated carbon, and seaweed [7,23,24], as well as inorganic adsorbents like powdered marble wastes [25], was previously reported. A recent review on the adsorption of metals by using clay minerals revealed that these minerals are effective toward removing various toxic metal contaminants from aqueous solutions [19]. For example, montmorillonite in its natural and modified forms is considered as a cheap and abundant material having high cation exchange capacity and surface area to remove various metal cations such as Cd^{2+}, Cr^{3+}, Pb^{2+}, Hg^{2+}, etc. [19,26,27]. The use of metal oxides which have favourable sorption to metals in terms of high capacity and selectivity has also been widely investigated [28]. In recent years, the application of titanium dioxide (TiO_2) as an adsorbent which is relatively cheap and non-toxic has been studied for the removal of toxic aquatic metal pollutants from aqueous solutions and showed a good adsorption performance [29,30]. Among other oxides, silica (SiO_2) has also received considerable

attention, because of the large surface area and the ability to effectively adsorb metal ions from aqueous solutions [31].

Although the use of the aforementioned adsorbents for the removal of various metals from water has been extensively investigated, the limited number of studies has been done so far on the Al removal by clay minerals and metal oxides. Most of the reported studies focused on the synthesis of the adsorbing material, and the adsorption isotherms and kinetics, and limited work has been carried out on the effect of ions usually present in natural water bodies and wastewater on the removal of metals by adsorption [23,25,32,33].

In this study, the adsorption of Al in aqueous solution on montmorillonite K10, TiO_2, and SiO_2 was investigated. The main objectives are: (i) to assess the effect of pH on the solubility and adsorption of Al and to determine adsorption kinetic and isotherm parameters, and (ii) to investigate the effect of anions (Cl^-, SO_4^{2-}, HCO_3^-) and cations (Na^+, Ca^{2+}, Mg^{2+}) on the removal of Al by adsorption on K10, TiO_2, and SiO_2.

5.2 Materials and Methods

5.2.1 Chemicals

Aluminum nitrate nonahydrate ($Al(NO_3)_3.9H_2O$; 99.997% trace metals basis), montmorillonite K10, and high-purity grade ($\geq$ 99%) silica gel (SiO_2; particle size 250–500 µm) were purchased from Sigma-Aldrich, Canada. Titanium dioxide (TiO_2; Aeroxide P25 anatase – 80%, rutile – 20%; particle size 30 nm) was obtained from Evonik Corporation (Piscataway, New Jersey, USA). The surface areas of K10, TiO_2, and SiO_2 are 250 $m^2\ g^{-1}$, 50 $m^2\ g^{-1}$, and 300 $m^2\ g^{-1}$, respectively. Hydrochloric acid (HCl) and sodium hydroxide (NaOH) were acquired from Caledon Laboratory Chemicals (Georgetown, Ontario, Canada). Polypropylene syringe filters (0.45 µm) were bought from VWR International (Mississauga, Ontario, Canada). All chemicals were used without further purification. All solutions were prepared in doubly distilled water that

was passed through 18.2 MΩ water purification system (Thermo Scientific, Barnstead™ Easypure™ RODi) (Milli-Q water).

5.2.2 Adsorption Experiments

All experiments were conducted in 125 mL flasks at room temperature (24±1 °C). Al solutions were prepared by dissolving a required amount of $Al(NO_3)_3.9H_2O$ salt in 800 mL of Milli-Q. The initial concentration of Al was 2 mg/L. The pH of the solution was adjusted using 0.5 M HCl and/or 0.5 M NaOH, followed by the addition of the desired amount of adsorbent. The experiments were carried out in an orbital shaker (MaxQ 4000, the Barnstead|Lab-line) at 200 rpm. The collected samples (10 mL) were filtered through 0.45 µm syringe filters to remove the adsorbent. The filtered samples were analyzed for Al concentration.

To investigate the effect of ions usually present in various waters (e.g. groundwater and wastewater) on the removal of Al by adsorption, inorganic ions – Cl^-, HCO_3^-, SO_4^{2-}, Ca^{2+}, Mg^{2+}, and Na^+ were added individually to the Al solution prior to the addition of adsorbent. After the pH adjustment samples were collected and analyzed for Al concentration to rule out any interaction between Al and the ion in the absence of adsorbent.

5.2.3 Analytical Methods

The concentration of aluminum was measured by the inductively coupled plasma – optical emission spectrometry (ICP-OES). The plasma produces temperatures of around 8000 °C making the elements in the sample excited and the concentrations of the elements under consideration can be measured [34]. The most commonly used spectral line for light absorption by aluminum atoms at the wavelength of 309.2 nm was applied in the method [35]. The aluminum concentration was determined by ICP-OES as an average of five replicates. Metrohm 780 pH Meter was used to measure the solution pH.

5.2.4 Adsorption Kinetic and Isotherm Models

A pseudo-first order and pseudo-second order adsorption kinetic models used to describe the adsorption rate are calculated as follows [36,37]:

$$q_t = q_e(1 - exp(-k_1 t)) \quad (5.1)$$

$$q_t = (q_e^2 k_2 t)/(1 + q_e k_2 t) \quad (5.2)$$

where k_1 and k_2 are the pseudo-first and pseudo-second order rate constants in (min^{-1}) and (g (mg min) $^{-1}$) respectively, q_e is the amount of Al adsorbed at equilibrium (mg g^{-1}), and q_t is the amount of Al on the surface of the adsorbent (mg g^{-1}) at any time *t*. The amount of Al adsorbed was calculated using the following equation:

$$q_e = (C_0 - C_e)V/m \quad (5.3)$$

where *V* is the volume of solution (L), *m* is the mass of the adsorbent (g), and C_0 and C_e are the initial and equilibrium concentrations of Al (mg L^{-1}), respectively. The percentage removal was obtained by using equation (5.4).

$$Al\ Removal\ \% = (C_0 - C_e)/C_0 \times 100 \quad (5.4)$$

Three adsorption isotherm models were used to describe the experimental data. The Langmuir adsorption isotherm [38] is expressed as follows:

$$q_e = (Q_0 b C_e)/(1 + bC_e) \quad (5.5)$$

where Q_0 is the maximum monolayer coverage capacity (mg g^{-1}) and *b* is the Langmuir isotherm constant (L mg^{-1}). The Freundlich's adsorption isotherm [36,39] is given by the following equation:

$$Q_e = K_F C_e^{1/n} \quad (5.6)$$

where *n* is the Freundlich intensity parameter, which indicates the magnitude of the adsorption driving force or the surface heterogeneity, K_F is Freundlich isotherm constant

related to adsorption capacity (mg g^{-1})/(mg L^{-1})^n. A joint adsorption isotherm that combines both Langmuir and Freundlich adsorption isotherm models has been proposed by Sips in 1948 [40] and is given as:

$$q_e = (K_S C_e^{\beta_S})/(1 + a_S C_e^{\beta_S}) \tag{5.7}$$

where K_S is the Sips isotherm model constant (L g^{-1}), β_S is the Sips isotherm model exponent, and a_S is the Sips isotherm model constant (L mg^{-1}).

The parameters of adsorption kinetic and isotherm models were calculated by non-linear regression analysis tool, Origin® 8.6 software. The standard error of regression *S* showing the average distance of the data points from the fitted lines that has the same units as the response variable (mg g^{-1}) was used to analyze the fitting degree of kinetic and isotherm models with the laboratory tests data. In non-linear regression, *S* is a more meaningful estimate of the goodness-of-fit rather than the coefficient of determination R^2 [41].

5.3 Results and Discussion

5.3.1 Effect of pH on the Solubility and Adsorption of Al

Initially, the effect of pH on the solubility of Al in aqueous solution was investigated at the pH range of 2.0–7.0. This experiment was conducted in the absence of any adsorbent to ensure that any Al removal is only due to precipitation. The results revealed that Al underwent to precipitation at pH > 4.0 with an increasing trend: Al precipitation of 9.1%, 62.7%, and 93.6% at pH 5.0, 6.0, and 7.0, respectively was observed (Figure 5.1a). These results are in agreement with the observations of other reported studies on the solubility of Al in water [7]. The adsorption of Al by K10, TiO_2, and SiO_2 was then investigated at pH of 2.0, 3.0, and 4.0 as at the aforementioned pH range 2.0–4.0, Al is completely dissolved in water [35]. The contact time for these experiments was 1440 min (24 h).

As the results of laboratory tests showed, there was no Al removal by K10, TiO_2, and SiO_2 observed at pH 2.0 (Figure 5.1b). At pH 3.0, Al was removed by K10 only, but the

removal efficiency within 24 h of contact time was as low as 9.5%. There was no Al removal by TiO_2 and SiO_2 seen at pH values of 2.0 and 3.0. The highest removal of Al by all adsorbents used in the study was achieved at pH 4.0. The removal close to 90%, 54%, and 66% was obtained by K10, TiO_2, and SiO_2, respectively, at the same adsorbent dose of 2.0 g L^{-1} and initial Al concentration of 2 mg L^{-1}. Similar results showing the optimal pH value of 4.0 for Al adsorption from acidic aqueous solution were mentioned in other studies [7,42]. Therefore, pH 4.0 was used for adsorption kinetic and isotherm studies, as well as to investigate the effect of ions on Al adsorption by K10, TiO_2, and SiO_2.

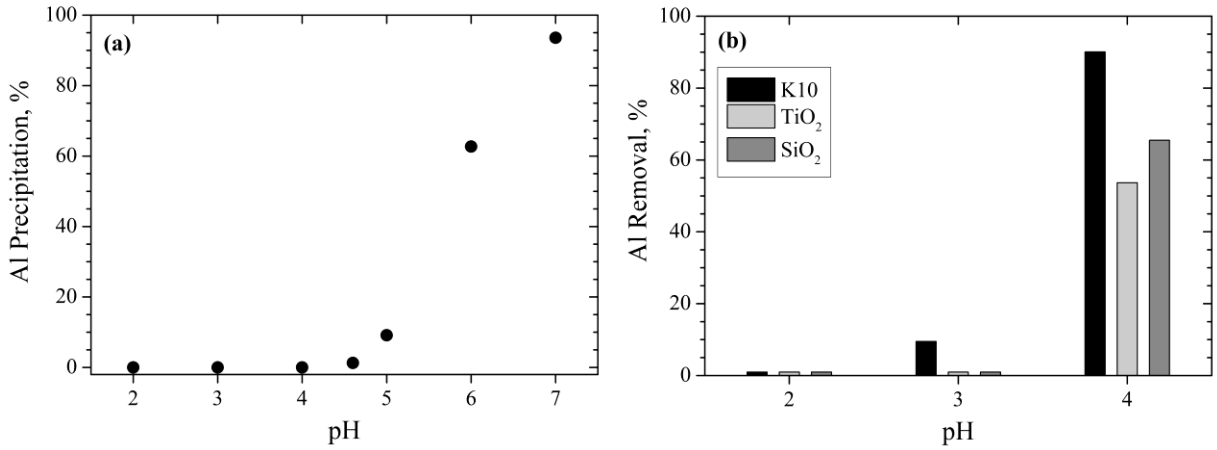

Figure 5.1: Effect of pH on the solubility (a) and adsorption (b) of Al by various adsorbents. Experimental conditions: $[Al]_0$ = 2 mg L^{-1}; [K10] = [TiO_2] = [SiO_2] = 2.0 g L^{-1}; contact time = 24 h; T = 24±1 °C.

5.3.2 Effect of Initial Al Concentration and Contact Time

The effect of contact time on the adsorption of Al by K10, TiO_2, and SiO_2 was investigated at two initial Al concentrations – 2 mg L^{-1} and 5 mg L^{-1}. The equilibrium time of 120 min for K10, 240 min for both TiO_2 and SiO_2 at pH 4.0 was revealed (Figure 5.2). There was no significant effect on the adsorption of Al after this period of time.

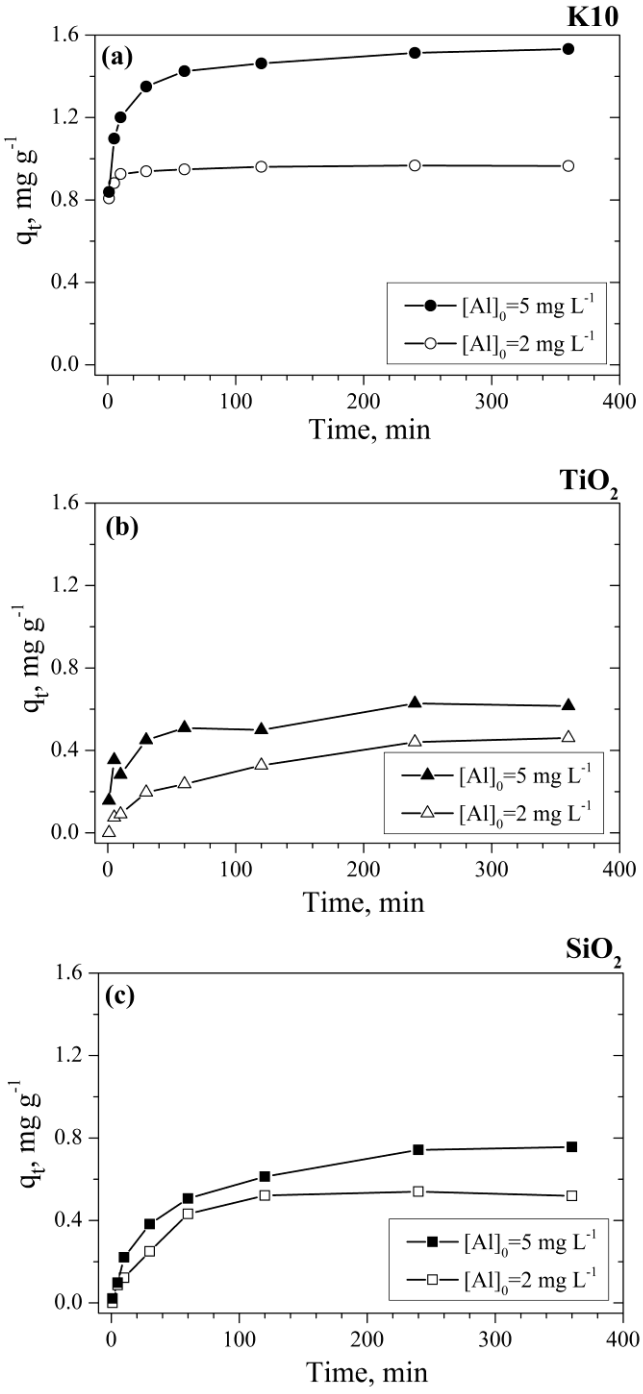

Figure 5.2: Effect of contact time and Al initial concentration on Al removal by K10 (a), TiO_2 (b), and SiO_2 (c). Experimental conditions: [K10] = [TiO_2] = [SiO_2] = 2.0 g L^{-1}; T = 24±1 °C; pH = 4.0.

The adsorption capacities (q_e) of all studied adsorbents increased with an increase of the initial concentration of Al. The reason of such a phenomenon can be connected with the increased driving force at the higher Al concentration which overcomes mass transfer resistance resulting in higher adsorption capacities [37]. Results obtained showed clearly that K10 exhibits a higher adsorption capacity compare to both TiO_2 and SiO_2. For TiO_2 and SiO_2, q_e was higher at higher initial Al concentration, as shown in Figure 5.2. The adsorption capacities of both TiO_2 and SiO_2 were almost similar with a slightly higher capacity of SiO_2 to adsorb Al at pH 4.0 (Figure 5.2b,c).

5.3.3 Adsorption Kinetics

A pseudo-first order and a pseudo-second order kinetic models were used to fit the experimental data obtained at pH 4.0 (Figure 5.3). The rate of Al adsorption on K10 was better described by the pseudo-second order model. The calculated *S* values of pseudo-first and pseudo-second order models were similar, however, *S* value of pseudo-second order model was slightly lower (Table 5.1). Additionally, the adsorption capacity q_e calculated using the pseudo-second order kinetic model was closer to the q_e^{test} value. These results (i.e. a better fit of pseudo-second order kinetic model) suggested that chemisorption most likely controls the adsorption of Al on K10 [43,44]. In the case of TiO_2, the obtained *S* values for both kinetic models were similar, however, the q_e^{test} value was equal to the calculated using the pseudo-first kinetic model q_e value. The adsorption of Al on SiO_2 followed better a pseudo-first order kinetic model as indicated by the calculated *S* values. Among adsorbents tested, K10 had a much higher adsorption rate (Figure 5.3, Table 5.1). It is worth mentioning that K10 required approximately 30 min to achieve an Al concentration below the limit of 0.20 mg L^{-1}.

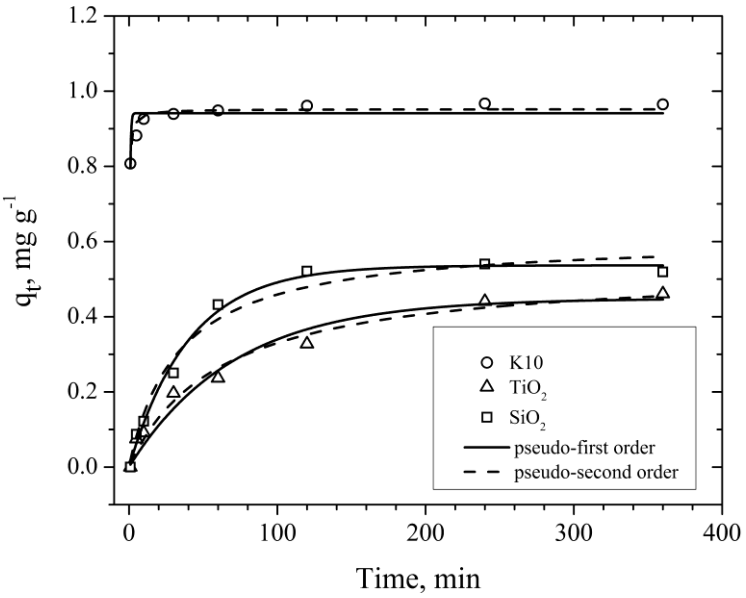

Figure 5.3: Laboratory test data and fitted curves of pseudo-first and pseudo-second order kinetic models of the Al adsorption by K10, TiO_2, and SiO_2. Experimental conditions: $[Al]_0$ = 2 mg L^{-1}; [K10] = [TiO_2] = [SiO_2] = 2.0 g L^{-1}; pH = 4.0; T = 24±1 °C.

Table 5.1: Adsorption kinetic models fitting parameters of Al adsorption on 2.0 g L^{-1} K10, TiO_2 and SiO_2 at pH 4.0 and room temperature (T = 24±1 °C) based on the results of testing.

Adsorbent	q_e^{test} *), mg g^{-1}	Kinetic model					
		Pseudo-first order			Pseudo-second order		
		k_1, min^{-1}	q_e, mg g^{-1}	S, mg g^{-1}	k_2, g (mg min) $^{-1}$	q_e, mg g^{-1}	S, mg g^{-1}
K10	0.96	1.95	0.94	0.03	5.41	0.95	0.02
TiO_2	0.45	0.01	0.45	0.03	0.03	0.53	0.03
SiO_2	0.53	0.03	0.54	0.02	0.05	0.61	0.04

*) q_e^{test} was determined based on laboratory tests by using equation (5.3).

5.3.4 Adsorption Isotherms

The adsorption equilibrium data of Al removal from aqueous solution on K10, TiO_2, and SiO_2 were obtained at room temperature (24±1 °C) and pH 4.0. The concentrating range of adsorbents was 1.0–5.0 g L^{-1}. Figure 5.4 shows fitted adsorption equilibrium data using isotherms models given by the equations (5.6), (5.5), and (5.7) for two-parameter Freundlich and Langmuir isotherm models, and a three-parameter Sips isotherm model, respectively.

According to the results (Figure 5.4, Table 5.2), the adsorption data of Al on K10, TiO_2, and SiO_2 showed a satisfactory agreement with Freundlich adsorption isotherm model indicating the heterogeneous surface property of the adsorbents. For K10 and SiO_2, the determined Freundlich model constant *n* was higher than 1 (Table 5.2). This suggests nonhomogeneous multilayer adsorption of Al on K10 and SiO_2 [44]. A slightly lower capability of the Langmuir isotherm model to describe the adsorption equilibrium data on SiO_2 was indicated by the higher *S* value, while Al adsorption data on K10 can be reasonably described by the three isotherms. The Langmuir model parameters for Al adsorption on TiO_2 were found to be negative therefore no physical meaning could be withdrawn.

The Sips isotherm model is a combined form of Langmuir and Freundlich expressions [45] and the model parameters were fitted using the following constraints K_S, β_S, $a_S > 0$ where β_S can vary between 0 and 1 [40]. The three-parameter model reduced to the Freundlich isotherm that can be explained by the low adsorbate concentrations [40,45]. Results showed that the Freundlich isotherm model was more preferred to describe the Al adsorption equilibrium data on TiO_2 and SiO_2 than both the Langmuir and Sips adsorption isotherm models while Freundlich and Sips isotherm models were more applicable to simulate the adsorption behaviour of Al on K10 (Table 5.2).

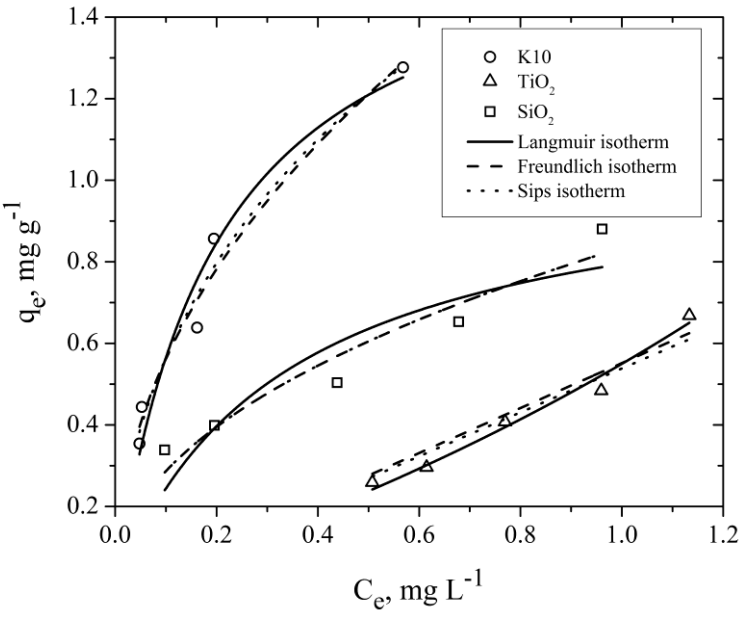

Figure 5.4: Fitted curves of Langmuir, Freundlich, and Sips isotherm equations for equilibrium data of Al adsorption on K10, TiO_2, and SiO_2. Experimental conditions: $[Al]_0$ = 2 mg L^{-1}; [K10] = [TiO_2] = [SiO_2] = 1.0–5.0 g L^{-1}; pH = 4.0; T = 24±1 °C.

Table 5.2: Adsorption isotherm models fitting parameters of Al adsorption on K10, TiO_2 and SiO_2 at pH 4.0 and room temperature (T = 24±1 °C).

Adsorbent	Isotherm model									
	Langmuir			Freundlich			Sips			
	Q_0, mg g^{-1}	b, L mg^{-1}	S, mg g^{-1}	K_F, (mg g^{-1}) /(mg L^{-1})^n	n	S, mg g^{-1}	K_S, L g^{-1}	β_S	a_S, L mg^{-1}	S, mg g^{-1}
K10	1.69	5.01	0.09	1.69	2.09	0.07	2.51	0.59	0.57	0.08
TiO_2	–	–	–	0.55	1.00	0.04	0.54	1.00	10^{-16}	0.04
SiO_2	1.06	2.99	0.10	0.83	2.15	0.07	0.83	0.46	10^{-16}	0.07

Among adsorbents tested, the use of K10 for Al removal at pH 4.0 is the most effective as the adsorption rate is relatively high and the small adsorbent doses are sufficient to significantly decrease Al concentration. A lower amount of K10 than TiO_2 or SiO_2 was needed to decrease Al concentration below the standard limit of 0.20 mg L^{-1}. The concentration of Al decreased from its initial concentration to 0.19 mg L^{-1} by 2.0 g L^{-1} of K10. The similar effect can be achieved by using 5.0 g L^{-1} of SiO_2 while adding the same concentration of TiO_2 could remove not more than about 72%. It is worth mentioning that the increase of both TiO_2 and SiO_2 doses had a significant effect on Al removal where the use of 5.0 g L^{-1} improved the percentage Al removal almost twice compared to 1.0 g L^{-1}, whereas the same doses of K10 provided the enhancement of Al removal in about 1.5 times (Table S5.1 of Appendix E).

5.3.5 Effect of Ions on the Adsorption of Al

The effect of water constituents such as ions on the removal of contaminants is important for the development of water treatment technologies. The effects of divalent cations (Ca^{2+} and Mg^{2+}), monovalent cation (Na^{+}), and anions (Cl^{-}, SO_4^{2-}, and HCO_3^{-}) usually present in surface waters, groundwater, and wastewater, on the Al adsorption on tested materials were investigated. The concentrations of the individually mixed ions were chosen to be relevant to concentrations found in the natural water bodies and wastewater [46]. The solution pH was adjusted to 4.0 before the ions addition. The further pH adjustment was needed only after HCO_3^{-} ions addition to Al solution, while the addition of other ions did not influence the pH value. The adjusted pH remained unchanged throughout the tests. Samples of the Al-ion solution prior to the addition of adsorbent were taken and analyzed for Al concentration to rule out any interaction between the ion and Al. The *t*-confidence interval procedure (*t*-test) with a 95% confidence interval comparing two independent groups representing the results of adsorbent-Al (control) and adsorbent-Al-ion experiments was applied using Minitab® 17.1.0 software to laboratory test data. It allowed to conclude the presence of a statistically significant difference between Al removal by adsorbents tested and Al adsorption in the presence of ions under consideration (Tables S5.2, S5.3, and S5.4 of Appendix E).

The results showed that in the case of K10 no statistically significant effect was observed by adding Na^+, Cl^-, SO_4^{2-} or HCO_3^- ions to the solution. The removal of Al by K10 was negatively affected by the presence of Ca^{2+} and Mg^{2+} ions – the removal decreased from 89.2% (control) to 35.5% and to 64.0%, for Ca^{2+} and Mg^{2+}, respectively (Figure 5.5a). There was no apparent effect of Mg^{2+} ions seen in the case of Al removal by TiO_2 while a presence of Ca^{2+} ions caused the adverse effect on Al adsorption and the Al removal decreased from 53.7% (control) to 44.5% (Figure 5.5b). The removal of Al by SiO_2 was negatively affected by both Ca^{2+} and Mg^{2+} ions, as well as SO_4^{2-} ions, where the Al removal decreased from 65.5% (control) to 47.4%, 54%, and 43.2%, respectively (Figure 5.5c).

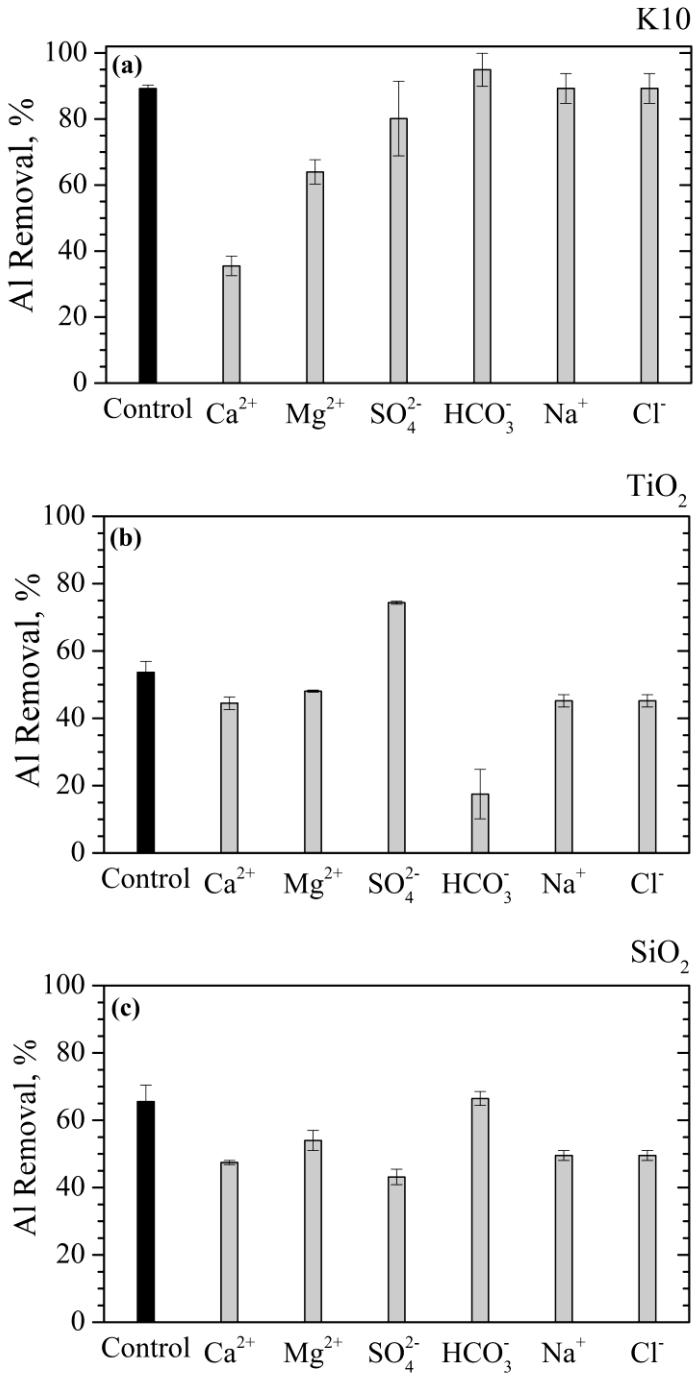

Figure 5.5: Effect of calcium (Ca^{2+}; $CaCl_2$), magnesium (Mg^{2+}; $MgCl_2.6H_2O$), sulfate (SO_4^{2-}; Na_2SO_4), bicarbonate (HCO_3^-; $NaHCO_3$), sodium (Na^+; NaCl), and chloride (Cl^-; NaCl) on Al adsorption on K10 (a), TiO_2 (b), and SiO_2 (c) at equilibrium time. Experimental conditions: $[Al]_0$ = 2 mg L^{-1}; [K10] = [TiO_2] = [SiO_2] = 2.0 g L^{-1}; initial concentration of ions: $[Ca^{2+}]$ = [SO_4^{2-}] = 2 mM, $[Mg^{2+}]$ = $[HCO_3^-]$ = 1 mM, $[Na^+]$ = $[Cl^-]$ = 4 mM; pH = 4.0; T = 24±1 °C.

There was observed a negative effect on TiO_2 adsorption capacity in the presence of HCO_3^- ions in the solution – the adsorption efficiency lowered from 53.7% (control) to 17.5%, while the presence of SO_4^{2-} ions had a positive effect on TiO_2 performance where Al removal increased from 53.7% (control) to 74.3% (Figure 5.5b). It is worth mentioning that the Al adsorption efficiency using 2.0 g L^{-1} of TiO_2 in the presence of SO_4^{2-} ions was similar to the percentage of Al removal by the TiO_2 concertation of 5.0 g L^{-1} without SO_4^{2-} ions (Table S5.1 of Appendix E). As the ionic strength may be changing by adding ions, it is assumed that some of the observed effects on aluminum removal by K10, TiO_2, and SiO_2 may be related to the variation in ionic strength rather than the ions effect [47,48].

The results of current study on Al adsorption by K10, TiO_2, and SiO_2 were compared to literature data on Al removal from acidic aqueous solutions (pH close to 4.0) (Table 5.3). The adsorbents tested are within the group of effective materials presented in Table 5.3. Al removal reaches 54–97% during 120–240 min by using K10, TiO_2, and SiO_2. Among them, K10 exhibited a significantly higher adsorption rate. Laboratory tests showed that K10 dose of 2.0 g L^{-1} was enough to remove up to 80% of Al throughout the initial five minutes and up to 89% at the equilibrium time 120 min. A comparable effectiveness under the experimental conditions when the sorbent dose and initial Al concentration were close to the ones used in current study is achieved by adsorption on rice husk char removing 98% of Al within the 120 min of equilibrium time (Table 5.3). The increase of K10 dose from 2.0 g L^{-1} to 5.0 g L^{-1} allowed to obtain 97% of Al removal during 120 min. A relatively low adsorbent doses applied, a short equilibrium time and high performance toward the Al removal from acidic aqueous solution are the features witnessing in favour of tested and discussed in current study adsorbents compare to a number of others including some activated carbon materials and their modified forms.

Table 5.3: Performance of various adsorbents toward Al removal from acidic aqueous solution based on the results of current study and some literature data.

Sorbent	Reference	pH	Sorbent dose, g L^{-1}	$[Al]_0$, mg L^{-1}	Equilibrium (or contact) time, min	Al removal, %	Effect of ions study
Beach cast seaweed	[24]	4.0	2.5	10.0	30 *)	80	–
				100.0	30 *)	80	
Rice husk char	[42]	4.2	2.0	3.0	120	98	–
Granular activated carbon	[42]	4.2	4.0	3.0	120	N/A	–
Activated carbon	[49]	4.0	20.0	3.0	5	95 **)	–
Date-pit activated carbon	[7]	4.0	2.0	5.0	1440 *)	53 **)	–
				50.0	1440 *)	18 **)	
BDH activated carbon	[7]	4.0	2.0	5.0	1440 *)	54 **)	–
				50.0	1440 *)	18 **)	
K10	Current study	4.0	2.0	2.0	120	89	+
			5.0		120	97	
TiO_2	Current study	4.0	2.0	2.0	240	54	+
			5.0		240	72	
SiO_2	Current study	4.0	2.0	2.0	240	66	+
			5.0		240	95	

*) Contact time.
**) Al removal % calculated using equations (5.3), (5.4) and the literature sources data.
Presence (+) or absence (−) of the ions tests results.
N/A: not applicable.

5.4 Conclusions

In this study, the adsorption of aluminum from aqueous solution on three adsorbents: K10, TiO_2, and SiO_2 at acidic conditions was examined. The effects of pH, initial aluminum concentration, contact time, adsorbent amount, and ions such as calcium, magnesium, sulphate, bicarbonate, sodium, and chloride were investigated. The laboratory tests showed that at pH 2.0, 3.0, and 4.0, the aluminum nitrate salt was found

to be completely soluble. The maximum adsorption capacities of K10, TiO_2 and SiO_2 were obtained at pH 4.0. The aluminum uptake by K10, TiO_2, and SiO_2 was up to 97.4%, 71.9%, and 94.6%, respectively at the 5.0 g L^{-1} adsorbents dose. The equilibrium time of 120 min for K10, 240 min for both TiO_2 and SiO_2 at pH 4.0 was revealed. The results showed that K10 exhibited significantly faster adsorption rates compare to TiO_2 and SiO_2. The K10 adsorbent removed more than 80% of aluminum concentration within the first five minutes of contact time. The equilibrium data of aluminum adsorption on TiO_2 and SiO_2 were described most satisfactory by the Freundlich isotherm model indicating a heterogeneous surface property of the adsorbents. Aluminum adsorption data on K10 can be reasonably described by the three isotherm models examined. Based on the experimental results it was found that various ions can negatively influence the adsorption of aluminum by the studied adsorbents. The presence of calcium and magnesium ions in the solution caused the highest negative effect on aluminum removal by K10, while the presence of HCO_3^- and SO_4^{2-} ions gave the highest negative effects on aluminum removal by TiO_2 and SiO_2, respectively.

5.5 References

[1] B. Thalmann, U. von Gunten, R. Kaegi, Ozonation of municipal wastewater effluent containing metal sulfides and metal complexes: kinetics and mechanisms, Water Res. 134 (2018) 170–180. doi:10.1016/j.watres.2018.01.042.

[2] A. Ali, A. Gul, A. Mannan, M. Zia, Efficient metal adsorption and microbial reduction from Rawal Lake wastewater using metal nanoparticle coated cotton, Sci. Total Environ. 639 (2018) 26–39. doi:10.1016/j.scitotenv.2018.05.133.

[3] I. Perez-Alvarez, H. Islas-Flores, L.M. Gomez-Olivan, D. Barcelo, M. Lopez De Alda, S. Perez Solsona, L. Sanchez-Aceves, N. SanJuan-Reyes, M. Galar-Martínez, Determination of metals and pharmaceutical compounds released in hospital wastewater from Toluca, Mexico, and evaluation of their toxic impact, Environ. Pollut. 240 (2018) 330–341. doi:10.1016/j.envpol.2018.04.116.

[4] C.T. Driscoll, W.D. Schecher, The chemistry of aluminum in the environment, Environ. Geochem. Health. 12 (1990) 28–49. doi:10.1007/BF01734046.

[5] Agency for Toxic Substances and Disease Registry (ATSDR), Toxicological Profile for Aluminum, Atlanta, GA, 2008.

[6] E. Lydersen, S. Löfgren, R.T. Arnesen, Metals in Scandinavian surface waters: effects of acidification, liming, and potential reacidification, Crit. Rev. Environ. Sci. Technol. 32 (2002) 73–295. doi:10.1080/10643380290813453.

[7] S.A. Al-Muhtaseb, M.H. El-Naas, S. Abdallah, Removal of aluminum from aqueous solutions by adsorption on date-pit and BDH activated carbons, J. Hazard. Mater. 158 (2008) 300–307. doi:10.1016/j.jhazmat.2008.01.080.

[8] J. Namiésnik, A. Rabajczyk, The speciation of aluminum in environmental samples, Crit. Rev. Anal. Chem. 40 (2010) 68–88. doi:10.1080/10408340903153234.

[9] Z. Wang, X. Wei, J. Yang, J. Suo, J. Chen, X. Liu, X. Zhao, Chronic exposure to aluminum and risk of Alzheimer's disease: a meta-analysis, Neurosci. Lett. 610 (2016) 200–206. doi:10.1016/j.neulet.2015.11.014.

[10] C.E. Cicero, G. Mostile, R. Vasta, V. Rapisarda, S.S. Signorelli, M. Ferrante, M. Zappia, A. Nicoletti, Metals and neurodegenerative diseases. A systematic review, Environ. Res. 159 (2017) 82–94. doi:10.1016/j.envres.2017.07.048.

[11] U.S. Environmental Protection Agency (USEPA), 2018 Edition of the Drinking Water Standards and Health Advisories Tables, Washington, DC, 2018. https://www.epa.gov/sites/production/files/2018-03/documents/dwtable2018.pdf.

[12] D. Popugaeva, K. Kreyman, A.K. Ray, Study of aluminium in groundwater using chemometric methods, Environ. Technol. (2018). doi:10.1080/09593330.2018.1544667.

[13] S. Kumari, A.K. Singh, A.K. Verma, N.P.S. Yaduvanshi, Assessment and spatial

distribution of groundwater quality in industrial areas of Ghaziabad, India, Env. Monit Assess. 186 (2014) 501–514. doi:10.1007/s10661-013-3393-y.

[14] M. Ferrante, S.S. Signorelli, L.S. Ferlito, A. Grasso, A. Dimartino, C. Copat, Groundwater-based water wells characterization from Guinea Bissau (Western Africa): a risk evaluation for the local population, Sci. Total Environ. 619–620 (2018) 916–926. doi:10.1016/j.scitotenv.2017.11.176.

[15] C. Bakar, H.I.Ö. Karaman, A. Baba, F. Şengünalp, Effect of high aluminum concentration in water resources on human health, case study: Biga Peninsula, northwest part of Turkey, Arch. Environ. Contam. Toxicol. 58 (2010) 935–944. doi:10.1007/s00244-009-9435-3.

[16] I.O. Dolganova, N.S. Belinskaya, E.N. Ivashkina, V.V. Martemyanova, E.V. Tkachev, Improving the efficiency of technology producing ethylbenzene by using mathematical modeling, Fundam. Res. 8 (2013) 595–600. http://www.fundamental-research.ru/ru/article/view?id=31964.

[17] M.J. Gardner, S.D.W. Comber, Aluminium speciation in effluents and receiving waters, J. Environ. Monit. 5 (2003) 902–905. doi:10.1039/b308409d.

[18] S.D.W. Comber, M.J. Gardner, J. Churchley, Aluminium speciation: implications of wastewater effluent dosing on river water quality, Chem. Speciat. Bioavailab. 17 (2005) 117–128. doi:10.3184/095422905782774874.

[19] M.K. Uddin, A review on the adsorption of heavy metals by clay minerals, with special focus on the past decade, Chem. Eng. J. 308 (2017) 438–462. doi:10.1016/j.cej.2016.09.029.

[20] P.T. Srinivasan, T. Viraraghavan, K.S. Subramanian, Aluminium in drinking water: an overview, Water SA. 25 (1999) 47–55.

[21] Z. Aly, A. Graulet, N. Scales, T. Hanley, Removal of aluminium from aqueous solutions using PAN-based adsorbents: characterisation, kinetics, equilibrium and thermodynamic studies, Environ. Sci. Pollut. Res. 21 (2014) 3972–3986.

doi:10.1007/s11356-013-2305-6.

[22] W. Wang, H. Yang, H. Zhao, Z. Jiang, Transfer and transport of aluminum in filtration unit, J. Environ. Sci. 19 (2007) 897–901. doi:10.1016/S1001-0742(07)60149-1.

[23] P.M. Choksi, V.Y. Joshi, Adsorption kinetic study for the removal of nickel(II) and aluminum(III) from an aqueous solution by natural adsorbents, Desalination. 208 (2007) 216–231. doi:10.1016/j.desal.2006.04.081.

[24] P. Lodeiro, Á. Gudiña, L. Herrero, R. Herrero, M.E. Sastre de Vicente, Aluminium removal from wastewater by refused beach cast seaweed. Equilibrium and dynamic studies, J. Hazard. Mater. 178 (2010) 861–866. doi:10.1016/j.jhazmat.2010.02.017.

[25] S.E. Ghazy, S.E. Samra, A.M. Mahdy, S.M. El-Morsey, Kinetic investigation of the removal of aluminum from water samples by adsorption onto powdered marble wastes, Sep. Sci. Technol. 40 (2005) 1797–1815. doi:10.1081/SS-200064573.

[26] C.O. Ijagbemi, M. Baek, D. Kim, Montmorillonite surface properties and sorption characteristics for heavy metal removal from aqueous solutions, J. Hazard. Mater. 166 (2009) 538–546. doi:10.1016/j.jhazmat.2008.11.085.

[27] L. de Pablo, M.L. Chávez, M. Abatal, Adsorption of heavy metals in acid to alkaline environments by montmorillonite and Ca-montmorillonite, Chem. Eng. J. 171 (2011) 1276–1286. doi:10.1016/j.cej.2011.05.055.

[28] M. Hua, S. Zhang, B. Pan, W. Zhang, L. Lv, Q. Zhang, Heavy metal removal from water/wastewater by nanosized metal oxides: a review, J. Hazard. Mater. 211–212 (2012) 317–331. doi:10.1016/j.jhazmat.2011.10.016.

[29] Y.C. Sharma, V. Srivastava, V.K. Singh, S.N. Kaul, C.H. Weng, Nano-adsorbents for the removal of metallic pollutants from water and wastewater, Environ. Technol. 30 (2009) 583–609. doi:10.1080/09593330902838080.

[30] I. Ali, New generation adsorbents for water treatment, Chem. Rev. 112 (2012) 5073–5091. doi:10.1021/cr300133d.

[31] M.E. Mahmoud, I.M.M. Kenawy, M.A.H. Hafez, R.R. Lashein, Removal, preconcentration and determination of trace heavy metal ions in water samples by AAS via chemically modified silica gel N-(1-carboxy-6-hydroxy) benzylidenepropylamine ion exchanger, Desalination. 250 (2010) 62–70. doi:10.1016/j.desal.2009.09.009.

[32] W.J. Walker, C.S. Cronan, H.H. Patterson, A kinetic study of aluminum adsorption by aluminosilicate clay minerals, Geochim. Cosmochim. Acta. 52 (1988) 55–62. doi:10.1016/0016-7037(88)90056-7.

[33] G. Brown, A.C.D. Newman, The reactions of soluble aluminium with montmorillonite, J. Soil Sci. 24 (1973) 339–354. doi:10.1111/j.1365-2389.1973.tb00770.x.

[34] P. Chowdhury, S. Athapaththu, A. Elkamel, A.K. Ray, Visible-solar-light-driven photo-reduction and removal of cadmium ion with Eosin Y-sensitized TiO2 in aqueous solution of triethanolamine, Sep. Purif. Technol. 174 (2017) 109–115. doi:10.1016/j.seppur.2016.10.011.

[35] G. Sposito, The Environmental Chemistry of Aluminum, 2nd edition, Lewis Publishers, Boca Raton, FL, 1996.

[36] H.N. Tran, S.-J. You, A. Hosseini-Bandegharaei, H.-P. Chao, Mistakes and inconsistencies regarding adsorption of contaminants from aqueous solutions: a critical review, Water Res. 120 (2017) 88–116. doi:10.1016/j.watres.2017.04.014.

[37] X. Xie, R. Deng, Y. Pang, Y. Bai, W. Zheng, Y. Zhou, Adsorption of copper(II) by sulfur microparticles, Chem. Eng. J. 314 (2017) 434–442. doi:10.1016/j.cej.2016.11.163.

[38] I. Langmuir, The constitution and fundamental properties of solids and liquids. Part I. Solids, J. Am. Chem. Soc. 38 (1916) 2221–2295. doi:10.1021/ja02268a002.

[39] H.M.F. Freundlich, Over the adsorption in solution, J. Phys. Chem. 57 (1906) 385–471.

[40] R. Sips, On the structure of a catalyst surface, J. Chem. Phys. 16 (1948) 490–495. doi:10.1063/1.1746922.

[41] A.-N. Spiess, N. Neumeyer, An evaluation of R2 as an inadequate measure for nonlinear models in pharmalogical and biochemical research: a Monte Carlo approach. BMC Pharmacol. 10 (2010) 1–11. doi:http://www.biomedcentral.com/1471-2210/10/6.

[42] T.S. Singh, B. Parikh, K. Pant, Investigation on the sorption of aluminium in drinking water by low-cost adsorbents, Water SA. 32 (2006) 49–54. doi:http://dx.doi.org/10.4314/wsa.v32i1.5239.

[43] Z. Li, L. Wu, H. Liu, H. Lan, J. Qu, Improvement of aqueous mercury adsorption on activated coke by thiol-functionalization, Chem. Eng. J. 228 (2013) 925–934. doi:10.1016/j.cej.2013.05.063.

[44] H.S. Niasar, H. Li, T. Venkateswara Rao Kasanneni, M.B. Ray, C. Xu, Surface amination of activated carbon and petroleum coke for the removal of naphthenic acids and treatment of oil sands process-affected water (OSPW), Chem. Eng. J. 293 (2016) 189–199. doi:10.1016/j.cej.2016.02.062.

[45] K.Y. Foo, B.H. Hameed, Insights into the modeling of adsorption isotherm systems, Chem. Eng. J. 156 (2010) 2–10. doi:10.1016/j.cej.2009.09.013.

[46] K. Manoli, G. Nakhla, A.K. Ray, V.K. Sharma, Oxidation of caffeine by acid-activated ferrate(VI): effect of ions and natural organic matter, AIChE J. 63 (2017) 4998–5006. doi:10.1002/aic.15878.

[47] Z. Reddad, C. Gerente, Y. Andres, P. Le Cloirec, Adsorption of several metal ions onto a low-cost biosorbent: kinetic and equilibrium studies, Environ. Sci. Technol. 36 (2002) 2067–2073. doi:10.1021/es0102989.

[48] Y.H. Li, J. Ding, Z. Luan, Z. Di, Y. Zhu, C. Xu, D. Wu, B. Wei, Competitive adsorption of Pb2+, Cu2+ and Cd2+ ions from aqueous solutions by multiwalled carbon nanotubes, Carbon. 41 (2003) 2787–2792. doi:10.1016/S0008-6223(03)00392-0.

[49] P.G. Pour, M.A.L.I. Takassi, T. Hamoule, Removal of Aluminum from Water and Industrial Waste Water, Orient. J. Chem. 30 (2014) 1365–1369. doi:http://dx.doi.org/10.13005/ojc/300356.

Chapter 6

6 Removal of Aluminum from Alkaline Aqueous Solution by Adsorption on TiO_2 and Vermiculite Concrete-Supported Ferric Oxyhydroxide

6.1 Introduction

The contamination of natural water sources with toxic metals has been recognized as one of the severe environmental problems nowadays [1–3]. Although several adverse health effects of metals have been known for a long time, the exposure to the metals goes on, and is even increasing in some areas [4]. Aluminum (Al) is the most plentiful metal in the Earth's crust and due to this is widely distributed in the environment [5]. The natural processes such as Al leaching from minerals as well as anthropogenic influence including the application of Al-based coagulants/catalysts for various technological processes such for example as water treatment and alkylation are within the typical sources of Al release to the aquatic environments where the metal speciation and solubility is influenced by solution pH [5–8]. The excessive concentrations of Al are observed in both acidic and alkaline surface and ground waters [9–11].

Drinking water is one of the main sources of Al exposure to human [12,13]. Various studies have implicated that Al accumulation in human body can cause neurotoxicity leading to the increased risk of neurological disorders such as Alzheimer's disease [14–16]. Several federal agencies and organizations developed health regulations and recommendations for Al in water. For example, the recommended secondary standard of Al level in drinking water in accordance with U.S. Environmental Protection Agency is set at a concentrating range of 0.05–0.20 mg L^{-1} [17]. According to a recent World Health Organization global overview of national regulations and standards for drinking water quality, the majority of countries specify the limit of Al concentration equals to 0.20 mg L^{-1} [18].

The problem of elevated Al concentrations in natural water sources is widespread [19–22]. The prohibitive Al concentration in the surface water, spring water, and groundwater

are the serious health concerns when the water is used for the local water supply [11,21,23]. Especially alarming situations appear when prohibitive Al concentration is observed in drinking water. For example, the groundwater located in the southern part of the Khibiny alkaline massif (Kola Peninsula, Russia) belonging to the Baltic hydrogeological massif over the past three decades became one of the essential sources of household water supply in the area. According to the recent results of Khibiny water intake field dataset assessment, the concentrations of Al in the groundwater varying within 0.19–1.81 mg L^{-1} that exceed the drinking water guidelines of 0.20 mg L^{-1} up to nine times [20]. To date, there is no a reliable solution solving the problem of elevated aluminum concentrations in the alkaline groundwater that is feasible to implement in the Khibiny area and facilitate the household water supply management satisfying health regulations.

Among available water treatment technologies adsorption is considered as a reliable method for the removal of various metals from aqueous solutions offering numerous advantages including cost-effectiveness, flexibility in design and operation as well as a wide variety of adsorbents available [24]. The key aspect is finding the effective adsorbent that is capable to remove the target metal pollutant from aqueous solutions effectively. Despite numerous adsorbents have been tested to remove metal pollutants from aqueous solutions just a limited number of investigations were dedicated to the adsorption of Al. Among them, only a few investigations describe Al removal by means of adsorption from alkaline aqueous solutions (pH $\geq$ 8.0) [25,26]. Most studies on Al adsorption are focused on the application of organic or having the organic component materials at the solution where the pH values are within the acidic range [27–29]. The number of studies investigating the effect of ions common for the natural water bodies such as Ca^{2+}, Mg^{2+}, SO_4^{2-}, HCO_3^-, Na^+, and Cl^- on Al removal by adsorption is also limited [12,30,31].

In present work the adsorption of Al from aqueous solution on titanium dioxide (TiO_2) and vermiculite concrete-supported ferric oxyhydroxide (VC) [32] is studied considering the physico-chemical composition of Khibiny alkaline massif groundwater [20]. The main objectives of study are: (i) to examine based on the results of laboratory tests the

adsorption kinetics and isotherms and (ii) to investigate the effect of major characterizing Khibiny groundwater chemical composition ions on the removal of Al by adsorption on TiO_2 and VC.

6.2 Materials and Methods

6.2.1 Characteristics of Khibiny Alkaline Massif Groundwater

According to the results of "Central" water intake field data (Khibiny alkaline massif, Kola Peninsula) assessment, the groundwater is characterized by strong alkaline conditions and elevated Al concentrations. During 1999–2012 Al concentration in the groundwater varied within 0.19–1.81 mg L^{-1} exceeding the drinking water guideline up to nine times. The variation of pH values was insignificant within the monitoring period with a mean value of 9.56. The application of chemometric methods to the analysis of monitored field data (Chapter 3) revealed that among ions characterizing the chemical composition of groundwater, Cl^-, SO_4^{2-}, and NO_3^- are associated with Al concentration changes.

6.2.2 Chemicals Used

Aeroxide TiO_2 P25 (80:20% anatase/rutile) was purchased from Evonik Degussa Corporation, USA. The vermiculite concrete-supported ferric oxyhydroxide adsorbent (VC) samples [32] and supportive information were received from Tomsk Polytechnic University, Tomsk, Russia. The surface areas and particle size TiO_2 and VC are 50 m^2 g^{-1} and 30 nm, and 188 m^2 g^{-1} and < 0.1 mm, respectively [32]. Aluminum nitrate nonahydrate ($Al(NO_3)_3.9H_2O$; 99.997% trace metals basis) from Sigma-Aldrich, Canada was used to prepare aluminum solutions. Hydrochloric acid (HCl) and sodium hydroxide (NaOH) were obtained from Caledon Laboratory Chemicals, Canada. Polypropylene 0.45 µm syringe filters and 0.20 µm membrane disk filters were acquired from VWR International, Canada and Pall Corporation, USA, respectively. All solutions were prepared in doubly distilled water (18.2 MΩ) that passed through Barnstead™

Easypure^{TM} RODi water purification system (Thermo Scientific, Canada) (Milli-Q water). All chemicals were used as received.

6.2.3 Analytical Methods

The solution pH was measured using a Metrohm 780 pH Meter. Aluminum concentration was determined as an average of five replicates by using inductively coupled plasma – optical emission spectrometry (ICP-OES). The plasma generates temperatures of around 8000 °C, and at this temperature, all the elements in the sample are excited and the concentrations of the elements under consideration are determined [33]. The most commonly used spectral line for light absorption by Al atoms at the wavelength of 309.2 nm was applied in the method [34].

6.2.4 Adsorption Testing Procedure

Aluminum solutions were prepared by dissolving a required amount of $Al(NO_3)_3.9H_2O$ salt in 800 mL of Milli-Q water. The solution pH was adjusted to 9.0 by using 0.5 M NaOH, followed by the filtration of the solution through 0.20 µm disk filters to filter out the insoluble aluminum hydroxide flocs and 10 mL sample was taken to analyze for initial Al concentration. At pH adjusted to 9.0 after the filtration the initial concentration of Al was 2 mg L^{-1}. All adsorption experiments were conducted in 500 mL beakers at room temperature (24±1 °C). The desired amount of adsorbent was added to Al solution, followed by a rapid mixing at room temperature (24±1 °C). The collected samples (10 mL each) were filtered through 0.45 µm syringe filters to remove the adsorbent particles. The filtered samples were analyzed for Al concentration.

To explore the effect of ions associated with elevated Al concentration in the Khibiny alkaline massif groundwater in accordance with the results of field data analysis (Chapter 3) on the removal of Al by adsorption, the inorganic anions – Cl^-, SO_4^{2-}, and NO_3^- were added separately to the Al solution before the adsorbent addition. The samples were taken and analyzed for Al concentration in the absence/presence of adsorbent. The

concentrations of the individually mixed ions were chosen to be relevant to concentrations measured in Khibiny alkaline massif groundwater (Chapter 3).

The uptake and percentage removal of Al by tested adsorbents was calculated using the following equations:

$$q_e = (C_0 - C_e)V/m \quad (6.1)$$

$$Al\ Removal\ \% = (C_0 - C_e)/C_0 \times 100 \quad (6.2)$$

where q_e is the amount of Al adsorbed at equilibrium (mg g^{-1}), V is the volume of solution (L), m is the mass of the adsorbent (g), and C_0 and C_e are the initial and equilibrium concentrations of Al (mg L^{-1}), respectively.

6.2.5 Adsorption Kinetic and Isotherm Models Used

The pseudo-first order and pseudo-second order adsorption kinetic models [35,36] used to describe adsorption mechanism and rate are given as follows:

$$q_t = q_e(1 - exp(-k_1 t)) \quad (6.3)$$

$$q_t = (q_e^2 k_2 t)/(1 + q_e k_2 t) \quad (6.4)$$

where k_1 (min^{-1}) and k_2 (g (mg min) $^{-1}$) are the pseudo-first and pseudo-second order rate constants, respectively, q_t is the amount of Al adsorbed (mg g^{-1}) at any time t (min).

Langmuir, Freundlich, and Sips adsorption isotherm models were used to examine the experimental data. The Langmuir adsorption isotherm [37] is represented as follows:

$$q_e = (Q_0 b C_e)/(1 + bC_e) \quad (6.5)$$

where Q_0 is the maximum monolayer coverage capacity (mg g^{-1}) and b is the Langmuir isotherm constant (L mg^{-1}). The Freundlich's adsorption isotherm [35,38] is determined according to the following equation:

$$Q_e = K_F C_e^{1/n} \quad (6.6)$$

where n is the Freundlich intensity parameter indicating the magnitude of the adsorption driving force or the surface heterogeneity, K_F is Freundlich isotherm constant related to adsorption capacity (mg g^{-1})/(mg L^{-1})^n. A joint adsorption isotherm combining both Langmuir and Freundlich adsorption isotherm models known as Sips or Langmuir-Freundlich adsorption isotherm model [39] is given as:

$$q_e = (K_S C_e^{\beta_S})/(1 + a_S C_e^{\beta_S}) \quad (6.7)$$

where K_S is the Sips isotherm model constant (L g^{-1}), β_S is the Sips isotherm model exponent, and a_S is the Sips isotherm model constant (L mg^{-1}).

The adsorption kinetic and isotherm models' parameters were obtained by non-linear regression analysis tool, Origin® 8.6 software. To identify the best-fit kinetic and isotherm models with the experimental data, the standard error of regression S showing the average distance of the data points from the fitted lines and has the response variable units (mg g^{-1}) was calculated. In non-linear regression, S is a more meaningful estimate of the goodness-of-fit rather than the coefficient of determination R^2 [40].

6.3 Results and Discussion

6.3.1 Adsorption of Al on TiO_2 and Vermiculite Concrete-Supported Ferric Oxyhydroxide

6.3.1.1 Effect of pH on the Solubility and Adsorption of Al

The solubility of $Al(NO_3)_3.9H_2O$ in aqueous solution was tested in the pH range 3.0–11.0 for two initial Al concentrations (2.5 and 100 mg L^{-1}) in the absence of any adsorbent. The results revealed that Al underwent to precipitation at pH > 3.5–4.0 depending on its initial concentration (Figure 6.1a). The minimum solubility of Al was observed at the neutral pH where the dominant form of Al is the insoluble $Al(OH)_3^0$ [34,41]. $Al(OH)_3^0$ dissolves in acidic or in the alkaline solutions making the investigation of Al adsorption

more appropriate at the aforementioned solution conditions [41]. Up to 40–60% of dissolved Al returned to the solution as pH reached the values of 8.5–9.0. The adsorption of Al on TiO_2 and VC was then investigated at pH 3.0, 4.0, and 9.0 (Figure 6.1b).

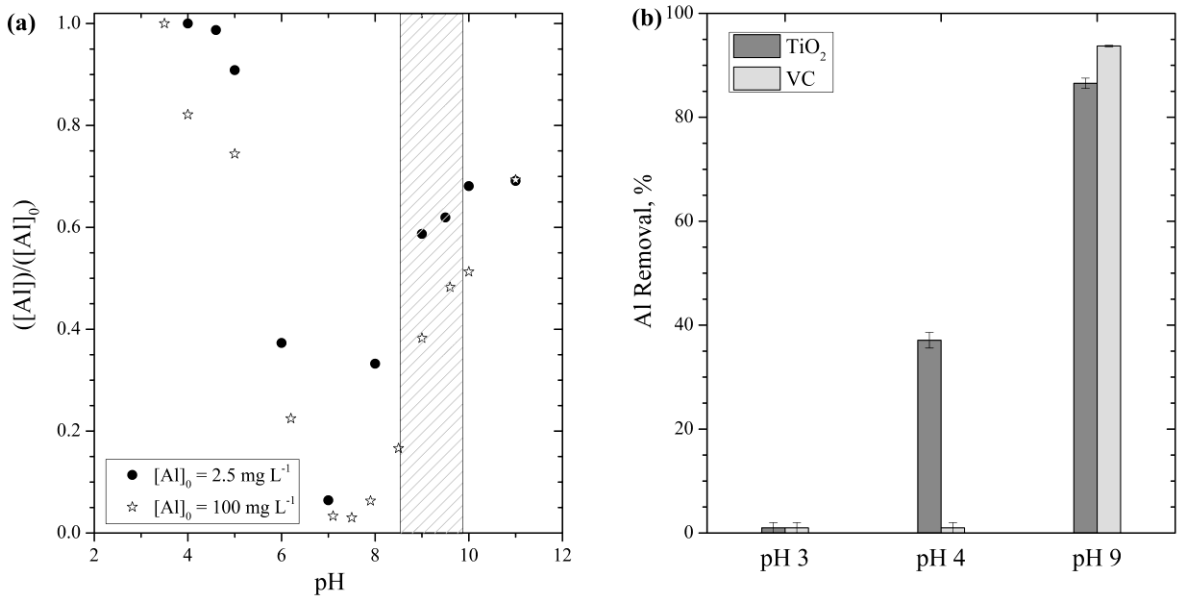

Figure 6.1: Effect of pH on Al solubility (a) and Al adsorption (b). Experimental conditions: $[Al]_0$ = 2 mg L^{-1}; $[TiO_2]$ = [VC] = 1.0 g L^{-1}; contact time = 240 min; T = 24±1 °C; [Al] –current concentrations of Al; shaded area denotes pH range of field data of "Central" water intake.

The results of laboratory tests in acidic conditions revealed that TiO_2 was more efficient than VC toward Al removal. The removal efficiency within 240 min of contact time reached 37% at pH 4.0 while no removal by both adsorbents at pH 3.0 was observed (Figure 6.1b). An additional set of experiments to investigate how TiO_2 adsorbent could influence the Al concentration change under UV irradiation at pH 4.0 was performed. The results expectedly were in a good agreement with the theory and showed no effect on Al removal that can be explained by a more negative Al^{3+} redox potential (E^0) of −1.67 V

(T = 25 °C) than the conduction band of the semiconductor photocatalyst [42,43] (Figure S6.1 of Appendix F).

In the alkaline aqueous solution – that is one of the distinctive features of Khibiny massif groundwater – the highest Al removal at pH 9.0 on TiO_2 and VC reached up to 87 and 94%, respectively. The adsorption capacity of TiO_2 at pH 9.0 was compared with the effectiveness of another inorganic adsorbent – ZnO. The results obtained were in favour of TiO_2 and showed that at the equilibrium it is more effective and capable to remove from water 70–74% more of Al than ZnO (Figure S6.2 of Appendix F).

An assumption of a possible Al precipitation during the adsorption process at alkaline conditions (simultaneous adsorption–precipitation) was made and a set of experiments by means of a so-called "tea-bag" procedure [44,45] was performed using different TiO_2 and VC doses (Figure S6.3 of Appendix F). The results of "tea-bag" experiments confirmed that adsorption dominated in the Al removal process and can be responsible for up to 75–80% Al removal (if the total removal amount is taken as 100%). The precipitation did not have a leading role and the amount of Al precipitated slightly varied depending on the adsorbent tested (Table S6.1 of Appendix F).

6.3.1.2 Adsorption Kinetics

The analysis of Al adsorption kinetics on TiO_2 and VC was conducted using the adsorbent doses of 0.25 g L^{-1} and 0.75 g L^{-1}. The results revealed that at pH 9.0 TiO_2 exhibited a significantly higher adsorption rate compare to VC – the period of 30 min and 240 min were needed to reach the equilibrium of Al adsorption on TiO_2 and VC, respectively (Figure 6.2).

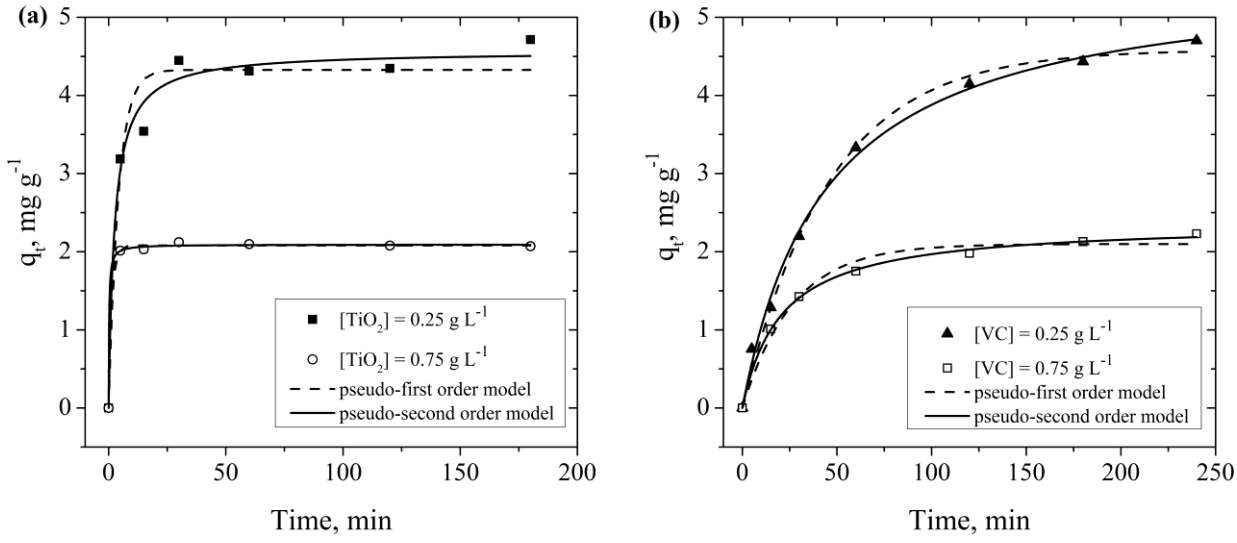

Figure 6.2: Laboratory test data and fitted curves of pseudo-first and pseudo-second order kinetic models of the Al adsorption by TiO_2 (a) and VC (b). Experimental conditions: $[Al]_0$ = 2 mg L^{-1}; pH = 9.0; T = 24±1 °C.

The results of fitting laboratory test data kinetic models (Table 6.1) showed that the rate of Al adsorption on both TiO_2 and VC was better described by the pseudo-second order model (equation 6.4). The calculated *S* values corresponding to pseudo-first and pseudo-second order models for the experimental data by using various doses of each adsorbent evidenced that in most cases the pseudo-second order model is more appropriate to describe Al adsorption kinetics on adsorbents tested. A better fit (lower *S* values) to the pseudo-second order kinetic model suggested that aluminum adsorption behaviour on TiO_2 and VC most likely occurs by chemisorption mechanism [46,47].

Table 6.1: Adsorption kinetic models fitting parameters of Al adsorption on TiO_2 and VC at pH 9.0 and room temperature (T = 24±1 °C) based on the results of testing.

Adsorbent	Dose, g L^{-1}	q_e^{test} *) mg g^{-1}	Kinetic model					
			Pseudo-first order			Pseudo-second order		
			k_1, min^{-1}	q_e, mg g^{-1}	S, mg g^{-1}	k_2, g (mg min) $^{-1}$	q_e, mg g^{-1}	S, mg g^{-1}
TiO_2	0.25	4.45 **)	0.33	4.33	0.36	0.09	4.57	0.22
	0.75	2.12	0.69	2.08	0.03	2.36	2.09	0.03
VC	0.25	4.70 ***)	0.02	4.58	0.14	0.01	5.58	0.10
	0.75	2.23	0.04	2.10	0.11	0.02	2.37	0.03

*) q_e^{test} was calculated based on laboratory tests using equation (6.1).

**) Equilibrium time: 30 min.

***) Equilibrium time: 240 min.

The results of laboratory tests showed that within the first five min of contact time the doses 0.25 g L^{-1} and 0.75 g L^{-1} of TiO_2 were capable to remove up to 41% and 76% of Al, respectively while that using VC required 60–120 min to achieve similar Al removal (46% and 77%, respectively) (Table S6.2a,b of Appendix F). In this set of tests, the pH value was stable throughout the experiments with respect to the adjusted pH 9.0 prior the adsorbent addition (Table S6.3 of Appendix F).

6.3.1.3 Adsorption Isotherms

The performance of TiO_2 and VC was studied by measuring Al adsorption amount at adsorbents doses of 0.25÷2.0 g L^{-1}, room temperature (24±1°C) and pH 9.0 (Tables S6.4, S6.5 of Appendix F). The obtained equilibrium data based on three replicates were fitted by using two-parameter Langmuir and Freundlich isotherm models, and a three-parameter Sips isotherm model (Figure 6.3).

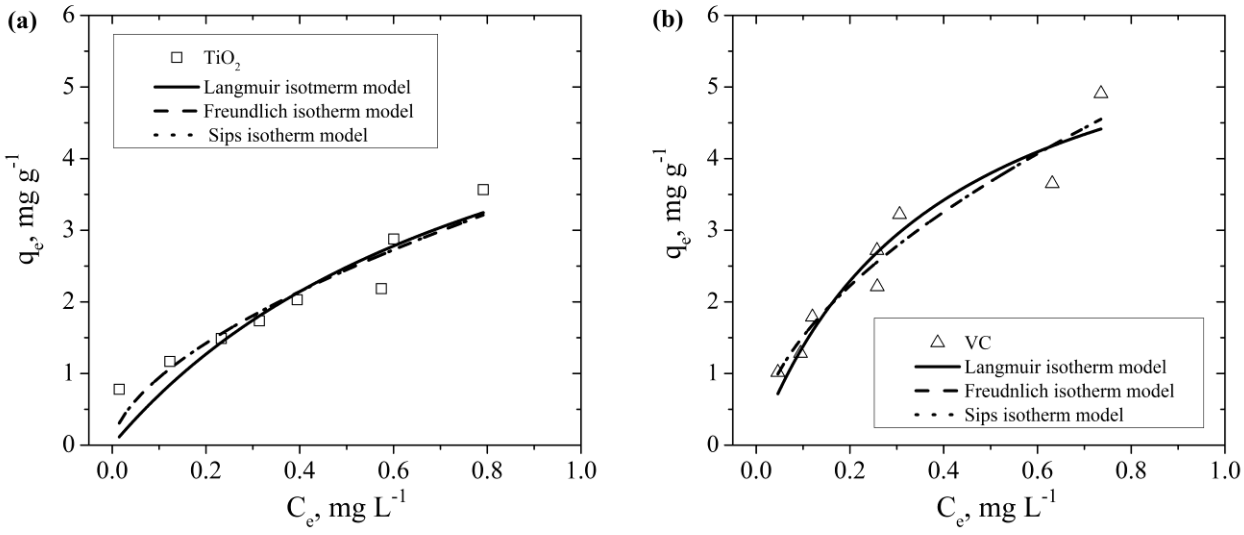

Figure 6.3: Fitted curves of Langmuir, Freundlich, and Sips isotherm equations for equilibrium data of Al adsorption on TiO_2 (a) and VC (b). Experimental conditions: $[Al]_0$ = 1.85±0.1 mg L^{-1}; $[TiO_2]$ = [VC] = 0.25–2.0 g L^{-1}; pH = 9.0; T = 24±1 °C.

In accordance with isotherm classification [48], the obtained isotherms curve shapes indicates L3-behaviour in which the slope steadily falls with a rise in adsorbate concentration because vacant sites in the adsorbent surface become more difficult to find with progressive covering of the surface. The maximum TiO_2 and VC adsorption capacities were similar and had values of 6.85 mg g^{-1} and 6.75 mg g^{-1}, respectively. The equilibrium data were fitted most satisfactory with Freundlich adsorption isotherm model as the calculated *S* values showed (Table 6.2). For both TiO_2 and VC the obtained Freundlich model constant $n > 1$ indicates a nonhomogeneous multilayer Al adsorption [47]. According to the calculated Sips isotherm parameters, the model has been reduced to the Freundlich isotherm (Table 6.2) that can be explained by the relatively low adsorbate concentrations [39,49].

Table 6.2: Adsorption isotherm models fitting parameters of Al adsorption on TiO_2 and VC at pH 9.0 and room temperature (T = 24±1 °C).

Adsorbent	Isotherm model									
	Langmuir			Freundlich			Sips			
	Q_0, mg g^{-1}	b, L mg^{-1}	S, mg g^{-1}	K_F, (mg g^{-1})/(mg L^{-1})^n	n	S, mg g^{-1}	K_S, L g^{-1}	β_S	a_S, L mg^{-1}	S, mg g^{-1}
TiO_2 *)	6.85	1.14	0.40	3.69	1.69	0.32	3.69	0.59	10^{-17}	0.32
VC **)	6.75	2.57	0.40	5.39	1.81	0.36	5.39	0.55	10^{-7}	0.36

*) Equilibrium time: 30 min.

**) Equilibrium time: 240 min.

6.3.2 Joint Use of TiO_2 and Vermiculite Concrete-Supported Ferric Oxyhydroxide

The adsorption capacity of both adsorbents tested toward Al removal from aqueous solution was found to be similar while the adsorption rate and time necessary to reach the equilibrium drastically differed – 30 min and 240 min were required in case of TiO_2 and VC, respectively. Based on the results of Al adsorption kinetic and isotherm studies revealing the advantages of tested adsorbents — the high initial rate of Al adsorption on TiO_2 and the high removal capacity of VC and TiO_2 — the investigation of a joint performance of these adsorbents in a form of one aggregate multicomponent adsorbent (MA) was further undertaken. The MA was prepared by mixing the various doses of TiO_2 and VC and then tested to examine the adsorption kinetics, isotherms, and effect of ions on Al adsorption. The procedure of this set of tests was kept similar to the one described in 6.2.4.

6.3.2.1 Effect of Adsorbents Addition Sequence

The effect of addition of TiO_2 followed by VC in 30 min and vice versa on the Al removal from aqueous solution was investigated at pH 9.0 and room temperature (24±1 °C). A typical example of the effect of adsorbents addition sequence on Al removal is shown on Figure 6.4a. According to the results, a slightly better Al removal (up to 82% within 60 min) was achieved in the case when TiO_2 was added to the solution prior to the VC (Figure 6.4b). The solution pH in both experiments remained approximately the same (Table S6.6 of Appendix F).

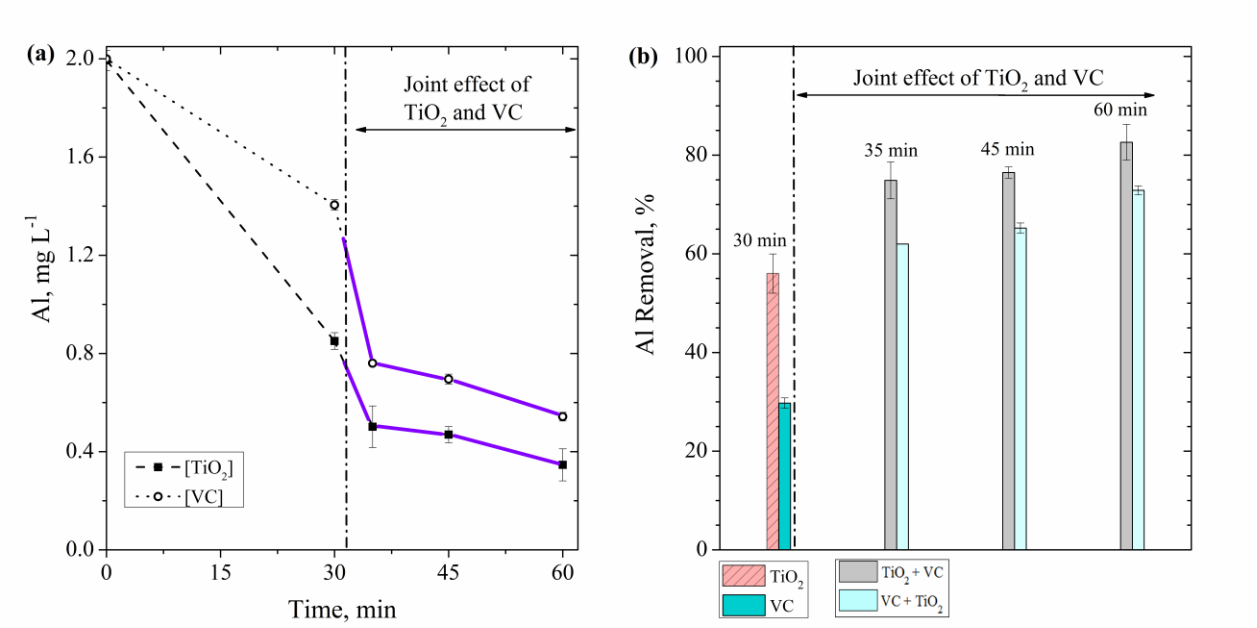

Figure 6.4: Effect of adsorbents addition sequence to aqueous solution (a) and the percentage Al removal from the solution (b). Experimental conditions: $[Al]_0$ = 2 mg L^{-1}; $[TiO_2]$ = [VC] = 0.25 g L^{-1}; pH = 9.0; T = 24±1 °C. Dash dotted line indicates the time when TiO_2 or VC was added as a second adsorbent to the solution.

The results of adsorption kinetics for TiO_2 and VC evidenced the possibility of using both adsorbents simultaneously and still have the advantages of both components: the high initial rate of Al adsorption on TiO_2 and high adsorption capacity of VC and TiO_2. The experiment on Al adsorption from aqueous solution using 0.50 g L^{-1} MA (simultaneously

added 0.25 g L^{-1} of both TiO_2 and VC) showed 78% Al removal within 60 min of contact time. The results of Al adsorption on TiO_2 and VC added simultaneously or in a sequence were similar and showed the removal up to 72–82%. Taking into consideration the removal efficiency, the investigation of MA adsorption kinetics and isotherms was carried out.

6.3.2.2 Adsorption Kinetics and Isotherms

The adsorption kinetic and equilibrium data of Al removal from aqueous solution on MA were obtained at pH 9.0 and room temperature (24±1°C) (Figure 6.5, Table 6.3). The MA adsorbent doses used to acquire kinetic and equilibrium data correspond to the summation of TiO_2 and VC doses in an equal proportion, for example, the MA doses of 0.25 g L^{-1} and 0.50 g L^{-1} correspond to 0.125 g L^{-1} [TiO_2] + 0.125 g L^{-1} [VC] and 0.25 g L^{-1} [TiO_2] + 0.25 g L^{-1} [VC], respectively (Table S6.7 of Appendix F).

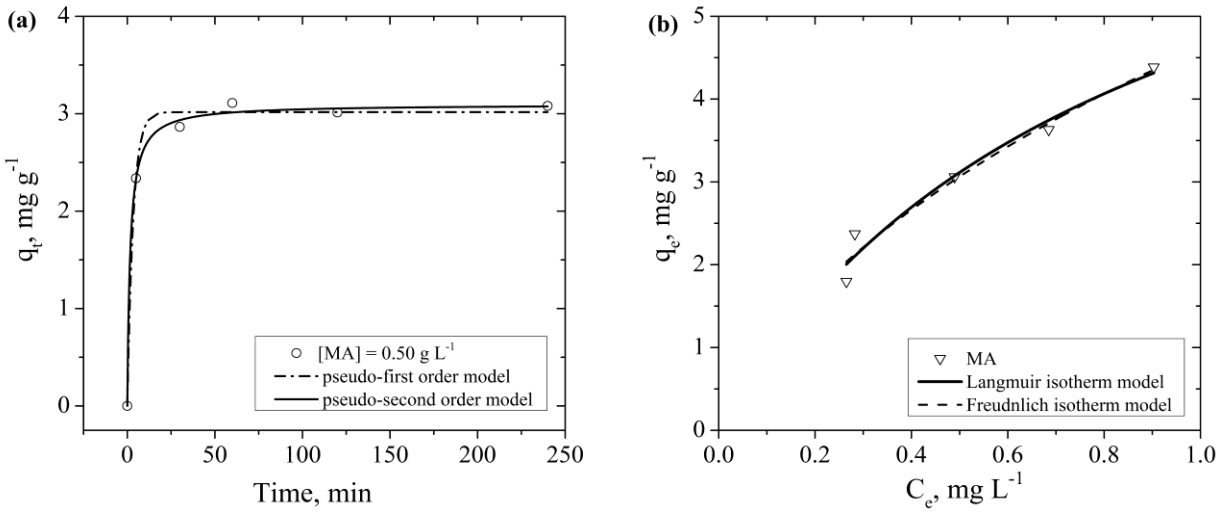

Figure 6.5: Fitted curves of pseudo-first and pseudo-second order kinetic models (a) Langmuir and Freundlich isotherm models (b) of data obtained in laboratory tests on Al adsorption by MA. Experimental conditions: $[Al]_0$ = 2 mg L^{-1}; pH = 9.0; T = 24±1 °C; [MA] = 0.25–1.0 g L^{-1}.

Table 6.3: The fitted parameters of adsorption kinetic (a) and adsorption isotherm (b) models of Al adsorption on MA at pH 9.0 and room temperature (T = 24±1 °C) based on the results of testing.

(a)

Kinetic model	Parameter	Value
Pseudo-first order	k_1, min^{-1}	0.30
	q_e, mg g^{-1}	3.02
	S, mg g^{-1}	0.09
Pseudo-second order	k_2, g (mg min) $^{-1}$	0.20
	q_e, mg g^{-1}	3.09
	S, mg g^{-1}	0.06

(b)

Isotherm model	Parameter	Value
Langmuir	Q_0, mg g^{-1}	8.28
	b, L mg^{-1}	1.21
	S, mg g^{-1}	0.21
	ARE, %	5.66 *)
	E^2	0.13 **)
Freundlich	K_F, (mg g^{-1})/(mg L^{-1})^n	4.66
	n	1.62
	S, mg g^{-1}	0.20
	ARE, %	5.61 *)
	E^2	0.13 **)

*) $ARE = (100/N)\sum_{i=1}^{N}(|q_e^{test} - q_e^{calc}|/q_e^{test})$ where *ARE* is the average relative error. *N* is number of experimental data points, q_e^{calc} values were calculated by using the isotherm model equations (6.5)–(6.7), q_e^{test} values were calculated based on laboratory tests data by using equation (6.1).

**) $E^2 = \sum_{i=1}^{N}(q_e^{test} - q_e^{calc})^2$ where E^2 is the sum of squared errors.

The adsorption kinetic data were better described by pseudo-second order model according to the calculated *S* values (Table 6.3a) that evidences in favour of chemisorption process controlling Al adsorption [46,47]. The results of experiments showed that Al adsorption on MA reached equilibrium within 60 min of contact time (Figure 6.5a) that is 30 min longer than in case of TiO_2 but four times faster than VC. Up to 50% of Al were removed within the first five min of contact time and more than 73% of Al were adsorbed within the first 30 min by using 0.50 g L^{-1} MA (Figure 6.5a). To compare, when TiO_2 worked alone the doses of 0.25 g L^{-1} and 0.50 g L^{-1} were capable to

decrease Al concentration up to 57% and 66% within 30 min (equilibrium time), respectively.

The laboratory test data were found to be well-fitted to both Langmuir and Freundlich isotherms models (Figure 6.5b) as the calculated *S* values suggested. To check this result, the error functions *ARE* and E^2 [50] were calculated (Table 6.3b). The obtained maximum monolayer coverage capacity of MA equal to 8.28 mg g^{-1} is higher than the individual TiO_2 and VC adsorption capacities by 18% (Table 6.2).

The scanning electron microscopy coupled with energy dispersive X-ray spectroscopy (SEM/EDX) analysis was used to characterize the surface of TiO_2, VC, and MA. The samples for SEM/EDX analysis were prepared using the experimental procedure described in 6.2.4. The initial Al concentration and adsorbent dose of 2 mg L^{-1} and 1.0 g L^{-1}, respectively were used. The images showing the morphology of TiO_2, VC, and MA surfaces before and after Al adsorption are presented in Figures S6.4, S6.5 of Appendix F and Figure 6.6, respectively.

According to SEM tests, surface morphology characteristics of adsorbents did not undergo significant changes due to the adsorption process (Figures S6.4a,c, S6.5a,c of Appendix F, Figure 6.6a,c) while EDX showed that aluminum ions attached to the surface of materials tested (Figures S6.4d, S6.5d of Appendix F, Figure 6.6d). Typical EDX spectra of unloaded and Al-adsorbed MA are shown on Figure 6.6b,d. The EDX spectrum of raw MA did not show Al ions on its surface while EDX spectrum of samples after adsorption evidenced the presence of aluminum ions on the surface of material tested. Similar results of SEM/EDX analysis were obtained in case of TiO_2 and VC (Figures S6.4, S6.5 of Appendix F).

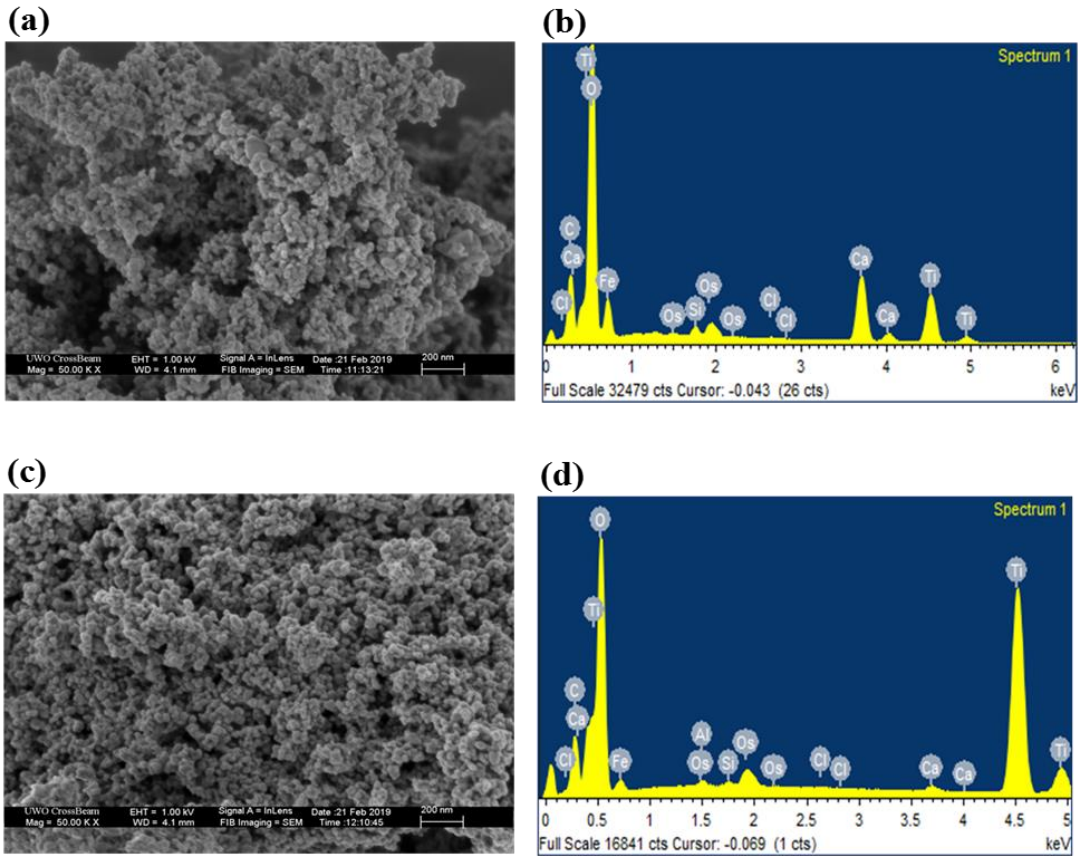

Figure 6.6: The results of SEM/EDX analysis of MA surface: before Al adsorption (a) and (b); after Al adsorption (c) and (d).

6.3.2.3 Effect of Ions and Adsorbent Dosing on Al Adsorption

The effect of anions NO_3^-, SO_4^{2-}, and Cl^- representing the constituencies of natural chemical composition of Khibiny alkaline massif groundwater which were identified based on the results of mathematical modelling (Chapter 3) as the key parameters associated with Al concentration variation was investigated in a set of laboratory tests. The solution pH was adjusted to 9.0 followed by the filtration removing insoluble Al flocs before the addition of certain amount of the ions. The ions were added to the solution individually. The presence of ions tested did not influence the pH value which remained stable throughout each experiment (Table S6.8 of Appendix F). Samples of the

Al-ion solution prior to the addition of adsorbent were taken and analyzed for Al concentration to eliminate any interaction between the ion and Al. The Al-ion-adsorbent samples were taken at equilibrium time of 30 min (TiO_2), 60 min (MA), and 240 min (VC) and analyzed for Al concentration.

The outcomes of this set of experiments indicated no apparent noticeable effect on Al removal by adsorbents tested in the presence of NO_3^-, SO_4^{2-}, and Cl^- ions (Figure 6.7a–c). The SO_4^{2-} and Cl^- ions presented in the solution had a light negative effect on aluminum adsorption by VC and MA that was within 6–14% of the control Al concentration. The presence of Cl^- ions in the solution influenced mostly the performance of MA adsorbent and lowered aluminum removal by 9.9% (Figure 6.7c). The apparent negative effects of tested ions were not detected for TiO_2 (Figure 6.7a). As the ionic strength may be changing by adding ions, it is assumed that some of the observed effects by adsorbents tested on Al removal could be related to the variation in the ionic strength rather than the direct ions effect [51,52].

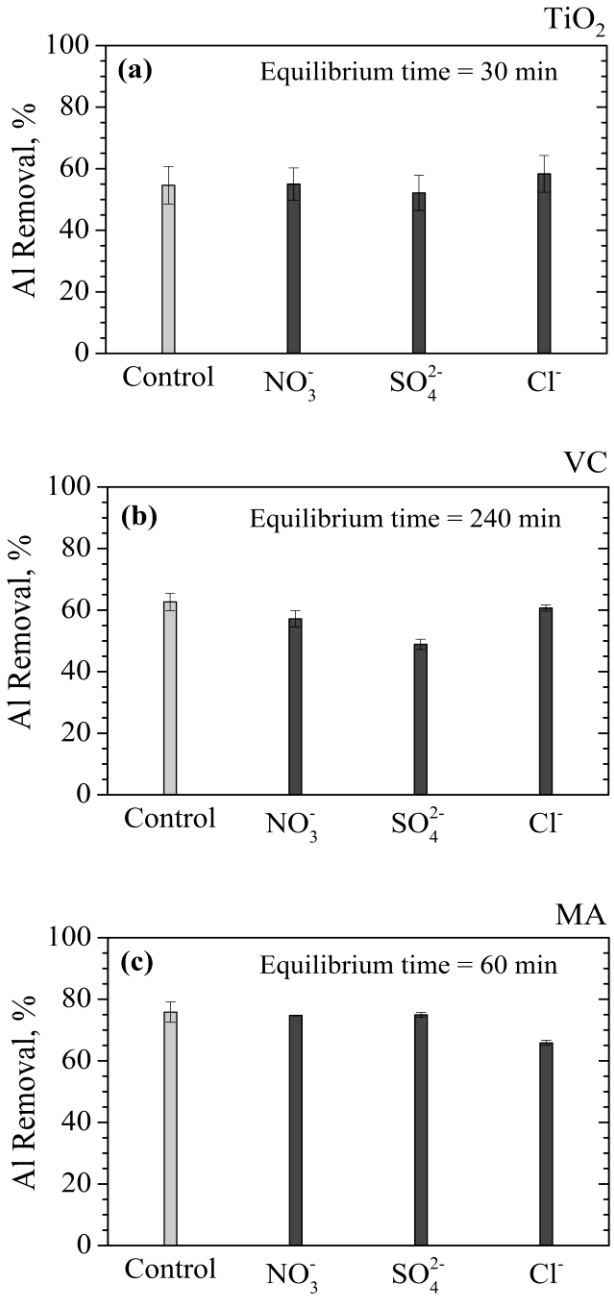

Figure 6.7: Effect of nitrate (NO_3^-, $NaNO_3$), sulphate (SO_4^{2-}; Na_2SO_4), and chloride (Cl^-; NaCl) on Al adsorption on TiO_2 (a), VC (b), and MA (c) at equilibrium time. Experimental conditions: $[Al]_0$ = 2 mg L^{-1}; [TiO_2] = [VC] = 0.25 g L^{-1}; [MA] = 0.50 g L^{-1}; initial concentration of ions: [NO_3^-] = 2.12 mg L^{-1}, [SO_4^{2-}] = 7.89 mg L^{-1}, [Cl^-] = 1.82 mg L^{-1}; pH = 9.0; T = 24±1 °C.

6.3.2.4 Effect of Multicomponent Adsorbent Dosing on Al Removal

The effect of adsorbent dosing on the Al removal was investigated considering the favourable outcomes obtained in the laboratory study on Al adsorption by MA. According to the results of adsorption kinetic and isotherm as well as the effect of ions studies, among adsorbents tested MA showed the highest adsorption capacity, a relatively high adsorption rate, and the insignificant changes in the presence of NO_3^-, SO_4^{2-}, and Cl^- anions on adsorption performance. The Al adsorption was tested at pH 9.0 and room temperature (24±1°C) using the following combinations of components doses ([TiO_2]/[VC], g L^{-1}): 0.25/0.75 g L^{-1}, 0.50/0.50 g L^{-1}, and 0.50/1.00 g L^{-1}. For the set of experiments, the initial Al concentration that is approximately seven times above the drinking water guideline was chosen in accordance with the *Q3* value of Al concentrations monitored in Khibiny alkaline massif groundwater for the period of 1999–2012 (Table 3.1 of Chapter 3).

The results of experiments revealed that the application of each tested dose combination was capable to decrease Al concentration below the drinking water guideline of 0.20 mg L^{-1} within 60 min of contact time (Figure 6.8). The total Al removal reached 87–95% depending on the MA dose (Table 6.4). The adsorption capacity and total effectiveness of the process can be easily controlled by changing the proportions between TiO_2 and VC when used jointly. This promotes the possibility of using optimization methods and developing a computer model/program to control the process of Al removal depending on the initial Al concentration in the water intake, adsorbent doses, and allowed contact time to reduce certain Al concentrations below the drinking water standards.

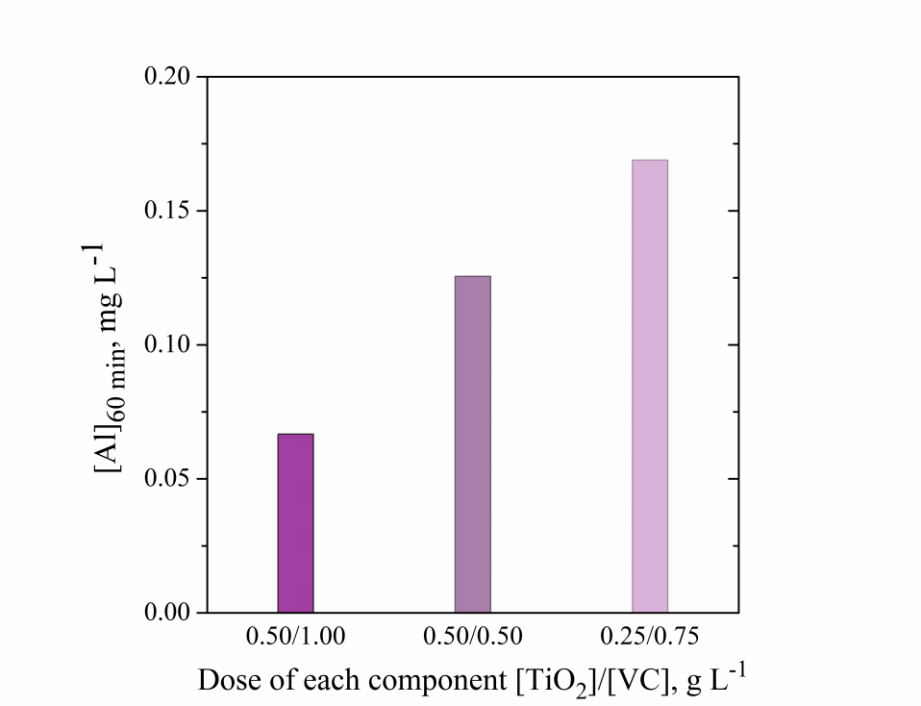

Figure 6.8: Effect of MA dosing on Al removal from water reflecting Khibiny alkaline massif groundwater conditions. Experimental conditions: $[Al]_0$ = 1.35 mg L^{-1}; pH = 9.0; T = 24±1 °C.

Table 6.4: Effect of multicomponent adsorbent dosing on Al removal from water reflecting Khibiny alkaline massif groundwater conditions.

MA *), g L^{-1}	$[Al]_0$, mg L^{-1}	$[Al]_{60\ min}$**), mg L^{-1}	Al removal, %	q_e, mg g^{-1}	pH
0.25/0.75	1.34	0.17	87.35	1.25	8.9
0.50/0.50	1.37	0.13	90.87	1.17	8.9
0.50/1.00	1.35	0.07	95.06	0.86	8.9

*) $[TiO_2]/[VC]$, g L^{-1}.

**) Concentration of aluminum at equilibrium.

The results of current study on Al adsorption considering the physico-chemical composition of Khibiny massif groundwater having elevated Al concentrations were compared to literature data on Al removal by various adsorbents from aqueous solutions (Table 6.5). It was found that the number of studies on Al removal from aqueous solutions by adsorption is limited and mostly focused on Al removal by organic or having an organic component materials at predominantly acidic pH range (pH < 6.0) [27,29,50,53]. In Table 6.5, the results on the performance of various adsorbents in alkaline aqueous solution are presented.

Table 6.5: Performance of various adsorbents toward Al removal from alkaline aqueous solution based on the results of current study and some literature data.

Sorbent	Reference	pH	Sorbent dose, g L^{-1}	Equilibrium time, min	Adsorption capacity, mg g^{-1}	Effect of ions study
Refuse derived char	[26]	8.0	2.0	120	40.0 *)	–
Granular activated carbon/$FeCl_3$	[25]	8.0	5.0	360	4.37	–
Granular activated carbon	[25]	8.0	5.0	360	3.0	–
MA	Current study	9.0	0.25÷1.0	60	8.28	+
TiO_2	Current study	9.0	0.25÷2.0	30	6.85	+
VC	Current study	9.0	0.25÷2.0	240	6.75	+

*) Adsorption capacity, mg g^{-1} calculated using the data reported in the journal article.
Presence (+) or absence (−) of the ions tests results.

The data indicate that TiO_2, VC, and MA have a comparable or even higher adsorption capacity toward Al removal at alkaline conditions compare to activated carbon materials (Table 6.5). Additionally, the equilibrium time of Al adsorption on TiO_2 and MA is significantly lower compare to the carbon and char-based adsorbents and even relatively low MA doses are capable to decrease Al concentrations below the drinking water guidelines. The strengths of adsorbents tested make MA a reliable and effective adsorbent for Al removal from the alkaline aqueous solution.

6.4 Conclusions

The adsorption of aluminum from aqueous solution reflecting the major features of physico-chemical composition of Khibiny alkaline massif groundwater (Kola Peninsula) was examined on titanium dioxide (TiO_2), vermiculite concrete-supported ferric oxyhydroxide (VC) [32], and a multicomponent adsorbent (MA) aggregating both TiO_2 and VC adsorbents. The effects of pH, initial aluminum concentration, contact time, adsorbent dose, and ions present in the Khininy alkaline massif groundwater were studied.

The results revealed that the adsorption rate followed the sequence of TiO_2 > MA > VC and the adsorption capacity can be ranged as MA > TiO_2 > VC. The adsorption kinetic data were well-fitted to the pseudo-second order kinetic model. The obtained kinetic data showed that aluminum adsorption on TiO_2 and MA exhibited a dramatically higher adsorption rate compare to VC. The contact time of 30 min, 60 min, and 240 min were needed to reach equilibrium, respectively. The adsorption equilibrium data on TiO_2 and VC were described most satisfactory by the Freundlich isotherm model indicating a heterogeneous surface property of the adsorbents while the adsorption process on MA can be reasonably characterized by both Freundlich and Langmuir isotherm models. The maximum adsorption capacities of VC, TiO_2, and MA were 6.75, 6.85, and 8.28 mg g^{-1}, respectively. Based on the experimental results, the presence of anions NO_3^-, SO_4^{2-}, and Cl^- identified as the parameters associated with Al concentration variability by earlier obtained mathematical models [20] insignificantly affected the adsorption of aluminum

on TiO_2, VC, and MA. It was found that the presence of SO_4^{2-} ions in the solution lowered aluminum removal by 13.8% in the case of VC. The Cl^- ions presented in the solution had a light negative effect on the efficiency of aluminum removal by MA decreasing it from 75.8% (control) to 65.9%. The apparent negative effect of ions was not detected for TiO_2 as the outcomes of laboratory tests showed. It is assumed that some of the observed effects on aluminum removal by adsorbents tested may be related to variation in the ionic strength.

The outcomes of current study are a necessary step to develop and implement a reliable method for treating Khibiny alkaline massif groundwater containing prohibitive aluminum concentrations. The implementation of adsorption process in the current technology at the Khibiny local water treatment facility can be an effective way to meet the drinking water standards.

6.5 References

[1] C.I. Adamu, T.N. Nganje, A. Edet, Heavy metal contamination and health risk assessment associated with abandoned barite mines in Cross River State, southeastern Nigeria, Environ. Nanotechnology, Monit. Manag. 3 (2015) 10–21. doi:10.1016/j.enmm.2014.11.001.

[2] X. Liu, Z.Q. Chen, B. Han, C.L. Su, Q. Han, W.Z. Chen, Biosorption of copper ions from aqueous solution using rape straw powders: optimization, equilibrium and kinetic studies, Ecotoxicol. Environ. Saf. 150 (2018) 251–259. doi:10.1016/j.ecoenv.2017.12.042.

[3] S.H. Peng, R. Wang, L.Z. Yang, L. He, X. He, X. Liu, Biosorption of copper, zinc, cadmium and chromium ions from aqueous solution by natural foxtail millet shell, Ecotoxicol. Environ. Saf. 165 (2018) 61–69. doi:10.1016/j.ecoenv.2018.08.084.

[4] L. Järup, Hazards of heavy metal contamination, Br. Med. Bull. 68 (2003) 167–182. doi:https://doi.org/10.1093/bmb/ldg032.

[5] J. Ščančar, R. Milačič, Aluminium speciation in environmental samples: a review, Anal. Bioanal. Chem. 386 (2006) 999–1012. doi:10.1007/s00216-006-0422-5.

[6] A.S. Cardwell, W.J. Adams, R.W. Gensemer, E. Nordheim, R.C. Santore, A.C. Ryan, W.A. Stubblefield, Chronic toxicity of aluminum, at a pH of 6, to freshwater organisms: empirical data for the development of international regulatory standards/criteria, Environ. Toxicol. Chem. 37 (2018) 36–48. doi:10.1002/etc.3901.

[7] C.T. Driscoll, R.D. Letterman, Chemistry and fate of Al(III) in treated drinking water, Environ. Enginering. 114 (1988) 21–37. doi:10.1061/(ASCE)0733-9372(1988)114:1(21).

[8] E.S. Khlebnikova, Intensification of the process obtaining ethylbenzene in a reactor unit with a preliminary mixing of reagents, Tomsk Polytechnic University, 2018.

[9] C.T. Driscoll, W.D. Schecher, The chemistry of aluminum in the environment, Environ. Geochem. Health. 12 (1990) 28–49. doi:10.1007/BF01734046.

[10] W.A. Scheider, B. Cave, J. Jones, Reclamation of Acidified Lakes near Sudbury Ontario by Neutralization and Fertilization, Rexdale, ON, 1975.

[11] C. Bakar, H.I.Ö. Karaman, A. Baba, F. Şengünalp, Effect of high aluminum concentration in water resources on human health, case study: Biga Peninsula, northwest part of Turkey, Arch. Environ. Contam. Toxicol. 58 (2010) 935–944. doi:10.1007/s00244-009-9435-3.

[12] Y.C. Rajan, B.S. Inbaraj, B.H. Chen, In vitro adsorption of aluminum by an edible biopolymer poly(γ-glutamic acid), J. Agric. Food Chem. 62 (2014) 4803–4811. doi:10.1021/jf5011484.

[13] D. Krewski, R.A. Yokel, E. Nieboer, D. Borchelt, J. Cohen, J. Harry, S. Kacew, J. Lindsay, A.M. Mahfouz, V. Rondeau, Human health risk assessment for aluminium, aluminium oxide, and aluminium hydroxide, J. Toxicol. Environ. Heal.

Part B. 10:S1 (2007) 1–269. doi:10.1080/10937400701597766.

[14] J. Nie, Neurotoxicity of Aluminum, in: Q. Niu (Ed.), Adv. Exp. Med. Biol., Springer, Singapore, 2018: pp. 99–111. doi:10.1007/978-981-13-1370-7_6.

[15] T.P. Flaten, Aluminium as a risk factor in Alzheimer's disease, with emphasis on drinking water, Brain Res. Bull. 55 (2001) 187–196.

[16] Z. Wang, X. Wei, J. Yang, J. Suo, J. Chen, X. Liu, X. Zhao, Chronic exposure to aluminum and risk of Alzheimer's disease: a meta-analysis, Neurosci. Lett. 610 (2016) 200–206. doi:10.1016/j.neulet.2015.11.014.

[17] U.S. Environmental Protection Agency (USEPA), 2018 Edition of the Drinking Water Standards and Health Advisories Tables, Washington, DC, 2018. https://www.epa.gov/sites/production/files/2018-03/documents/dwtable2018.pdf.

[18] World Health Organization (WHO), A Global Overview of National Regulations and Standards for Drinking-Water Quality, Switzerland, 2018. http://apps.who.int/iris/bitstream/handle/10665/272345/9789241513760-eng.pdf.

[19] C.M.C. de Meyer, J.M. Rodríguez, E.A. Carpio, P.A. García, C. Stengel, M. Berg, Arsenic, manganese and aluminum contamination in groundwater resources of Western Amazonia (Peru), Sci. Total Environ. 607–608 (2017) 1437–1450. doi:10.1016/j.scitotenv.2017.07.059.

[20] D. Popugaeva, K. Kreyman, A.K. Ray, Study of aluminium in groundwater using chemometric methods, Environ. Technol. (2018). doi:10.1080/09593330.2018.1544667.

[21] M. Frankowski, A. Zioła-Frankowska, I. Kurzyca, K. Novotný, T. Vaculovič, V. Kanický, M. Siepak, J. Siepak, Determination of aluminium in groundwater samples by GF-AAS, ICP-AES, ICP-MS and modelling of inorganic aluminium complexes, Environ. Monit. Assess. 182 (2011) 71–84. doi:10.1007/s10661-010-1859-8.

[22] T.G. Kazi, M.B. Arain, M.K. Jamali, N. Jalbani, H.I. Afridi, R.A. Sarfraz, J.A. Baig, A.Q. Shah, Assessment of water quality of polluted lake using multivariate statistical techniques: a case study, Ecotoxicol. Environ. Saf. 72 (2009) 301–309. doi:10.1016/j.ecoenv.2008.02.024.

[23] P.F. Henshaw, J.K. Bewtra, N. Biswas, Occurrence of aluminum, lead, and trihalomethanes in drinking water from the Great Lakes, J. Great Lakes Res. 19 (1993) 521–532. doi:10.1016/S0380-1330(93)71238-1.

[24] Y. Zhang, C. Zhu, F. Liu, Y. Yuan, H. Wu, A. Li, Effects of ionic strength on removal of toxic pollutants from aqueous media with multifarious adsorbents: a review, Sci. Total Environ. 646 (2019) 265–279. doi:10.1016/j.scitotenv.2018.07.279.

[25] M. Mahdavi, A. Ebrahimi, A.H. Mahvi, A. Fatehizadeh, F. Karakani, H. Azarpira, Experimental data for aluminum removal from aqueous solution by raw and iron-modified granular activated carbon, Data Br. 17 (2018) 731–738. doi:10.1016/j.dib.2018.01.063.

[26] C. Nobre, M. Gonçalves, D. Resende, C. Vilarinho, B. Mendes, Removal of Chromium and Aluminum from Aqueous Solutions Using Refuse Derived Char, in: L. Camarinha-Matos, A.J. Falcão, N. Vafaei, S. Najdi (Eds.), Technol. Innov. Cyber-Physical Syst., Springer International Publishing, Costa de Caparica, 2016: pp. 515–522. doi:DOI: 10.1007/978-3-319-31165-4_48.

[27] A. Saleh, M. Tuzen, A. Sarı, Magnetic activated carbon loaded with tungsten oxide nanoparticles for aluminum removal from waters, J. Environ. Chem. Eng. 5 (2017) 2853–2860. doi:10.1016/j.jece.2017.05.038.

[28] E. Moniri, H.A. Panahi, Y.G. Mohammadi, H. Gaforian, Removal of aluminum(III) from environmental samples by siliceous support grafted with poly[1-(N,N-bis-carboxymethyl)amino-3- allylglycerol-co-dimethylacrylamide] Brushes, Can. J. Chem. Eng. 92 (2014) 1414–1420. doi:10.1002/cjce.22003.

[29] P. Lodeiro, Á. Gudiña, L. Herrero, R. Herrero, M.E. Sastre de Vicente, Aluminium removal from wastewater by refused beach cast seaweed. Equilibrium and dynamic studies, J. Hazard. Mater. 178 (2010) 861–866. doi:10.1016/j.jhazmat.2010.02.017.

[30] A.A. Kumari, K. Ravindhranath, Removal of aluminium(III) from polluted waters using biosorbents derived from Achiranthus Aspera and Cassia Occidentalis, Int. J. Water Resour. Environ. Sci. 1 (2012) 8–19. doi:10.5829/idosi.ijwres.2012.1.1.1101.

[31] J.B. Neris, F.H.M. Luzardo, E.G.P. da Silva, F.G. Velasco, Evaluation of adsorption processes of metal ions in multi-element aqueous systems by lignocellulosic adsorbents applying different isotherms: a critical review, Chem. Eng. J. 357 (2019) 404–420. doi:10.1016/j.cej.2018.09.125.

[32] D. Martemianov, B. Xie, T. Yurmazova, M. Khaskelberg, F. Wang, C. Wei, S. Preis, Cellular concrete-supported cost-effective adsorbents for aqueous arsenic and heavy metals abatement, J. Environ. Chem. Eng. 5 (2017) 3930–3941. doi:10.1016/j.jece.2017.07.063.

[33] P. Chowdhury, S. Athapaththu, A. Elkamel, A.K. Ray, Visible-solar-light-driven photo-reduction and removal of cadmium ion with Eosin Y-sensitized TiO2 in aqueous solution of triethanolamine, Sep. Purif. Technol. 174 (2017) 109–115. doi:10.1016/j.seppur.2016.10.011.

[34] G. Sposito, The Environmental Chemistry of Aluminum, 2nd edition, Lewis Publishers, Boca Raton, FL, 1996.

[35] H.N. Tran, S.-J. You, A. Hosseini-Bandegharaei, H.-P. Chao, Mistakes and inconsistencies regarding adsorption of contaminants from aqueous solutions: a critical review, Water Res. 120 (2017) 88–116. doi:10.1016/j.watres.2017.04.014.

[36] X. Xie, R. Deng, Y. Pang, Y. Bai, W. Zheng, Y. Zhou, Adsorption of copper(II) by sulfur microparticles, Chem. Eng. J. 314 (2017) 434–442.

doi:10.1016/j.cej.2016.11.163.

[37] I. Langmuir, The constitution and fundamental properties of solids and liquids. Part I. Solids, J. Am. Chem. Soc. 38 (1916) 2221–2295. doi:10.1021/ja02268a002.

[38] H.M.F. Freundlich, Over the adsorption in solution, J. Phys. Chem. 57 (1906) 385–471.

[39] R. Sips, On the structure of a catalyst surface, J. Chem. Phys. 16 (1948) 490–495. doi:10.1063/1.1746922.

[40] A.-N. Spiess, N. Neumeyer, An evaluation of R2 as an inadequate measure for nonlinear models in pharmacological and biochemical research: a Monte Carlo approach. BMC Pharmacol.10 (2010) 1–11. doi:http://www.biomedcentral.com/1471-2210/10/6.

[41] J. Namiésnik, A. Rabajczyk, The speciation of aluminum in environmental samples, Crit. Rev. Anal. Chem. 40 (2010) 68–88. doi:10.1080/10408340903153234.

[42] D. Chen, A.K. Ray, Removal of toxic metal ions from wastewater by semiconductor photocatalysis, Chem. Eng. Sci. 56 (2001) 1561–1570. doi:10.1016/S0009-2509(00)00383-3.

[43] L. Pauling, General Chemistry, 3rd edition, W.H. Freeman and Company, San-Francisco, CA, 1970.

[44] B. Volesky, Biosorption and me, Water Res. 41 (2007) 4017–4029. doi:10.1016/j.watres.2007.05.062.

[45] A.H. Sulaymon, A.A.H. Faisal, Q.M. Khaliefa, Simultaneous adsorption–precipitation characterization as mechanisms for metals removal from aqueous solutions by cement kiln dust (CKD), Desalin. Water Treat. 57 (2016) 819–826. doi:10.1080/19443994.2014.976769.

[46] Z. Li, L. Wu, H. Liu, H. Lan, J. Qu, Improvement of aqueous mercury adsorption on activated coke by thiol-functionalization, Chem. Eng. J. 228 (2013) 925–934. doi:10.1016/j.cej.2013.05.063.

[47] H.S. Niasar, H. Li, T. Venkateswara Rao Kasanneni, M.B. Ray, C. Xu, Surface amination of activated carbon and petroleum coke for the removal of naphthenic acids and treatment of oil sands process-affected water (OSPW), Chem. Eng. J. 293 (2016) 189–199. doi:10.1016/j.cej.2016.02.062.

[48] C.H. Giles, D. Smith, A. Huitson, A general treatment and classification of the solute adsorption isotherm. I. Theoretical, J. Colloid Interface Sci. 47 (1974) 755–765. doi:https://doi.org/10.1016/0021-9797(74)90252-5.

[49] K.Y. Foo, B.H. Hameed, Insights into the modeling of adsorption isotherm systems, Chem. Eng. J. 156 (2010) 2–10. doi:10.1016/j.cej.2009.09.013.

[50] S.A. Al-Muhtaseb, M.H. El-Naas, S. Abdallah, Removal of aluminum from aqueous solutions by adsorption on date-pit and BDH activated carbons, J. Hazard. Mater. 158 (2008) 300–307. doi:10.1016/j.jhazmat.2008.01.080.

[51] Z. Reddad, C. Gerente, Y. Andres, P. Le Cloirec, Adsorption of several metal ions onto a low-cost biosorbent: kinetic and equilibrium studies, Environ. Sci. Technol. 36 (2002) 2067–2073. doi:10.1021/es0102989.

[52] Y.H. Li, J. Ding, Z. Luan, Z. Di, Y. Zhu, C. Xu, D. Wu, B. Wei, Competitive adsorption of Pb2+, Cu2+ and Cd2+ ions from aqueous solutions by multiwalled carbon nanotubes, Carbon. 41 (2003) 2787–2792. doi:10.1016/S0008-6223(03)00392-0.

[53] T.S. Singh, B. Parikh, K. Pant, Investigation on the sorption of aluminium in drinking water by low-cost adsorbents, Water SA. 32 (2006) 49–54. doi:http://dx.doi.org/10.4314/wsa.v32i1.5239.

Chapter 7

7 Conclusions and Recommendations

7.1 Major Conclusions

The current PhD research work is driven by the problem of elevated aluminum concentrations in the groundwater of the Khibiny alkaline massif (Kola Peninsula). This thesis reports a comprehensive analysis of the available field data between 1999–2012 of groundwater quality monitoring and analysis of the results of laboratory study of aluminum adsorption from aqueous solutions on various adsorbents. The quantitative statistical analysis and mathematical modelling including both univariate and multivariate statistical techniques, spectral analysis, and water quality index scores values calculations were considered. The removal of aluminum via adsorption for both alkaline and acidic aqueous solutions were studied. The summaries and major outcomes during the consequent steps of this research are presented in Chapters 3–6. The principal findings of the PhD research thesis are as follows:

- Statistical analysis and mathematical modelling:
    i. The univariate statistical analysis of the field dataset that includes 12 groundwater quality parameters identified by using the correlation matrix that at a statistically significant level (α-*level* = 0.05) pH, NO_3^-, SO_4^{2-}, Cl^- ions and TDS associated with aluminum concentrations variability of Khibiny massif groundwater. The multiple regression model after the multicollinearity check including NO_3^-, Cl^-, and pH explained up to 54% of aluminum concentrations temporal variation in groundwater.
    ii. The application of spectral analysis based on fast Fourier transform (FFT) algorithm to NO_3^-, Cl^-, pH, and aluminum time series allowed to identify three main frequency bands corresponding approximately to 5–7, 13–17, and 20–34 month periods. The fluctuations within these bands contributed mostly to the total temporal variation of major Khibiny groundwater quality parameters.

iii. The multivariate statistical analysis of field data using factor analysis/principal component analysis extraction method (FA/PCA) allowed the reduction of 12 groundwater quality parameters into four dominating influencing factors explaining 67.5% of the original dataset total variance. The hierarchical cluster analysis (HCA) applied to examine the similarities of 12 monitored groundwater quality parameters suggested the subdivision of data into three clusters where Al and pH formed a separate cluster.

iv. The calculated CCME Water Quality Index (WQI) scores values combining and evaluating the scope, frequency, and amplitude measures of variance described the water quality of Khibiny alkaline massif as fair to marginal and indicated its gradual deterioration during the monitoring period 1999–2012.

v. Although the field data analysis using chemometric methods has been done for one particular metal and groundwater source, the similar analysis, the developed algorithms and computer programs can be successfully applied to any other water sources and could be extended to other toxic metals in the natural water bodies.

- Laboratory study:

i. The removal of aluminum from acidic aqueous solution by adsorption on montmorillonite K10, TiO_2, and SiO_2 was studied. The effect of pH, initial aluminum concentration, contact time, adsorbent amount, and ions present in natural water bodies was investigated. The outcomes of laboratory tests showed that the adsorption rate and capacity of adsorbents were in the following orders K10 > $TiO_2 \geq SiO_2$ and K10 > SiO_2 > TiO_2, respectively. The aluminum removal up to 97% was achieved in 120 min using 5.0 g L^{-1} of K10 and the removal of 72–95% within 240 min using both TiO_2 and SiO_2. The presence of Ca^{2+}, Mg^{2+}, SO_4^2, HCO_3^- ions in the solution had a negative effect on the aluminum removal by adsorbents tested.

ii. In the alkaline aqueous solution considering the natural physico-chemical composition of Khibiny alkaline massif groundwater, TiO_2 and vermiculite concrete-supported ferric oxyhydroxide adsorbent displayed themselves as

effective adsorbents. The effects of pH, initial aluminum concentration, contact time, adsorbent dose, and ions associated according to the results of statistical analysis and mathematical modelling with aluminum concentration variability in the Khininy massif groundwater were investigated. The results revealed that TiO_2 exhibited a much higher aluminum adsorption rate and the equilibrium time was up to eight times less than in case of vermiculite concrete-supported ferric oxyhydroxide adsorbent while the capacities of both adsorbents were similar. Laboratory tests showed that 1.0 g L^{-1} of each adsorbent at pH 9.0 removed 86–93% of aluminum initially contained in water during the contact time of 30 min for TiO_2 and 240 min for vermiculite concrete-supported ferric oxyhydroxide adsorbent.

iii. It was shown that when TiO_2 and vermiculite concrete-supported ferric oxyhydroxide adsorbent worked jointly as a multicomponent adsorbent they were capable to remove up to 95% of aluminum within 60 min of contact time from alkaline aqueous solution and the changes of each component mass allow controlling the contact time and efficiency of aluminum removal. No apparent significant effect on aluminum removal in the presence of NO_3^-, SO_4^{2-}, and Cl^- at pH 9.0 was observed.

The current investigation is a necessary step preceding the development and implementation of a reliable technology to reach a desirable level of aluminum removal from Khibiny alkaline massif groundwater that is an important source of household water supply in the area. The outcomes of field data analysis and mathematical modelling together with the results of laboratory study of adsorbents identify and present a possible approach solving the problem of elevated aluminum concentrations in the household water of Khibiny alkaline massif area as well as other locations where the solution of this problem can improve living conditions or industrial technologies. The PhD thesis objectives were addressed.

7.2 Scientific Contribution

- The field dataset including the results of long-term monitoring of 12 physico-chemical characteristics of Khibiny alkaline massif groundwater was analyzed quantitatively for the first time by applying chemometric methods including both univariate and multivariate statistical techniques, spectral analysis based on fast Fourier transform (FFT) algorithm and water quality index. The mathematical models developed by using univariate and multivariate regression methods explained up to 54% of aluminum concentration variability and 67.5% of the original dataset total variance. The temporal and dominant frequency variability features of groundwater quality parameters were established, analyzed, and interpreted with the emphasis on the elevated aluminum concentrations.
- The gradual deterioration of Khibiny alkaline massif groundwater quality from fair to marginal category during the monitoring period 1999–2012 was revealed by calculated CCME Water Quality Index scores values.
- The results of testing of various adsorbents revealed that in the acidic aqueous solution the maximum aluminum uptake of 1.69 mg g^{-1} was shown by the montmorillonite K10 within 120 min while in the alkaline solution TiO_2 and vermiculite concrete-supported ferric oxyhydroxide adsorbent were most effective having the adsorption capacities of 6.85 mg g^{-1} and 6.75 mg g^{-1} at 30 min and 240 min of contact time, respectively. Testing revealed that when worked jointly as a multicomponent adsorbent they were capable to effectively remove aluminum from the alkaline aqueous solution where the maximum uptake reached 8.28 mg g^{-1} within 60 min and the changes of each component mass allow controlling the contact time to provide the required aluminum removal efficiency.
- The adsorbents tested – K10, SiO_2, TiO_2, and vermiculite concrete-supported ferric oxyhydroxide showed several advantages over the conventional adsorbents such for example as activated carbon materials and their modified forms investigated in relevant studies. The benefits of a faster kinetic rate, higher adsorption capacity, and the application of lower adsorbent doses decreasing aluminum concentrations below the drinking water guideline of 0.20 mg L^{-1} were obtained in current study.

7.3 Study Limitations

Study on adsorption of Al was conducted at acidic and alkaline aqueous solutions. According to the literature survey, elevated Al concentrations are presented in both acidic and alkaline surface and ground waters such as in the alkaline groundwater under consideration. The amphoteric nature of Al in aqueous solution dissolving in the acidic or in the alkaline solutions made the investigation of Al adsorption appropriate at the above-mentioned conditions. The photocatalytic process using TiO_2 as a photocatalyst could not be studied due to the more negative Al^{3+} (acidic conditions) and $Al(OH)_4^-$ (alkaline conditions) redox potentials (E^0) of −1.67 V and −2.35 V at T = 25 °C, respectively than the conduction band of TiO_2.

7.4 Recommendations

The current investigation on elevated aluminum level in the groundwater of Khibiny alkaline massif and the approach lowering it to the established guidelines by using statistical analysis, mathematical modelling as well as laboratory tests on adsorption as a reliable method for aluminum removal from aqueous solutions would require further investigation. The following research topics can be suggested:

- The experiments testing adsorbents performance toward aluminum removal from natural water of Khibiny alkaline massif is recommended as the current study was performed on simulated water.
- The investigation of adsorption on TiO_2 and vermiculite concrete-supported ferric oxyhydroxide adsorbent in a multi-element aqueous system in the presence of competing toxic metals such as cadmium, zinc, chromium could be beneficial.
- The life-cycle analysis study of adsorbents tested is suggested.
- Studying the adsorption of aluminum on TiO_2 and vermiculite concrete-supported ferric oxyhydroxide adsorbent adsorbents in a lab-scale and pilot-scale projects using continuous flow model systems is required.

- The development of computer model/program using optimization methods to control the process of aluminum removal depending on the initial aluminum concentration in the water intake, adsorbent doses, and allowed contact time is a necessary tool during the pilot-scale tests.

Appendices

Appendix A: Graphical abstract of work presented in Chapter 3.

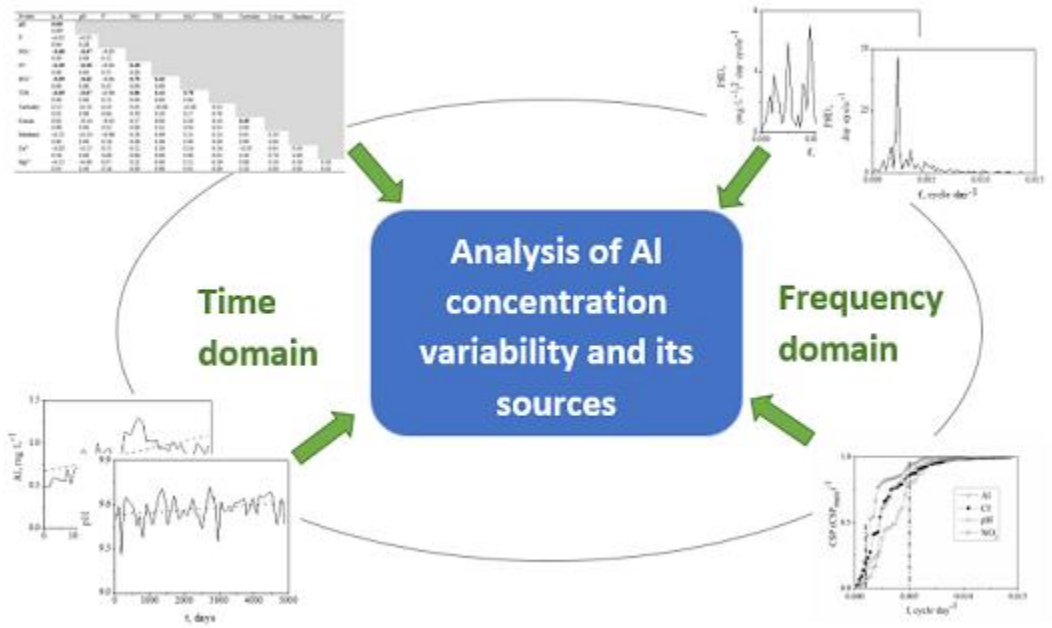

Appendix B: Supplementary material of Chapter 3.

Table S3.1: Averaged water quality parameters monitored from ten groundwater wells of "Central" water intake.

Year	Al, mg L^{-1}	pH	F^- mg L^{-1}	NO_3^-, mg L^{-1}	Cl^-, mg L^{-1}	SO_4^{2-}, mg L^{-1}	TDS, mg L^{-1}	Turbidity, mg L^{-1}	Colour, colour units	Hardness, mmol L^{-1}	Ca^{2+}, mmol L^{-1}	Mg^{2+}, mmol L^{-1}
1999	0.53	9.53	0.12	2.32	2.95	11.47	65.48	0.04	1.50	0.02	0.02	0.01
2000	0.56	9.47	0.08	3.57	1.60	8.94	66.64	0.02	0.00	0.03	0.00	0.03
2001	0.67	9.44	0.09	3.56	1.83	12.54	63.83	0.14	1.47	0.03	0.01	0.02
2002	0.92	9.61	0.09	2.68	1.86	9.71	58.18	0.16	2.15	0.03	0.03	0.00
2003	0.83	9.52	0.07	2.63	1.97	7.78	54.57	0.22	2.54	0.07	0.05	0.03
2004	0.88	9.53	0.13	2.38	2.40	8.13	56.91	0.16	0.98	0.04	0.80	0.00
2005	0.96	9.51	0.18	2.30	1.68	11.42	57.89	0.19	1.86	0.04	0.66	0.19
2006	1.24	9.65	0.15	1.64	1.33	6.83	51.44	0.40	1.76	0.01	0.00	0.16
2007	0.99	9.48	0.27	1.79	1.92	7.16	52.54	0.35	1.81	0.02	0.19	0.06
2008	0.97	9.55	0.21	1.91	1.28	5.12	54.77	0.42	1.66	0.01	0.07	0.05
2009	0.93	9.58	0.16	1.48	1.32	4.89	49.63	0.42	2.75	0.01	0.14	0.07
2010	0.90	9.58	0.08	1.35	1.69	5.26	50.08	0.37	1.32	0.01	0.08	0.03
2011	0.92	9.56	0.10	1.41	2.01	5.73	51.37	0.48	2.17	0.00	0.01	0.01
2012	0.90	9.54	0.12	1.25	1.69	6.56	51.52	0.37	1.03	0.01	0.00	0.00

Table S3.2: Assessment of candidate terms for the Al multiple regression model.

Model Term	Term Coefficient	p-value	VIF
Constant	−4.929	0.001	
pH	0.543	0.001	1.980
NO_3^-	−0.029	0.001	4.370
Cl^-	−0.042	0.018	1.270
SO_4^{2-}	0.000	**0.938**	2.840
TDS	−0.006	0.001	**4.830**

Table S3.3: Assessment of multiple regression model (Equation (3.4)) with predictors pH, NO_3^-, and Cl^-.

Model Term	Term Coefficient	p-value	VIF
Constant	−5.861	0.001	
pH	0.617	0.001	1.870
NO_3^-	−0.068	0.001	1.930
Cl^-	−0.057	0.001	1.210

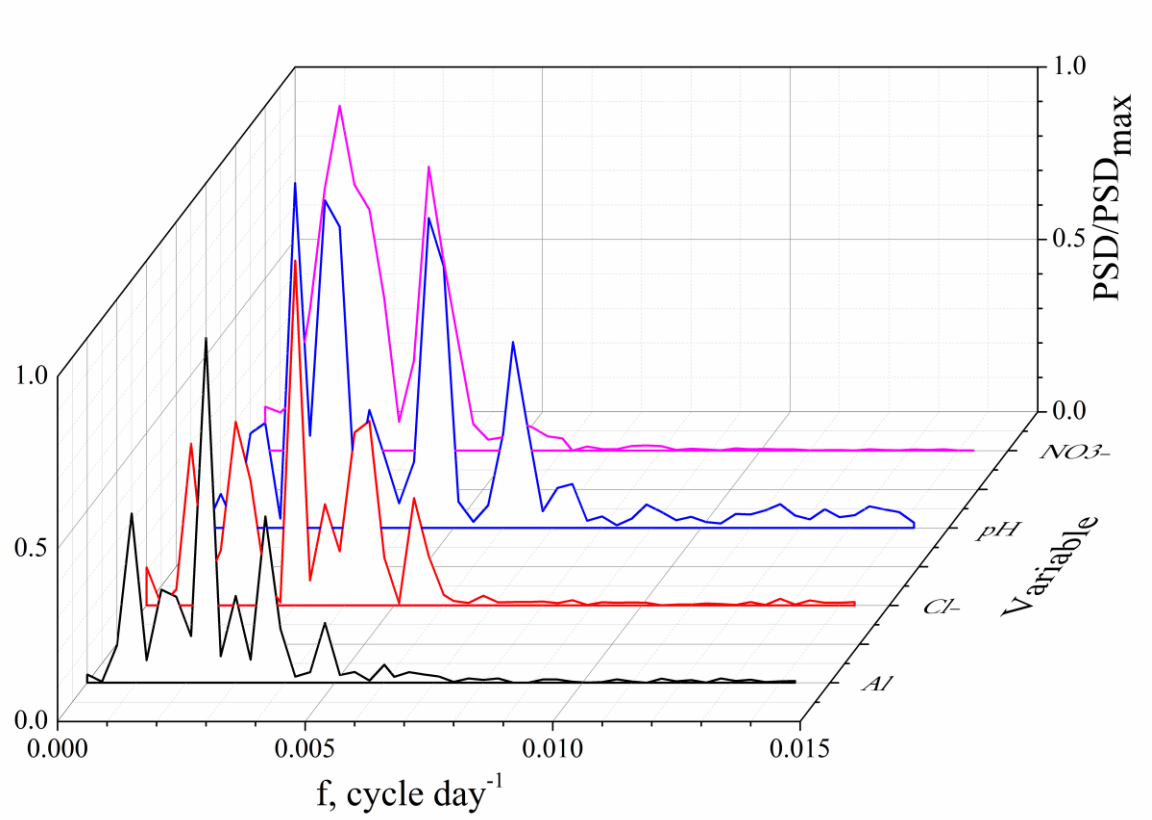

Figure S3.1: Calculated PSD estimates of Al, Cl^-, pH, and NO_3^- time series, well 10 of water intake "Central".

Appendix C: MATLAB code to calculate the results reported in 3.4.4 Spectral Analysis based on FFT.

```
% Aluminum time series
Cj_Al=fft(Al); % calculation of Fourier coefficients of
detrended and interpolated data using Fast Fourier
Transform (FFT) algorithm
N=length(Al); % set the length of data
Fs=0.028571428;% set sampling frequency = 1/35 (1/day)
Cj1_Al=Cj_Al(1:N/2+1); % we need only half of the result as
the result is mirrored
PSD_Al=(1/(Fs*N))*abs(Cj1_Al).^2; % calculation of PSD with
the scaling factor
PSD_Al(2:end-1)=2*PSD_Al(2:end-1); % additional factor of 2
is added
freq=0:Fs/N:Fs/2; % set frequency range, Fs/N is a
frequency resolution
% plot the results
fig1=figure;
plot(freq,PSD_Al, 'k') % plot PSD values as a function of
frequency
grid on % display grid on the graph
xlabel('Frequency (cycle/day)') % name x-axis
ylabel('PSD (mg/L).^2/(cycle/day)') % name y-axis
title('Calculated values of Al PSD, Well 1 1999-2012') %
title the graph
set(gca,'xtick', 0:0.0025:0.015) % set x-axis tick values
set(gca,'FontSize', 18) % set font size on the graph
saveas(fig1,'Calculated values of Al PSD, Well 1 1999-
2012.tif')% save the graph as image

% pH time series
Cj_pH=fft(pH); % calculation of Fourier coefficients using
Fast Fourier Transform algorithm
Cj1_pH=Cj_pH(1:N/2+1); % we need only half of the result as
the result is mirrored
PSD_pH=(1/(Fs*N))*abs(Cj1_pH).^2; % calculation of PSD with
the scaling factor
PSD_pH(2:end-1)=2*PSD_pH(2:end-1); % additional factor of 2
is added
% plot the results
fig2=figure;
plot(freq,PSD_pH, 'k') % plot PSD values as a function of
frequency
```

```
grid on % display grid on the graph
xlabel('Frequency (cycle/day)') % name x-axis
ylabel('PSD day/cycle') % name y-axis
title('Calculated values of pH PSD, Well 1 1999-2012') %
title the graph
set(gca,'xtick', 0:0.0025:0.015) % set x-axis tick values
set(gca,'FontSize', 18) % set font size on the graph
saveas(fig2,'Calculated values of pH PSD, Well 1 1999-
2012.tif')% save the graph as image

% Chloride time series
Cj_Cl=fft(Cl); % calculation of Fourier coefficients using
Fast Fourier Transform algorithm
Cj1_Cl=Cj_Cl(1:N/2+1); % we need only half of the result as
the result is mirrored
PSD_Cl=(1/(Fs*N))*abs(Cj1_Cl).^2; % calculation of PSD with
the scaling factor
PSD_Cl(2:end-1)=2*PSD_Cl(2:end-1); % additional factor of 2
is added
% plot the results
fig3=figure;
plot(freq,PSD_Cl, 'k') % plot PSD values as a function of
frequency
grid on % display grid on the graph
xlabel('Frequency (cycle/day)') % name x-axis
ylabel('PSD (mg/L).^2/(cycle/day)') % name y-axis
title('Calculated values of Cl.^- PSD, Well 1 1999-2012') %
title the graph
set(gca,'xtick', 0:0.0025:0.015) % set x-axis tick values
set(gca,'FontSize', 18) % set font size on the graph
saveas(fig3,'Calculated values of Cl.^- PSD, Well 1 1999-
2012.tif')% save the graph as image

% Nitrate time series
Cj_NO=fft(NO); % calculation of Fourier coefficients using
Fast Fourier Transform algorithm
Cj1_NO=Cj_NO(1:N/2+1); % we need only half of the result as
the result is mirrored
PSD_NO=(1/(Fs*N))*abs(Cj1_NO).^2; % calculation of PSD with
the scaling factor
PSD_NO(2:end-1)=2*PSD_NO(2:end-1); % additional factor of 2
is added
% plot the results
fig4=figure;
plot(freq,PSD_NO, 'k') % plot PSD values as a function of
frequency
grid on % display grid on the graph
```

```
xlabel('Frequency (cycle/day)') % name x-axis
ylabel('PSD (mg/L).^2/(cycle/day)') % name y-axis
title('Calculated values of NO_{3}.^- PSD, Well 1 1999-
2012') % title the graph
set(gca,'xtick', 0:0.0025:0.015) % set x-axis tick values
set(gca,'FontSize', 18) % set font size on the graph
saveas(fig4,'Calculated values of NO3- PSD, Well 1 1999-
2012.tif')% save the graph as image

% Cumulative spectral power estimates (CSP) calculation of
aluminum, pH, chloride, and nitrate time series
x=length(Time); % set the length of data
T=Time(x);
dF=1/T;% set frequency resolution
CSP_Al=dF*cumsum(PSD_Al);% calculation of CSP
CSP_pH=dF*cumsum(PSD_pH);% calculation of CSP
CSP_Cl=dF*cumsum(PSD_Cl);% calculation of CSP
CSP_NO=dF*cumsum(PSD_NO);% calculation of CSP
CSP_Al_max=max(CSP_Al);% calculation of max CSP value
CSP_pH_max=max(CSP_pH);% calculation of max CSP value
CSP_Cl_max=max(CSP_Cl);% calculation of max CSP value
CSP_NO_max=max(CSP_NO);% calculation of max CSP value
CSP_Al_N=CSP_Al/CSP_Al_max;% normalizing the CSP values
CSP_pH_N=CSP_pH/CSP_pH_max;% normalizing the CSP values
CSP_Cl_N=CSP_Cl/CSP_Cl_max;% normalizing the CSP values
CSP_NO_N=CSP_NO/CSP_NO_max;% normalizing the CSP values
%plot the results
fig5=figure;
plot(freq,CSP_Al_N,'-.r*','DisplayName','Al')
hold on
plot(freq,CSP_pH_N,':bs','DisplayName','pH')
hold on
plot(freq,CSP_Cl_N,'--mo','DisplayName','Cl.^-')
hold on
plot(freq,CSP_NO_N,'-ko', 'MarkerFaceColor',[0 0
0],'DisplayName','NO_{3}.^-')
grid on
xlabel('Frequency(cycle/day)')% name x-axis
ylabel('CSP/CSP_{max}')% name y-axis
title('Calculated CSP values, Well 1 1999-2012')
set(gca,'xtick', 0:0.0025:0.015) % set x-axis tick values
set(gca,'FontSize', 18) % set font size on the graph
legend({'Al','pH','Cl.^-','NO_{3}.^-'},'AutoUpdate','off')
saveas(fig5,'Calculated values of Al, pH, Cl-, and NO3-
CSP, Well 1 1999-2012.tif')% save the graph as image
```

```
%Lomb-Scargle periodogram method using detrended
noninterpolated data: aluminum time series
[LS,freq2]=plomb(Al_raw,Time_raw);
x_1=length(Time_raw); % set the length of data
T_1=Time(x_1);
dF_1=1/T_1;% set frequency resolution
CSP_LS_Al=dF_1*cumsum(LS);% calculation of CSP based on
Lomb-Scargle periodogram method
fig6=figure;
semilogy(freq,CSP_Al,'--mo','DisplayName','PSD based on
FFT')
hold on
semilogy(freq2,CSP_LS_Al,'--ks','DisplayName','PSD based on
Lomb-Scargle')
xlabel('Frequency (cycles/day)')
title('Calculated CSP estimates of Al with the application
of FFT algorithm and Lomb-Scargle method')
ylabel('CSP Al,(mg/L).^2')
saveas(fig6,'Calculated CSP estimates of Al with the
application of FFT algorithm and Lomb-Scargle method')%
save the graph as image
```

Appendix D: Supplementary material of Chapter 4.

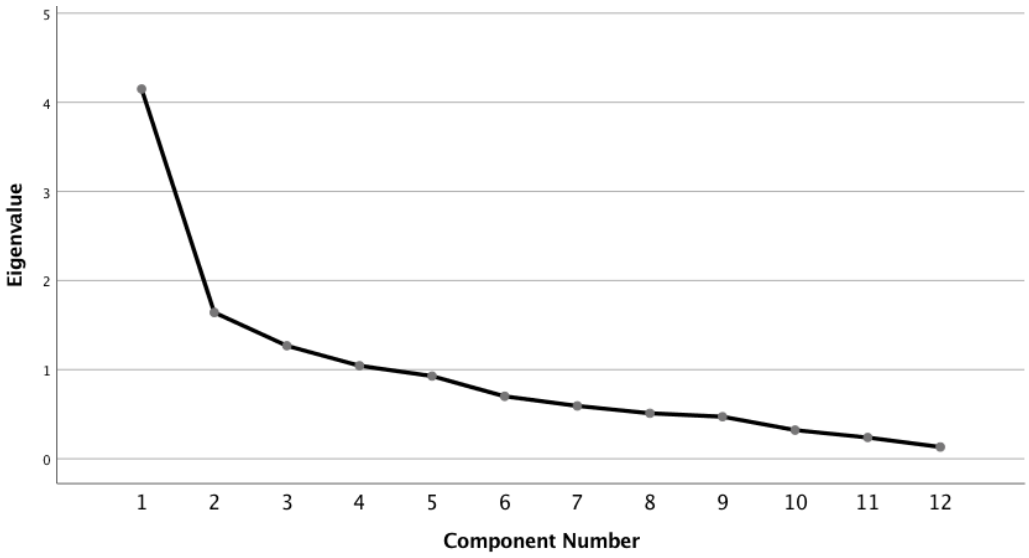

Figure S4.1: Scree plot to identify the number of components to be retained in the analysis to comprehend the underlying data structure.

Appendix E: Supplementary material of Chapter 5.

Table S5.1: Effect of adsorbent dose on percentage Al removal by K10, TiO_2 and SiO_2 at equilibrium time, pH 4.0 and room temperature (T = 24±1 °C).

Adsorbent dose, g L^{-1}	Percentage of Al removal (mean ± standard deviation)		
	K10	TiO_2	SiO_2
1.0	67.5 ± 0.8	37.1 ± 1.5	50.1 ± 3.3
2.0	89.2 ± 1.1	53.7 ± 4.6	65.5 ± 4.9
3.0	92.3 ± 0.7	61.5 ± 3.4	80.4 ± 3.3
4.0	97.1 ± 0.3	65.8 ± 3.7	89.1 ± 3.6
5.0	97.4 ± 0.2	71.9 ± 1.9	94.6 ± 1.4

Table S5.2: Effect of ions on the percentage Al removal by K10 based on the t-confidence interval procedure (*t*-test).

Ion	Estimate for difference*)	95% confidence interval for difference*)	p-value	Comment on null hypothesis	Presence of statistically significant difference
Ca^{2+}	53.7	(45.9, 61.6)	0.001 < 0.05	Rejected	Yes
Mg^{2+}	25.2	(15.7, 34.8)	0.008 < 0.05	Rejected	Yes
SO_4^{2-}	9.1	(–8.5, 26.7)	0.200 > 0.05	Accepted	No
Cl^-/Na^+ (NaCl)	–0.1	(–4.4, 4.3)	0.977 > 0.05	Accepted	No
HCO_3^-	–5.7	(–18.4, 7.0)	0.193> 0.05	Accepted	No

*) Null Hypothesis: $(\text{Average Al Removal})_{(\text{control})} - (\text{Average Al Removal})_{(\text{in ion presence})} = 0$

Table S5.3: Effect of ions on the percentage Al removal by TiO_2 based on the t-confidence interval procedure (*t*-test).

Ion	Estimate for difference*)	95% confidence interval for difference*)	p-value	Comment on null hypothesis	Presence of statistically significant difference
Ca^{2+}	9.2	(2.3, 16.1)	0.024 < 0.05	Rejected	Yes
Mg^{2+}	5.6	(−2.6, 13.8)	0.099 > 0.05	Accepted	No
SO_4^{2-}	–20.7	(–28.9, −12.5)	0.008 < 0.05	Rejected	Yes
Cl^-/Na^+ (NaCl)	8.5	(–0.16, 17.1)	0.052 > 0.05	Accepted	No
HCO_3^-	36.2	(16.2, 56.1)	0.016 < 0.05	Rejected	Yes

*) Null Hypothesis: $(\text{Average Al Removal})_{(\text{control})} - (\text{Average Al Removal})_{(\text{in ion presence})} = 0$

Table S5.4: Effect of ions on the percentage Al removal by SiO_2 based on the t-confidence interval procedure (*t*-test).

Ion	Estimate for difference*)	95% confidence interval for difference*)	p-value	Comment on null hypothesis	Presence of statistically significant difference
Ca^{2+}	18.1	(5.9, 30.3)	0.024 < 0.05	Rejected	Yes
Mg^{2+}	11.6	(1.1, 22.1)	0.040 < 0.05	Rejected	Yes
SO_4^{2-}	22.4	(9.0, 35.7)	0.019 < 0.05	Rejected	Yes
Cl^-/Na^+ (NaCl)	16.0	(3.7, 28.3)	0.031 < 0.05	Rejected	Yes
HCO_3^-	–0.9	(–14.1, 12.2)	0.791 > 0.05	Accepted	No

*) Null Hypothesis: $(\text{Average Al Removal})_{(\text{control})} - (\text{Average Al Removal})_{(\text{in ion presence})} = 0$

Appendix F: Supplementary material of Chapter 6.

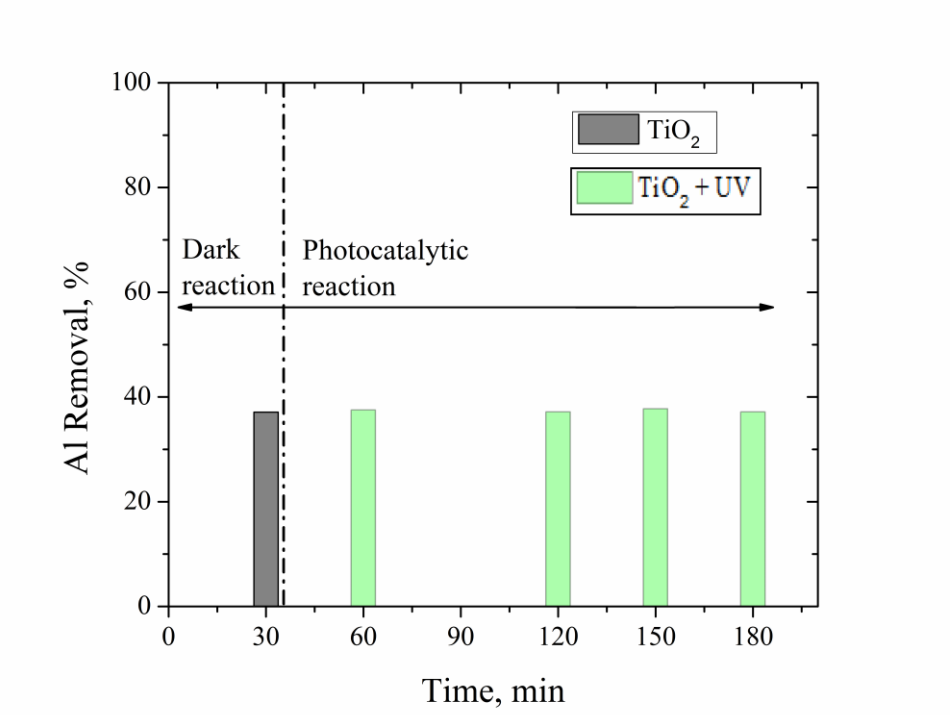

Figure S6.1: Effect of UV radiation on Al removal by TiO_2 *). Experimental conditions: $[Al]_0$ = 2 mg L^{-1}; $[TiO_2]$ = 1.0 g L^{-1}; pH = 4.0; T = 24±1 °C, light intensity = 100 mW cm^{-2}. Dash dotted line indicates the time when the UV radiation started.

*) The experimental procedure of this set of experiments was following the main steps as described in [1,2].

References

[1] P. Chowdhury, S. Athapaththu, A. Elkamel, A.K. Ray, Visible-solar-light-driven photo-reduction and removal of cadmium ion with Eosin Y-sensitized TiO2 in aqueous solution of triethanolamine, Sep. Purif. Technol. 174 (2017) 109–115. doi:10.1016/j.seppur.2016.10.011.

[2] G. Kumordzi, G. Malekshoar, E.K. Yanful, A.K. Ray, Solar photocatalytic degradation of Zn2+ using graphene based TiO2, Sep. Purif. Technol. 168 (2016) 294–301. doi:10.1016/j.seppur.2016.05.040.

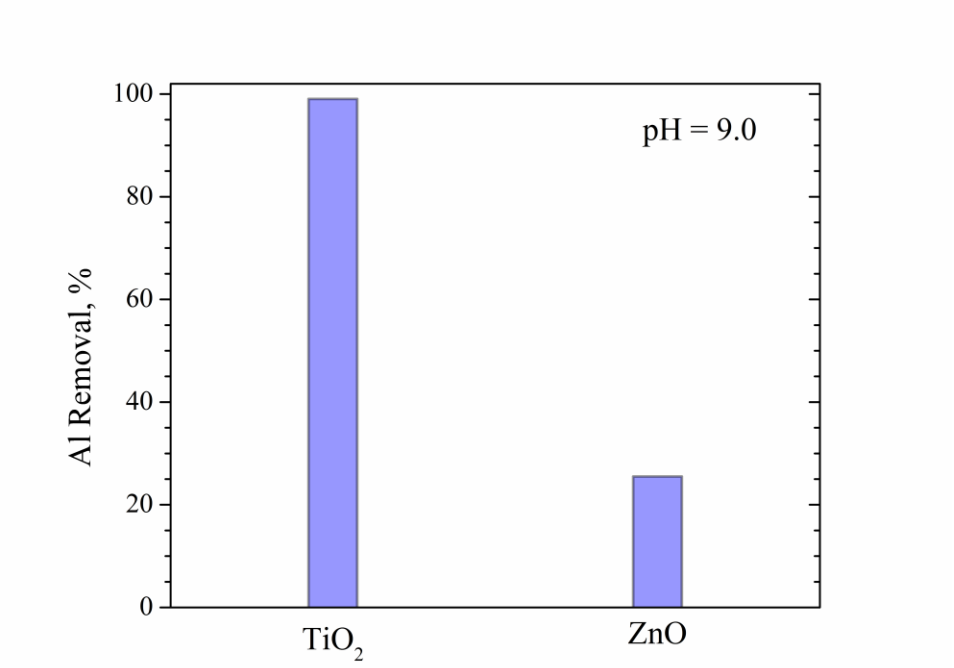

Figure S6.2: Al adsorption on nanomaterials [*)]. Experimental conditions: $[Al]_0$ = 2 mg L^{-1}; $[TiO_2]$ = [ZnO] = 2.0 g L^{-1}; equilibrium time = 30 min; pH = 9.0; T = 24±1 °C.

[*)] TiO_2 – titanium dioxide P25 nano powder was obtained from Evonik Corporation (Piscataway, New Jersey, USA). Surface areas 50 m^2 g^{-1}, particle size 30 nm;

ZnO – zinc oxide nano powder was purchased from Advanced Materials (Manchester, Connecticuit, USA). Surface area 35 m^2 g^{-1}, particle size 30 nm.

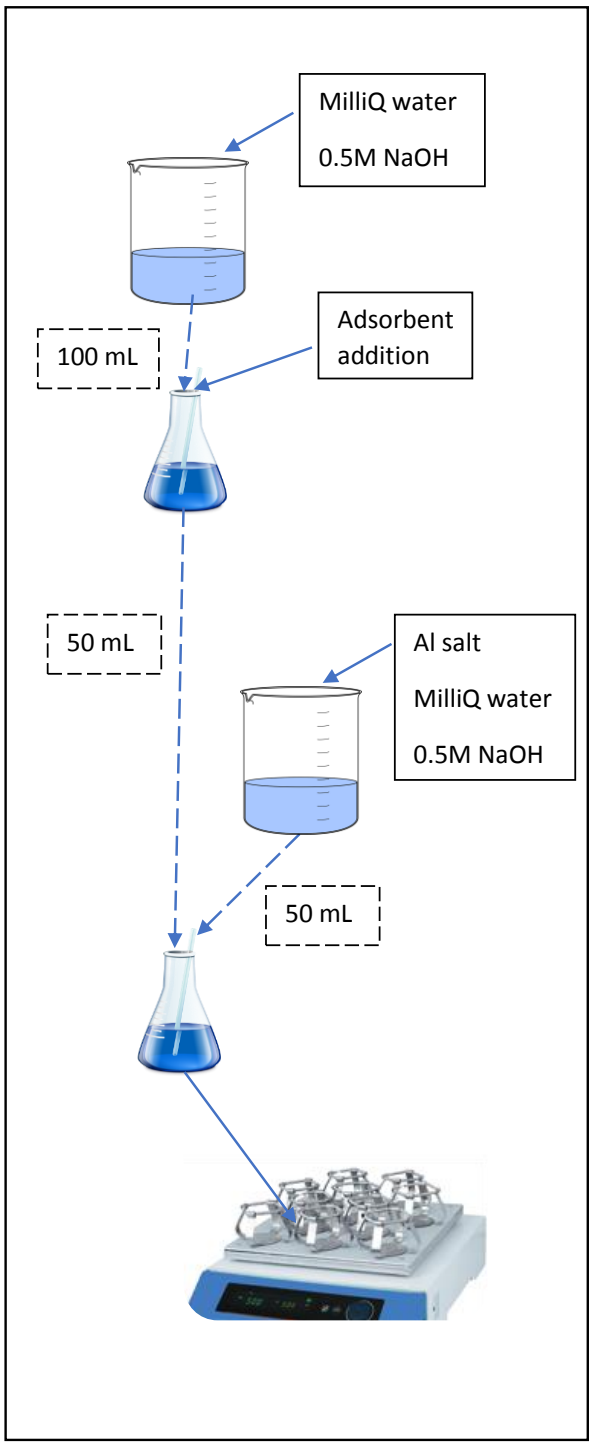

Figure S6.3: Main steps in the "tea-bag" experimental procedure.

Table S6.1: Percentage of Al removed by adsorption and precipitation on different TiO_2 (a) and VC (b) doses based on the results of the "tea-bag" experiments. Experimental conditions: $[Al]_0$ = 2 mg L^{-1}; mixing time = 30 min (TiO_2), 240 min (VC); T = 24±1 °C.

(a)

TiO_2, g L^{-1}	Precipitation, %	Adsorption, %	Total Al removal, %	Adjusted pH	Final pH
0.375	22.4	35.2	57.7	9.0	8.2
0.500	25.5	40.5	65.9	9.0	8.2
0.625	19.8	65.9	85.7	9.0	8.2
1.000	20.7	75.5	96.2	9.0	8.2

(b)

VC, g L^{-1}	Precipitation, %	Adsorption, %	Total Al removal, %	Adjusted pH	Final pH
0.750	19.8	65.9	85.7	9.0	8.3
1.500	20.7	75.5	96.2	9.0	8.3

Table S6.2: Adsorption kinetics data of Al adsorption on TiO_2 (a) and VC (b) obtained at pH = 9.0 and room temperature T = 24 ± 1 °C.

(a)

0.25 g L^{-1} TiO_2				0.75 g L^{-1} TiO_2			
Contact time, min	Al, mg L^{-1}	q_t, mg g^{-1}	Al removal, %	Contact time, min	Al, mg L^{-1}	q_t, mg g^{-1}	Al removal, %
0	1.96	0.00	0	0	1.99	0.00	0
5	1.17	3.19	41	5	0.48	2.01	76
15	1.08	3.54	45	15	0.46	2.03	77
30	0.85	4.45	57	30	0.40	2.12	80
60	0.88	4.31	55	60	0.41	2.10	79
120	0.88	4.35	55	120	0.43	2.08	78
180	0.78	4.71	60	180	0.44	2.07	78

(b)

0.25 g L^{-1} VC				0.75 g L^{-1} VC			
Contact time, min	Al, mg L^{-1}	q_t, mg g^{-1}	Al removal, %	Contact time, min	Al, mg L^{-1}	q_t, mg g^{-1}	Al removal, %
0	1.82	0.00	0	0	1.92	0.00	0
5	1.63	0.75	10	5	–	–	–
15	1.50	1.29	18	15	1.16	1.01	40
30	1.27	2.20	30	30	0.85	1.42	56
60	0.99	3.33	46	60	0.61	1.75	68
120	0.78	4.15	57	120	0.43	1.98	77
180	0.71	4.43	61	180	0.32	2.13	83
240	0.64	4.70	65	240	0.25	2.23	87

Table S6.3: The pH measurement during the adsorption kinetic experiments with 0.25 g L^{-1} and 0.75 g L^{-1} TiO_2 and vermiculite concrete-supported adsorbent. Experimental conditions $[Al]_0$ = 2 mg L^{-1}; T = 24 ± 1 °C.

Contact time, min	pH 0.25 g L^{-1} TiO_2	pH 0.75 g L^{-1} TiO_2	pH 0.25 g L^{-1} VC	pH 0.75 g L^{-1} VC
0	9.05	9.05	9.01	9.01
5	9.18	9.14	8.80	9.00
15	9.17	9.15	8.81	9.07
30	9.12	9.14	8.79	9.07
60	9.12	9.06	8.85	9.15
120	9.16	9.18	8.80	9.09
180	9.11	9.18	8.77	9.00
240	–	–	8.69	8.88

Table S6.4: Effect of adsorbent dose on percentage Al removal by TiO_2 at equilibrium time 30 min, pH 9.0 and room temperature (T = 24±1 °C).

Adsorbent dose, g L^{-1}	Percentage of Al removal (mean ± standard deviation)	Final pH
0.250	53.30 ± 8.2	9.08
0.375	64.54 ± 3.65	9.12
0.500	65.92 ± 4.77	9.12
0.625	76.01 ± 8.47	9.12
0.750	80.57 ± 0.23	9.17
1.000	86.54 ± 0.99	9.12
1.500	93.40 ± 3.36	9.00
2.000	99.05 *)	9.00

*) The test was not replicated.

Table S6.5: Effect of adsorbent dose on percentage Al removal by VC at equilibrium time 240 min, pH 9.0 and room temperature (T = 24±1 °C).

Adsorbent dose, g L^{-1}	Percentage of Al removal (mean ± standard deviation)	Final pH
0.250	62.67 ± 2.82	8.88
0.375	68.43 ± 4.90	8.90
0.500	84.08 ± 2.40	8.73
0.625	86.83 ± 8.81	8.81
0.750	86.52 ± 0.87	8.96
1.000	93.72 ± 0.14	8.87
1.500	95.31 *)	8.85
2.000	97.78 *)	8.75

*) The test was not replicated.

Table S6.6: The Al removal and pH measurement during the experiments investigating the effect of adsorbents addition sequence. Experimental conditions $[Al]_0$ = 2 mg L^{-1}; $[TiO_2]$ = [VC] = 0.25 g L^{-1}; T = 24 ± 1 °C.

(a)

Contact time, min	Al Removal, % 0.25 g L^{-1} TiO_2	pH 0.25 g L^{-1} TiO_2
0	–	8.92
30	56.7 ± 4.0 *)	9.07
35	74.9 ± 3.7 **)	8.89
45	76.5 ± 1.2 **)	8.84
60	82.6 ± 3.6 **)	8.82

(b)

Contact time, min	Al Removal, % 0.25 g L^{-1} VC	pH 0.25 g L^{-1} VC
0	–	8.98
30	29.8 ± 1.1 ***)	8.83
35	62.0 ****)	8.96
45	65.2 ± 1.0 ****)	8.93
60	72.9 ± 0.9 ****)	8.88

*) Al removal by TiO_2.

**) Al removal by joint TiO_2 +VC.

***) Al removal by VC.

****) Al removal by joint VC +TiO_2.

Table S6.7: Effect of adsorbent dose on percentage Al removal by MA at equilibrium time 60 min, pH 9.0, and room temperature (T = 24±1 °C).

Adsorbent dose *), g L^{-1}	Percentage of Al removal (mean ± standard deviation)	Final pH
0.250	54.84	9.02
0.375	67.84	9.03
0.500	75.80 ± 3.29	9.06
0.750	86.73 ± 3.89	8.86
1.000	87.11 ± 1.63	8.92

*) [MA] = [TiO_2] + [VC] were taken in equal proportions.

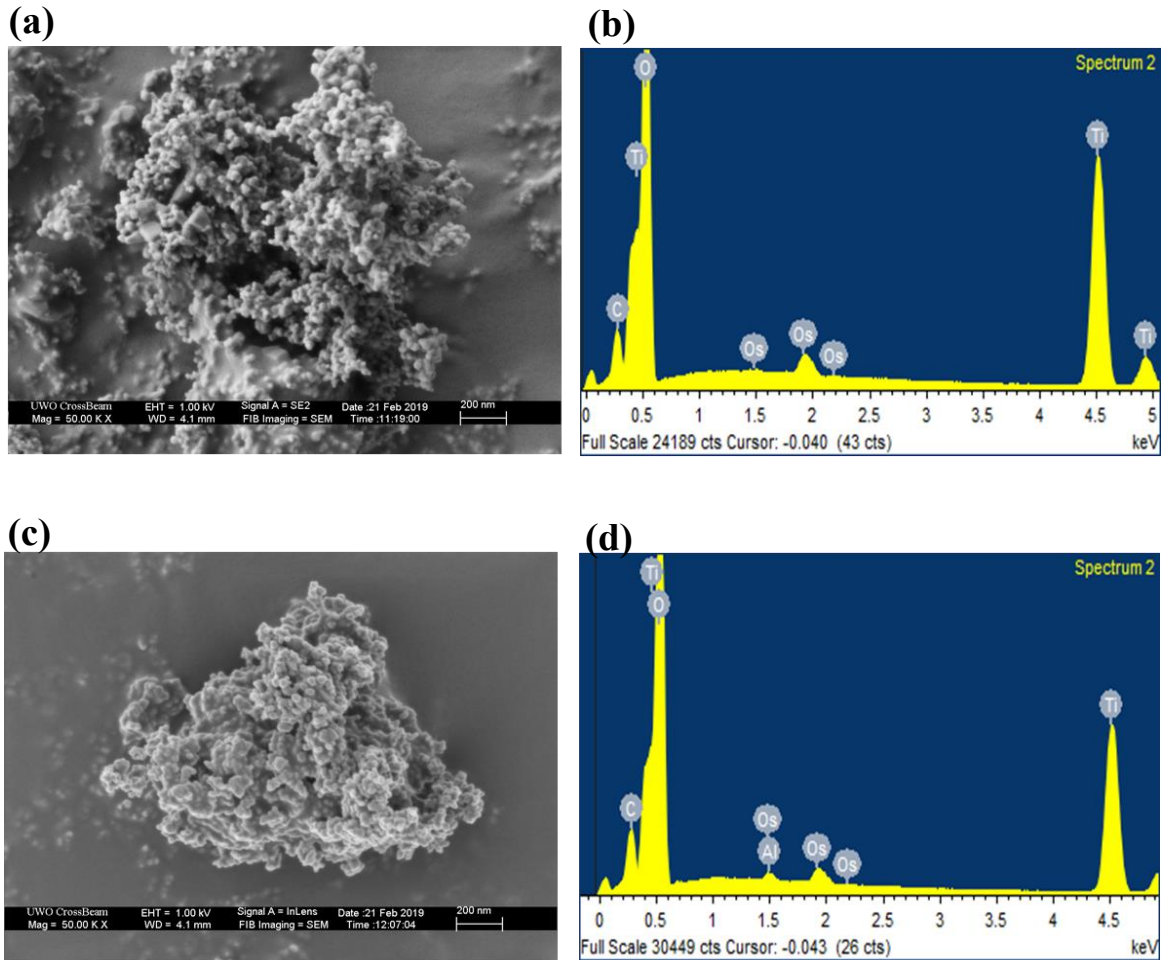

Figure S6.4: The results of SEM/EDX analysis of TiO_2 surface: before Al adsorption (a) and (b); after Al adsorption (c) and (d).

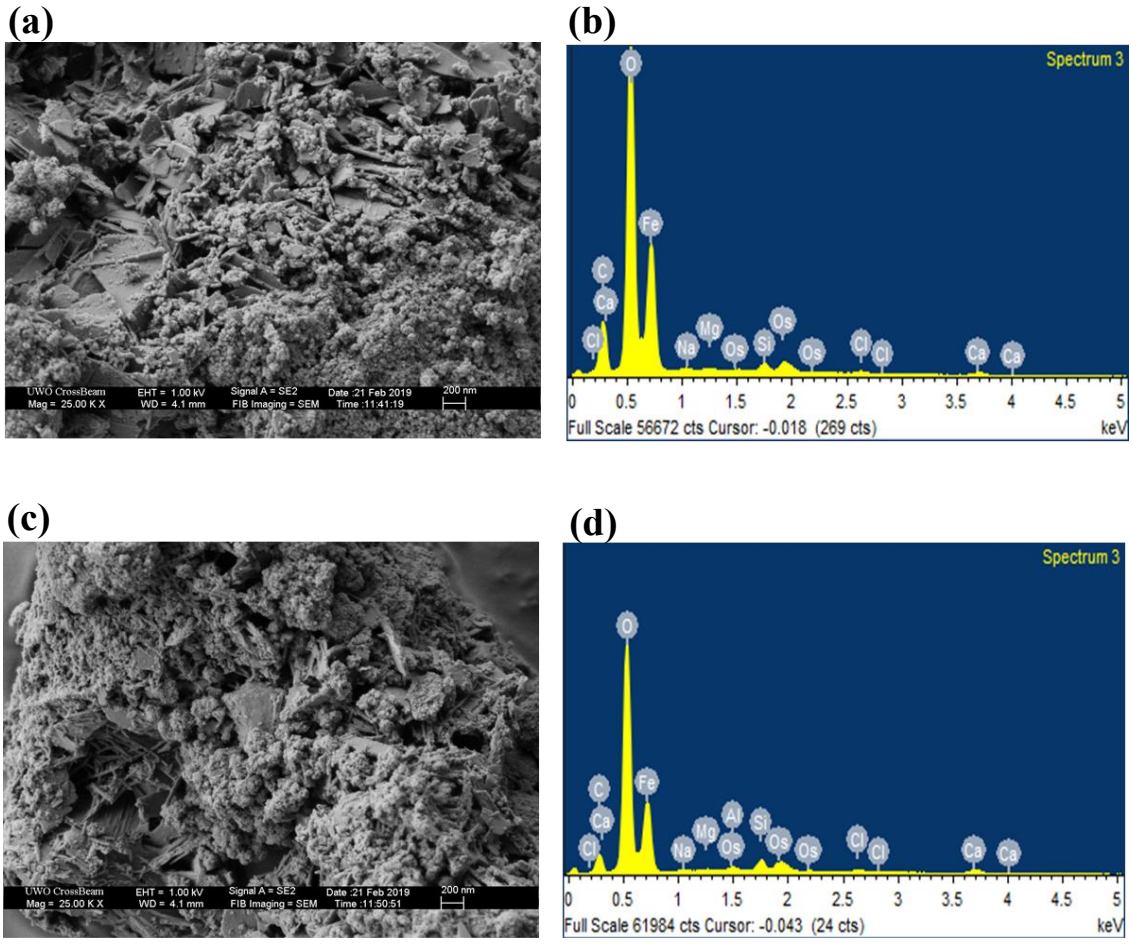

Figure S6.5: The results of SEM/EDX analysis of VC surface: before Al adsorption (a) and (b); after Al adsorption (c) and (d).

Table S6.8: Effect of ions on Al adsorption by 0.25 g L^{-1} TiO_2 (a), 0.25 g L^{-1} VC (b), and 0.50 g L^{-1} MA (c) at equilibrium time, pH 9.0, and room temperature (T = 24±1 °C), initial concentration of ions: [NO_3^-] = 2.12 mg L^{-1}, [SO_4^{2-}] = 7.89 mg L^{-1}, [Cl^-] = 1.82 mg L^{-1}.

(a) Equilibrium time = 30 min		
	Al removal, %	Final pH
Control	54.64 ± 6.09	9.10
NO_3^-	54.99 ± 5.28	9.14
SO_4^-	52.13 ± 5.68	8.97
Cl^-	58.33 ± 5.98	9.01

(b) Equilibrium time = 240 min		
	Al removal, %	Final pH
Control	62.67 ± 2.82	8.88
NO_3^-	57.19 ± 2.62	9.15
SO_4^-	48.88 ± 1.66	9.10
Cl^-	60.67 ± 1.00	9.06

(c) Equilibrium time = 60 min		
	Al removal, %	Final pH
Control	75.80 ± 3.29	9.06
NO_3^-	74.76 ± 0.11	8.86
SO_4^-	74.94 ± 0.80	8.83
Cl^-	65.84 ± 0.78	9.05

Curriculum Vitae

Name: Daria Popugaeva

Post-secondary Education and Degrees:

Saint Petersburg State University of Aerospace Instrumentation
Saint Petersburg, Russia
2008–2012 B.Eng. System Analysis and Logistics;
System Theory and Management

Western University
London, Ontario, Canada
2014–2019 Ph.D. Chemical and Biochemical Engineering;
Environmental and Green Engineering

Honours and Awards:

Nominee of the Graduate Student Teaching Assistant (GSTA) Awards of Excellence. 2018

1st Degree Diploma, The International Forum-Contest of Young Researchers "Topical Issues of Rational Use of Natural Recourses", Saint Petersburg Mining University, Saint Petersburg, Russia. 2016

Related Work Experience:

Research Intern
Trojan Technologies, London, Ontario, Canada
May–August 2016

Graduate Research Assistant
Western University, London, Ontario, Canada
2014–2019

Graduate Teaching Assistant
Western University, London, Ontario, Canada
2014–2019

Conference Presentations:

Popugaeva, D., Ray, A.K., Kreyman, K. Analysis and control of aluminum concentration in groundwater based on field data and laboratory experiments. Ontario Water Works Association (OWWA) & Trade Show, Ottawa, ON, Canada (May 6–8, 2019)

Popugaeva, D., Ray, A.K., Kreyman, K. Analysis and control of Al concentration in groundwater based on mathematical modeling and laboratory tests. American Institute of Chemical Engineers (AIChE) Annual Meeting, Pittsburgh, PA, USA (October 28–November 2, 2018)

Popugaeva, D., Ray, A.K., Kreyman, K. Analysis and control of aluminum level in groundwater. Water Environment Association of Ontario (WEAO) 47th Annual Technical Symposium & OPCEA Exhibition, London, ON, Canada (April 15–17, 2018)

Popugaeva, D., Ray, A.K., Kreyman, K. Study of Al(III) in groundwater using chemometric methods. Canadian Society for Chemical Engineering (CSChE) 67th Canadian Chemical Engineering Conference, Edmonton, AB, Canada (October 22–25, 2017)

Popugaeva, D., Ray, A.K., Kreyman, K. Decreasing Al(III) level in water for water reuse via low-cost adsorbents. The NSERC CREATE TWNER 5th Annual Workshop, Western University, London ON, Canada (February 22, 2017)

Popugaeva, D. Al(III) removal from aqueous solution. The International Forum-Contest of Young Researchers "Topical Issues of Rational Use of Natural Recourses", Saint Petersburg Mining University, Saint Petersburg, Russia (April 20–22, 2016)

Popugaeva, D., Ray, A.K., Kreyman, K. Decreasing Al(III) level in water for water reuse. The NSERC CREATE TWNER 4th Annual Workshop, Western University, London ON, Canada (October 29, 2015)

Popugaeva, D., Ray, A.K., Kreyman, K. Decreasing Al^{3+} level in water: field data analysis and laboratory experiments. The NSERC CREATE TWNER 3rd Annual Workshop: Western University, London ON, Canada (February 18, 2015)

Popugaeva, D. Environmental impact of logistics operations. The International Forum Competition of Young Researchers "Topical Issues of Rational Use of Natural Recourses", Saint Petersburg Mining University, Saint Petersburg, Russia (April, 2012)

Refereed Publications:

Popugaeva, D., Kreyman, K., Ray, A.K. (2018). Study of aluminium in groundwater using chemometric methods. Published in *Environmental Technology* https://doi.org/10.1080/09593330.2018.1544667

Popugaeva, D., Kreyman, K., Ray, A.K. Assessment of Khibiny Alkaline Massif Groundwater Quality using Statistical Methods and Water Quality Index. Submitted to *The Canadian Journal of Chemical Engineering* (under review)

Popugaeva, D., Manoli, K., Ray, A.K., Kreyman, K. Removal of aluminum from aqueous solutions by adsorption on montmorillonite K10, TiO_2, and SiO_2: Kinetics, Isotherms, and Effect of Ions. In preparation for the submission

Popugaeva, D., Ray, A.K., Kreyman, K. Aluminum removal from alkaline aqueous solution by adsorption on TiO_2 and vermiculite concrete-supported adsorbent. Prepared for the submission to *The Canadian Journal of Chemical Engineering*

Refereed Conference Proceedings:

Popugaeva, D. (2016, April). Al(III) removal from aqueous solution. In V.L. Trushko, L.S. Sinkov & U.M. Sichuk (Eds.), Topical Issues of Rational Use of Natural Recourses: The International Forum-Contest of Young Researchers, Saint Petersburg, Russia, April 20–22, 2016 (p.115–117). Saint Petersburg: Saint Petersburg Mining University Press. ISBN:978-5-94211-757-3

Popugaeva, D. (2014, April). Major steps for the efficient Al(III) removal from potable water. In V.L. Trushko, L.S. Sinkov & U.M. Sichuk (Eds.), Topical Issues of Subsoil Usage: The International Forum Competition of Young Researchers, Saint Petersburg, Russia, April 23–25, 2014 (p.102–103). Saint Petersburg: Saint Petersburg Mining University Press. ISBN:978594211688